Horizon 2020
European Union funding
for Research & Innovation

REDUCTION OF
RADIOLOGICAL
ACCIDENT
CONSEQUENCES

Action	Research and Innovation Action NFRP-2018-1
Grant Agreement #	847656
Project name	**R**eduction of **R**adiological **C**onsequences of design basis and design extension **A**ccidents
Project Acronym	R2CA
Project start date	01.09.2019
Deliverable #	D2.7.
Title	Reassessment of reactor tests cases
Author(s)	Tadas Kaliatka (LEI) Andrii Berezhnyi, Andriy Krushynskyy, Stanislav Sholomitsky, Denis Ruban (ARB) Anis Bousbia, Albert Malkhasyan (Bel V) Nikolaus Müllner, Raphael Zimmerl (BOKU) Luis E. Herranz, Rafael Iglesias (CIEMAT) Stefano Ederli, Fulvio Mascari (ENEA) Matthias Jobst (HZDR) Sebastien Belon, Katia Dieschbourg, Nathalie Girault, François Kremer, Dorel Obada (IRSN) Berta Bürger, Zoltán Hózer, Katalin Kulacsy (EK) Dmytro Gumenyuk, Yuriy Vorobyov, Olexandr Kotsuba (SSTC-NRS) Paul Foucaud (TRACTEBEL) Adam Kecek, Jan Klouzal, Pavel Kral (UJV-NRI) Asko Arkoma, Brahim Dif,Szogradi Marton (VTT)
Version	01
Related WP	WP2 METHO - Methodologies
Related Task	T2.5. Reassessment of reactor test cases - Quantification of gains (LEI)
Lead organization	LEI
Submission date	31.01.2024
Dissemination level	PU

This project has received funding from the Euratom research and training programme 2014-2018 under the grant agreement n° 847656

History

Date	Submitted by	Reviewed by	Version (Notes)
11.12.2023	Tadas Kaliatka (LEI) Paul Foucaud (TE)	Nathalie Girault (IRSN)	01

Contents

Abbreviations

AFW	Auxiliary Feed Water
BRU-A	Steam dump valve to-atmosphere
BWR	Boiling Water Reactor
CVCS	Chemical and Volume Control System
DBA	Design Basis Accident
DEC	Design Extension Conditions
DG	Diesel Generator
ECCS	Emergency Core Cooling System
EFW	Emergency Feedwater
EOP	Emergency Operating Procedures
EPR	European Pressurised Reactor
FA	Fuel Assemblies
FP	Fission products
HFP	Hot Full Power
HPIS	High Pressure Injection System
IE	Initiating Event
LOCA	Loss of Coolant Accident
LOOP	Loss Of Offsite Power
LPCI	Low Pressure Coolant Injection
LPIS	Low Pressure Injection System
LWR	Light Water Reactor
MCP	Main Cooling Pump
MFW	Main Feed Water
MSIV	Main Steam Isolation Valve
MSLB	Main Steam Line Break
PCT	Peak Cladding Temperature
PORV	Power Operated Relief Valve
PWR	Pressurized Water Reactor
PRZ	Pressurizer
RCS	Reactor Cooling System
RHRS	Residual Heat Removal System
RPV	Reactor Pressure vessel
RV	Relief Valve
RWST	Refuelling Water Storage Tank
SCRAM	Safety Control Rod Axe Man
SDA	Steam Dump to Atmosphere
SEG	Senior Expert Group
SG	Steam Generator
SG SRV	Steam Generator Safety Relief Valves
SG SV	Steam Generator Safety Valve
SGTR	Steam Generator Tube Rupture
SI	Safety Injection
SLB	Steam Line Break
SLBOUT	Steam Line Break Out of containment
VVER	Water Water Energy Reactor
WP	Work Package

1 Introduction

The R2CA project (Reduction of Radiological Consequences of design basis and extension Accidents) targeted the development of harmonized methodologies and innovative management approaches for the evaluation and the reduction of the consequences of DBA and DEC-A accidents in operating and foreseen nuclear power plants in Europe. For both purposes, the development of calculation methodologies has been conducted with the goal of better estimating the safety limits using fewer conservative and decoupled approaches and considering more realistic assumptions. It is expected that this will reinforce the confidence on these safety limits for conditions up to the first extended design domain (DEC-A) and will help a more accurate quantification of the potential changes to be considered for the forthcoming NPP operation conditions (i.e. increase of the fuel burn-up with NPP long term operation, use of new types of fuel rods, for example accident tolerant fuel). It is also expected that this will also allow the identification of new accident management measures and devices and will support the optimization of the associated emergency population protection measures. Finally, more realistic assessments of the radiological consequences of DBA-type accidents are also expected in a context where the development of small module reactors (SMRs) potentially in close proximity to housing is envisaged in the near future.

Improvements of evaluation tools were supported by the reassessment of the existing experimental and analytical databases. To this end, a dedicated database was built during the project, covering more than forty experimental programs including thousands of tests (integral and analytical as well as NPP measurements) which were relevant for phenomena occurring during LOCA and SGTR and for DBA or DEC-A conditions of interest.

In this document are presented the results, analyses and conclusions from first set of the simulation runs of selected Loss Of Coolants Accidents (LOCA) and Steam Generator Tube Ruptures (SGTR) in different kinds of LWRs (PWRs, BWR, VVERs and EPR) within DBA and DEC-A conditions. These transients, being by nature completely different and involving different physical phenomena, have been selected at the very beginning of the project by a dedicated Senior Expert Group (SEG) as representative scenarios to quantify the gains obtained by code and methodology improvements. The main outcomes from the first set of the simulations allowed to identify the needs in terms of code/model improvements, reduction of the conservatisms in the modelling assumptions and/or upgrade of the calculation chains including more detailed (mechanistic) computer codes. These improvements were provided in project work packages dedicated to R&D which result could be found in their dedicated deliverables [1], [2], [3], **Erreur ! Source du renvoi introuvable.**, [4], [5].

The results of the first set of simulations become the reference point for a second set of simulations of the same LOCA and SGTR transients performed after the improvements. In this report, reassessments of the calculation results using the improvements of the evaluation tools and methodologies are comparing with the first set of the simulations, mostly through the radiological consequence evaluations. Analyses of these comparisons in turn have served as a basis to formulate recommendations for a harmonization of the calculation methodologies and for a more realistic evaluation of the radiological consequences of these transients.

In the second set of the simulations, mostly the more realistic assumptions and approaches were used which can then be used for uncertainty evaluations. Uncertainty evaluations are difficult in such analyses especially considering the numerous calculation tools used in the calculation chains to provide the radiological consequences of the selected transients. In the project, a specific uncertainty evaluation methodology was however developed [13] [14], which one of the applications is presented at the end of this report.

A schematic view of the main project activities led for the LOCA and SGTR transient modelling and calculations is presented in the Figure 1 and Figure 2 below.

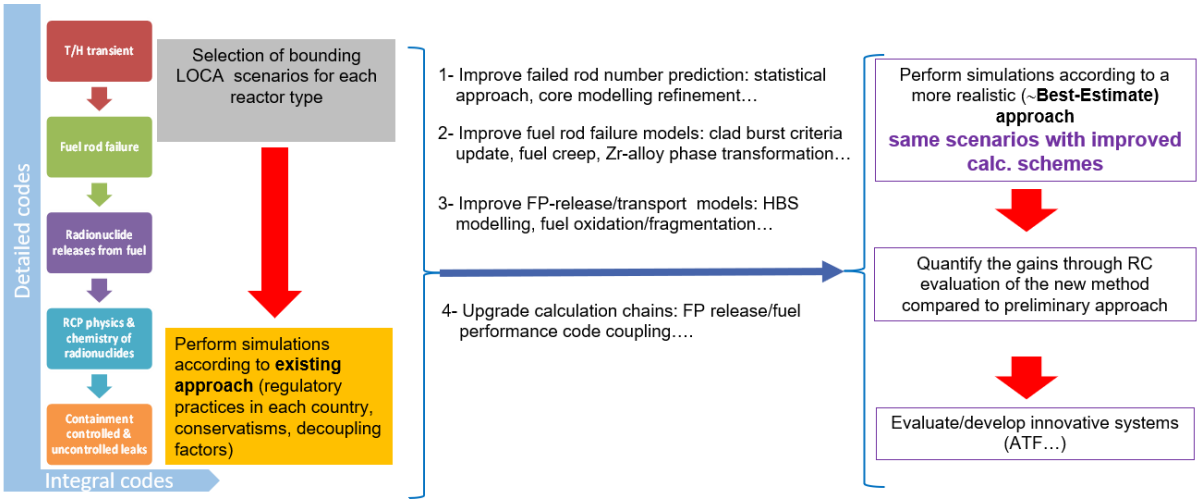

Figure 1. Illustration of the project activities for the LOCA transient.

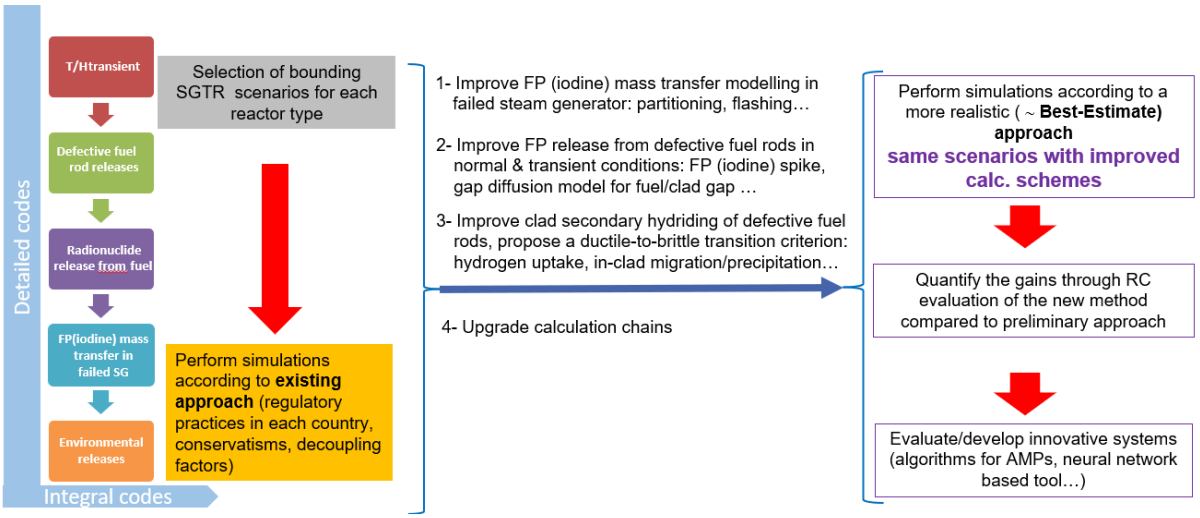

Figure 2. Illustration of the project activities for the SGTR transient.

2 First set of reactor test case simulations

The first runs of simulations of the reactor cases selected by the SEG have been performed using existing simulation tools of various details and at different scales in available calculation schemes in each partner's organization involved. These calculations have provided a large range of results that were post-processed and analysed and provided the environmental activity releases and associated short-term radiological consequences in the NPP vicinity. It covered a broad scope of LWR designs (BWR, EPR, PWR, VVER) as indicated in Table 1. In total 13 organizations participated in this work, with LEI as leading organization. Most of these organizations have provided LOCA and/or SGTR simulations for DBA and/or DEC-A conditions. The list of organizations involved, their analysed type of reactor, the chosen scenario and accidental conditions are presented in Table 1.

Organization	Type of reactor	LOCA		SGTR	
		DBA	DEC-A	DBA	DEC-A
ARB	VVER-440;	+	+	+	+
	VVER-1000	+	+	+	+
Bel V	PWR-1000	-	-	+	+
BOKU	PWR-1300,	-	-	+	+
	VVER-1000	-	-	+	+
CIEMAT	PWR-1000	-	-	+	+
ENEA	PWR-900	+	+	-	-
HZDR	PWR-Konvoi	+	+	-	-
IRSN	PWR-900	+	+	+	-
LEI	BWR-4	-	+	-	-
EK	VVER-440	+	-	+	-
SSTC-NRS	VVER-1000	+	+	+	+
TRACTEBEL	PWR-1000	-	-	+	+
UJV-NRI	VVER-1000	+	-	+	-
VTT	EPR-1600	+	-	-	-
	VVER-1000	-	+	-	-

Table 1. Partners participated in the first set of the simulations, type of reactors, accident scenarios and conditions.

2.1 Summary of analysed reactor types

As mentioned already in Table 1 different reactor types have been analysed.

- VVER type reactors have been analysed by 6 partners:
  - VVER -1000 was analysed by ARB, SSTC-NRS, UJV-NRI, BOKU and VTT. This is a 3000 MW_{th} and 1000 MW_e reactor with four primary loops, four MCPs and four horizontal SGs.
  - VVER-440 was analysed by ARB and EK. Both partners analysed the six-loop reactor with 2 turbines. However, EK analysed upgraded version of VVER-440 with 1485 MW_{th} and 500 MW_e while ARB analysed VVER-440 with 1375 MW_{th} and 440 MW_e
- 8 partners analysed PWR type reactors.
  - PWR–900 was analysed by IRSN and ENEA. This is a three-loop 2775 MW_{th} and 900 MW_e reactor.
  - PWR–1000 was analysed by TRACTEBEL, Bel V and CIEMAT. This is a three-loop 3000 MW_{th} reactor and 1000 MW_e reactor.
  - PWR-1300 was analysed by BOKU. This is a four-loop 3750 MW_{th} and 1300 MW_e reactor.
  - PWR Konvoi was analysed by HZDR. This is a four-loop 3950 MW_{th} and 1485 MW_e reactor.
  - EPR 3rd generation Pressurised Water Reactor analysed by VTT. This is a four-loop 4500 MW_{th} and 1660 MW_e power.
- 1 partner analysed a BWR reactor.
  - BWR-4 was analysed by LEI. This is a 2381 MW_{th} reactor with a Mark I containment and two recirculation loops.

Some partners used generic reactor models and other partners used real plant configuration. This explains why some information is marked as being confidential.

2.2 Summary of selected scenarios

Hereunder a summary of the different performed simulations (and their associated scenarios) is represented. Firstly, for the LOCA and secondly for the SGTR:

2.2.1 LOCA scenarios at DBA and DEC-A conditions

For almost all reactor types LOCA simulations have been performed. In collaboration with the SEG it was decided that no common specific scenario would be used for all partners since the purpose of the project is not benchmarking but comparing radiological consequences evaluated from initial and updated calculations. Therefore, all partners were free to use their own scenarios. For the DBA case, most of the partners were considered Large Break LOCA (LB LOCA), while IRSN and ENEA considered Intermediate Break LOCA (IB LOCA) for DBA and Small Break LOCA (SB LOCA) for DEC-A. ARB analysed different sizes of the break. For the LOCA scenarios, in order to have DEC-A conditions mostly one additional failure was considered. Hereunder the most important data of the different LOCA-scenarios are listed.

- VVER LOCA scenarios:
  - For VVER-1000 LOCA scenarios, the DBA and DEC-A conditions were modelled by ARB, SSTC-NRS, UJV-NRI and VTT. For DBA case, all partners assumed LB LOCA in cold leg and LOOP, no operator actions, conservative initial and boundary conditions. However, partners used different assumptions for operation/availability of the safety systems. ARB decided additionally to analyse different sizes of the break. UJV-NRI provided analysis only for DBA conditions. For DEC-A scenarios, ARB, SSTC-NRS decided to model the failure of the containment spray system, more realistic initial and boundary conditions were used for this analysis comparing to the DBA cases. VTT also used conservative initial and boundary conditions (aligned with other partners), but VTT model did not include containment and backpressure was fixed. ARB considers identical conservative sets of initial and boundary conditions for all LOCA scenarios within first and second set of the calculations to ensure a proper assessment of the impact of improved modelling of isotope behaviour on reducing radiological consequences.
  - The VVER-440 LOCA scenarios at DBA and DEC-A conditions were modelled by ARB and EK. ARB applied the same scenarios for DBA and DEC-A conditions as it is presented to VVER-1000. EK modelled only DBA conditions – guillotine break in the cold leg, no operator actions, conservative initial and boundary conditions. According to the standard DBA methodology, the worst single failure is considered, which in this case is the failure of one HA feeding into the upper plenum of the reactor. In addition, the coolant of the LPIS feeding into loop no. 4 is lost through the break.
- PWR LOCA scenarios:
  - DBA and DEC-A cases for PWR-900 were modelled by ENEA and IRSN. In the DBA scenario it was assumed a IB LOCA with a break of 16.3” in cold leg of loop 2 (without pressurizer) just downstream the primary pump; accident starts at nominal reactor power for ENEA case and with the reactor at 104% of nominal power in the IRSN case; LOOP is assumed at scram signal combined with the single failure of one over two emergency diesel generators. For DEC-A conditions a LOCA with a break of 4" in the hot leg (at primary vessel outlet) of the loop 2 (without pressurizer) was chosen by the two partners. Accident starts about 2 hours after an intermediate subcritical hot shutdown (at this time the reactor power is approximately 1% of the nominal one and primary pressure is around 70 bars); accumulators in this scenario were not available and delayed manual safety injection system has to be started by operators. ENEA used realistic initial and boundary conditions for both DBA & DEC-A scenarios while IRSN uses conservative ones for DBA and realistic for DEC-A
  - HZDR modelled LOCA scenario at DBA and DEC-A conditions for the PWR-Konvoi reactor. For both analyses it was assumed a double-ended guillotine break of cold leg loop 2 (loop connected to pressurizer) with the combination of LOOP. Regarding ECCS availability, single failure of one ECCS train was assumed, together with maintenance of one accumulator. For both calculations conservative initial and boundary conditions were used.

- VTT analysed LOCA DBA for EPR-1600. The work was not performed in the frame of R2CA project. However, in this project was presented a summary of work that have been done before and its main results. A double-ended break in a cold leg in combination of LOOP was analysed. Conservative initial and boundary conditions were used.

- BWR LOCA scenario for DEC-A conditions was analysed by LEI. For the scenario LB-LOCA, double-ended break of the main recirculation pipe for BWR-4 with delayed activation of LPCI system was assumed. Additionally, it was assumed that all ECCS, except LPCI, are not available after the start of accident. For calculations the realistic initial and boundary conditions were used.

2.2.2 SGTR scenarios at DBA and DEC-A conditions

SGTR simulations have been performed for all PWR designs. As for LOCA no common specific scenario was used by the partners. However, the chosen DBA scenarios correspond to condition IV accidents (limiting faults) of the Safety Analysis Report (SAR). For DEC-A scenarios, either it was chosen that one additional failure was considered (failure of another SG RV or SV: for VVER reactors for instance) or, as for PWRs for instance that, in addition, Main Steam Line Break occurs (MSLB) (from PSA studies).

- VVER SGTR scenarios:
  - For VVER-1000, the SGTR scenarios were modelled by ARB, BOKU, SSTC-NRS and UJV-NRI. ARB for DBA case assumed Steam Generator collector cover lift up (different diameters were analysed) and guillotine ruptures of SG tubes (it was assumed single, two and three ruptured tubes) with failure to close the BRU-A (Steam dump valve to-atmosphere) of affected SG after its opening. SSTC-NRS also assumed Steam Generator collector cover lift up for Dn100 mm. Both partners used conservative initial and boundary conditions for the analysis. BOKU and UJV-NRI assumed single SG tube rupture for DBA analysis with conservative conditions for UJV-NRI and realistic ones for BOKU. In the case of the SGTR analysis using DEC-A conditions BOKU and SSTC-NRS used additional failure - the BRU-A of the affected SG stuck open after the start of the accident. For ARB, a failure to close the SV SG, in addition to BRU-A, of the emergency SG after its opening was also assumed. All partners used nominal conditions. For DEC-A scenarios, BOKU assumed another case - double ended guillotine break of a SG tube in loop 4 with simultaneous MSLB in a non-isolable part of the steam line outside the containment.
  - For VVER-440, SGTR scenarios were modelled by ARB and EK. ARB applied almost the same scenarios as those described above for the VVER-1000 SGTR scenarios, for DBA and DEC-A conditions correspondingly, except that the single failure is assumed for the control SG SV of affected SG for the VVER-440 DBA case. For DEC-A scenarios, both BRU-A and control SG SV are assumed to be stuck open after the first opening and nominal conditions are assumed. EK modelled only DBA conditions – steam generator collector cover lift up together with 3 SG tube break with nominal conditions.
- PWR SGTR scenarios:
  - PWR-900 SGTR scenario at DBA conditions was modelled only by IRSN. For the DBA scenario, IRSN assumed a break of 1 SG tube on loop 2 (without PRZ) at the top of the U-bundle at full power together with the by-pass atmospheric steam Relief Valve (RV) of the failed SG blocked open after its first opening. No operator actions were considered, but 20 minutes after the transient onset automatic accident management procedures automatically triggered when specific thresholds are reached. Nominal conditions were used.
  - PWR – 1000 SGTR scenarios were analysed by Bel V, CIEMAT and TRACTEBEL. For the DBA case all partners decided to analyse a single U-tube double-ended break at full power at the top of the longest U-tube to enable a meaningful comparison of results. No operator actions were considered for 30 minutes, and the single failure related to a stuck open RV was applied on the RV of the affected SG. In the case of DEC-A conditions CIEMAT, Bel V and TRACTEBEL assumed 3

tubes, double-ended break at the bottom of the U-tube bundle on the cold leg side loop with PRZ (shortest tube) combined with MSLB outside containment before MSIV in case of TRACTEBEL and Bel V and after MSIV in the case of CIEMAT (isolable MSLB). Nominal conditions are assumed for the DEC-A case. For the DBA case, TRACTEBEL assumed conservative conditions while CIEMAT and Bel V assumed nominal conditions.

- PWR – 1300 SGTR scenarios at DBA and DEC-A conditions were modelled by BOKU. For the DBA conditions, double-ended break of 1 SG tube at top of the bundle was assumed. For DEC-A conditions, it is assumed an additional failure on the relief valve of the affected SG which is stuck open after first opening. In both DBA and DEC-A conditions, nominal conditions are assumed.

2.3 Summary of modelling methods and approaches

2.3.1 Modelling methods and approaches for LOCA scenarios

For the modelling of LOCA accidents and for the evaluation of their radiological consequences, it was needed to consider many phenomena and processes which are taking place in the reactor core (i.e. fuel rod bursts…), main reactor cooling circuit and containment (i.e. FP transport & physic-chemical behaviour…). These are then thermal hydraulic, thermo-mechanical and FP behaviour questions, which should be solved. However, to evaluate possible activities in the reactor cooling circuit, containment and environment it is needed to estimate the fission product releases during the accidental scenario and this product transfer from the burst fuel claddings to reactor cooling circuit, then to containment, and from there to the environment.
Different methodologies based on different modelling computer codes or process assessment methods were used by the R2CA partners for the simulation of the phenomena and processes occurring during LOCA accidents. R2CA partners indeed, based on their own experience, chose commonly used methods in their countries and existing modelling codes to simulate in an appropriate way their selected LOCA scenarios and to get main results of thermal hydraulic (core, primary circuit and containment) and fuel rod thermo-mechanical analysis as well as far as possible evaluation results of fission product release and transportation.
In general summarizing modelling approaches used by partners, it is possible to distinguish three types:

1. The thermal hydraulic, thermo-mechanical analyses were provided. Fission product transport and behaviour in the primary circuit and containment (whose releases from fuel were evaluated from the thermo-mechanical analysis) were also provided by computer codes. For these analyses, partners used complex modelling (coupled) computer codes.
2. Detailed thermal hydraulic and thermo-mechanical analyses were provided by computer codes. However, for the fission product release and behaviour it was made conservative assumptions.
3. The thermal hydraulic analyses were provided by modelling computer codes, but thermo-mechanical analyses were not provided. Instead of those, conservative assumptions – i.e. release from the fuel to the primary circuit of the entire contents of the gas gap at the beginning of the transient- were made. Considered such assumptions, the fission product behaviour was then simulated with varying degrees of details using computer codes.

Table 2 summarizes the main modelling computer codes and the approaches used for the analysis of the LOCA scenarios at DBA and DEC-A conditions. The parts marked in green colour are those that were changed/improved within the project by the involved partners. A summary of the improvements made by R2CA project partners is presented in Section 3.

Organization	Reactor type	Thermal hydraulics	Fuel rod thermal mechanics	FP transport and behaviour in primary circuit and containment
ARB	**VVER-440; VVER-1000;**	**ATHLET 3.2**	Not performed.	**COCOSYS 3.0** 100% of FP is released to containment.
EK	**VVER-440**	**ATHLET 1.1**	**FUROM-2.1.1** for fuel rod history. **FRAPTRAN-2.0** modified by EK	**CONTAIN** EK developed a methodology for the analysis of data. 100% of FP release to containment.
SSTC-NRS	**VVER-1000**	**RELAP5 Mod 3.2**	Not performed.	**MELCOR 2.2** 100% of FP release to containment.
UJV-NRI	**VVER-1000**	**ATHLET 3.1**	**TRANSURANUS**	**COCOSYS 2.4v4** 100% of FP release to containment. Containment design leak and ventilation systems
ENEA	**PWR-900**	**ASTEC 2.2.b**	**ASTEC 2.2.b**	**ASTEC 2.2.b**
HZDR	**PWR-Konvoi**	**ATHLET-CD 3.2**	**ATHLET-CD 3.2**	**ATHLET-CD 3.2** - FP release from fuel. 100% of FP release to containment, theoretical FP release to environment.
IRSN	**PWR-900**	**ASTEC 2.2**	**ASTEC 2.2**	**ASTEC 2.2**
VTT	**EPR-1600 (DBA conditions)**	**GENFLO, APROS**	**FRAPCON, FRAPTRAN-GENFLO**	Not performed.
	VVER-1000 (DEC-A conditions)	**GENFLO, APROS**	**FRAPCON, FRAPTRAN-GENFLO**	Not performed
LEI	**BWR-4**	**ASTEC 2.1.1.6**	**ASTEC 2.1.1.6**	**ASTEC 2.1.1.6**

Table 2. Modelling tools and modelling approaches used by partners for the first set of the LOCA analysis at DBA and DEC-A conditions.

2.3.2 Modelling methods and approaches for SGTR scenarios

For the modelling of SGTR accidents and for the evaluation of their radiological consequences, it is needed to consider many phenomena and processes taking place in the reactor core (i.e. FP spiking releases...), in main reactor cooling circuit, in the affected SG, (i.e. FP transport & behaviour) as well as in intact SGs. These are then not only thermal hydraulic questions, which should be solved but also physic-chemical ones. From the relatively low temperatures calculated in SGTR transients compared to LOCAs, fuel rod failures are not expected. To evaluate possible activities in the reactor cooling circuit, then in the affected SG and environment it is then needed, in addition to the primary circuit activity in normal operation conditions due to defective fuel rods and/or tramp uranium, to estimate fission product releases during the SGTR accident from leaking fuel rods and their transfer from the primary circuit, then to the affected SG, and from there to the environment. In general, leaking fuel rods have a primary defect but not simulated by the codes. On the other hand, fuel rod burst/failures can be modelled but doesn't occur in such scenarios.

There are different calculation methodologies using different modelling computer codes or process assessment methods for the evaluation of the phenomena and processes during SGTR accident. R2CA project partners, based

on their experience, chose methods and modelling codes to properly simulate SGTR scenarios including thermal hydraulic analysis, fission product releases from leaking fuel rods and their transportation to SGs. A common feature of these approaches is that, as already mentioned, there was no simulation of clad defect formation. In addition, none of the calculations considered the SG upper structures in their models.
In general summarizing modelling approaches used by partners it is possible to distinguish:

1. Different methods used for simulating the FP releases from defective fuel rods: either simple based-correlation models were used or assumptions (often based on NPP measurement feedbacks) for both primary circuit contamination in normal operation and transient conditions were considered.
2. Various levels of modelling for FP behaviour in the failed SG: either a detailed modelling of some or all the phenomena that could take place (i.e. flashing, atomization, partitioning….) was used or assumptions were used for FP distribution between the gaseous and liquid phases.

The list of FP considered also greatly differed from one partner to another. Some partners only considered I-131 while others considered a wide list of elements and isotopes mainly including noble gasses and volatile species.

Table 3 below, summarizes the main modelling computer codes and approaches used for the analyses of the SGTR scenarios at DBA and DEC-A conditions. The parts marked in green colour are those that were improved within the project. A summary of the improvements foreseen by R2CA project partners is presented in Section 3.

Organization	Type of reactor	Thermal hydraulics	FP transport and behaviour in primary circuit and steam generators
ARB	VVER-440; VVER-1000	ATHLET 3.2	ATHLET 3.2 + COCOSYS
EK	VVER-440	RELAP5 Mod 3.3	RING
SSTC-NRS	VVER-1000	RELAP5 Mod 3.2	Not performed. Assumed 100% release of FP from primary circuit to environment
UJV-NRI	VVER-1000	ATHLET 3.1	Conservative and simplified methodology developed by UJV-NRI
BOKU	VVER-1000; PWR1300	RELAP5-3D 4.0.3	RELAP5-3D 4.0.3
TRACTEBEL	PWR-1000	RELAPmod2.5 (for DBA case) MELCOR2.2 (for DEC-A case)	RELAPmod2.5 (for DBA case) MELCOR2.2 (for DEC-A case)
Bel V	PWR-1000	CATHARE2/V2.5_3/mod8.1	VBA-script
IRSN	PWR-900	ASTEC 2.2	ASTEC 2.2
CIEMAT	PWR-1000	MELCOR2.2	MELCOR2.2 – External functions

Table 3. Modelling tools and modelling approaches used by partners for the first set of the SGTR analysis at DBA and DEC-A conditions.

2.4 Main outcomes of reactor case simulations

In total 13 organizations participated in this work. These organizations have provided LOCA and/or SGTR simulations for VVER, PWR, EPR and BWR type reactors at DBA and/or DEC-A conditions.

2.4.1 LOCA calculation results

In total 9 partners analysed VVER (440 and 1000), PWR (900 and Konvoi), EPR-1600 and BWR-4 type reactors. Gained calculation results vary in wide range (Table 4 and Table 5). The calculated PCTs for the DBA case is varying from ~750 °C to ~1100 °C while for DEC-A case calculations the temperature varies from ~720 °C to ~2250 °C. Beyond the differences in scenarios, used simulation tools and their coupling schemes, the wide range of the received calculation results in terms of PCTs, number of fuel rod ruptures and activity released to the environment is due to many other factors, such as:

- Reactor types and their designs.
- Modelling approaches, such as core nodalization method, chosen models/correlations (i.e. for the cladding bursts).
- Individual assumptions for the initial parameters and conditions. Some partners used realistic initial conditions, however some others used conservative conditions (e.g. for DBA case some partners assumed initial reactor power higher than 100% in order to cover measurement uncertainties and set points of reactor protection system).
- Boundary conditions used for the calculations, for example HPIS and LPIS flowrate characteristics, design containment leakages and venting systems etc.
- The list of isotopes considered in the analyses and evaluations of the radiological consequences. Some partners used a long list of isotopes, while others considered only the five most important ones.

Some of the mentioned differences caused differences in PCTs calculated by partners and these differences were also reflected in other analysed parameters (thermo-mechanical analysis, number of failed rods, etc.).
Partners who provided thermo-mechanical analysis based on averaged fuel rod concept (i.e. when core was divided in concentric rings or averaged parameters were used for inherent groups) generally found, that there is no damage of fuel cladding in the case of analysed LOCA under DBA conditions and even in some cases under DEC-A conditions. For that reason, in some cases, several sensitivity calculations were performed, and the calculations, were penalized by using pessimistic conditions and hypotheses (for instance increasing the fuel rod linear heat rate, the initial reactor power, etc.) to meet the conditions of clad failures. In some calculations an average initial gap inventory was assumed for all the fuel rods and the gap content of the failed fuel rods during the LOCA transient was assumed to be released to the primary circuit. In other calculations, more conservative assumptions were used where the failure of all the core fuel rods was considered, and their corresponding gap content instantaneously released and transported to the containment or directly transferred to environment (in the case where the containment is not modelled) during the transient. This partly explains the wide range of predicted activity released into the environment, where the calculation results show that they are differing by 2 to 3 orders of magnitude for the VVER and PWR type reactors (for DBA cases). In addition, partners also considered different approaches for the activities releases into the environment from containment design leakages (unfiltered releases), considering or not the release from the auxiliary buildings too (filtered releases). Regarding the containment design leakages, most of the partners used simulation tools to calculate the release function in time considering the pressure difference between containment and environment while few others used conservative assumptions, for example considering the maximal containment design pressure for the calculation of FP release to environment.
Though the above listed differences in modelling approaches and assumptions could affect the range of the calculated integral activity released into the environment, several other factors played an important role. Indeed, the total activities released into the environment consists of the activities released into the environment carried by aerosols, together with liquid and gas releases depending on the assumptions made by partners (filtered or non-filtered releases, operation of venting system, etc.). Thus, they strongly depend on the calculated or assumed

containment inventory, on the FP distribution between the liquid and gaseous phases and for the iodine on whether chemistry is considered or not.
Activities released into the environment from liquid were always found small while activities released through aerosols were dependent on pressure, temperature, steam content in the containment, mass and energy of water, accident management strategies and other factors. As these aerosols are likely to condense onto containment surfaces and/or settle down to the containment sump, their calculated containment activity in the gas phase decreases and thus the activity likely to be released into the environment also decreases with time. Then, the main and more important contribution on the total activity release becomes the gaseous release through containment design leakage, which depends on the containment pressure but also whether the venting systems were considered or not. This activity release does not stop throughout the entire transient period under consideration but continuously decrease as the pressure in the containment is decreasing. Thus, it is important to consider a rather long time of calculation even if during the long-term phase, the activity increase in the environment is relatively low comparing to initial phase.

Reactor type	**Partner Used simulation tools/methods for initial inventory, T-H, T-M and FP.**	**Scenario (Initial event + failures)**	**Power[i] (% P_N)**	**PCT (°C)**	**Burst FA[ii] (%)**	**Activity in environment (Bq) at time (s)**
VVER 440	Partner ARB Initial inventory: Conservative data of the fuel designer, 4th year fuel cycle (EOC) T-H: ATHLET T-M: not performed FP: COCOSYS	DEGB in CL; LOOP Failure of DG-1	103.5	~1050	100[a]	~1.25 10^{14} at 80000
	Partner EK Initial inventory: ORIGEN code T-H: ATHLET T-M: FUROM and FRAPTRAN mod. EK FP: CONTAIN+EK methodology	DEGB in CL; 2/3 LPIS available	100	~900	100[a]	~9.5 10^{13} instant release
VVER 1000	Partner ARB Initial inventory: Conservative data of the fuel designer, 4th year fuel cycle (EOC) T-H, T-M, FP same as VVER 440	DEGB in CL; LOOP Failure of DG-1	104	~1100	100[a]	~1.9 10^{13} at 80000
	Partner SSTC-NRS Initial inventory: Fuel designer data, 4th year EOC. T-H: RELAP5 T-M: not performed. FP: MELCOR	DEGB in CL; LOOP Failure of DG-1	104	~880	100[a]	~2.04 10^{13} at 86400

	Partner UJV-NRI Initial inventory: Monte Carlo calculation T-H: ATHLET T-M: TRANSURANUS FP: COCOSYS	DEGB in CL; 3/4 HA available; 1/3 HPIS & LPIS available	104	~860	100[a]	~1.6 10^{11} at 60000
PWR 900	Partner IRSN Initial inventory: VESTA code, EOC, averaged inventory T-H, T-M, FP: ASTEC	IB in CL; LOOP Failure of ½ DG	104	~750	~33[c]	~3.5 10^{13} at 180000
PWR 900 Generic	Partner ENEA Initial inventory: provided by IRSN T-H, T-M, FP: ASTEC	IB in CL; LOOP Failure of ½ DG	100	~860	12.7[c]	6.13 10^{12} at 180000
PWR Konvoi	Partner HZDR Initial inventory: ATHLET-CD module (OREST/FIPISO) T-H, T-M, FP: ATHLET-CD	DEGB in CL; LOOP, 5/8 accus, 3/4 HPIS, 6/8 LPIS	106	~1050	10[a]	~5.84 10^{14} at 86400
EPR 1600	Partner VTT Initial inventory: CMS codes developed by Studsvik Scandpower. T-H: GENFLO, APROS T-M: FRAPTRAN-GENFLO FP: not performed	DEGB in CL; LOOP Delay of DG start	102	~900	1.4[c]	_

i: Operational power at beginning of the transient in % of nominal power P_N

ii: % of burst Fuel Assemblies: [a]: assumed & [c]: calculated

Table 4. LOCA analyzed scenarios and main calculation results (DBA conditions).

Reactor type	**Partner. Used simulation tools Main assumptions**	**Scenario (Initial event + failures)**	**Poweri (% PN)**	**PCT (°C)**	**Burst FA[ii] (%)**	**Activity in environment (Bq) at time (s)**
VVER 440	Partner ARB Initial inventory: Conservative data of the fuel designer, 4th year fuel cycle (EOC) T-H, T-M, FP: as DBA	DBA + failure of CSS	100	~720	100[a]	~1.2 10^{14} at 80000
VVER 1000	Partner ARB Initial inventory: Conservative data of the fuel designer, 4th year fuel cycle (EOC) T-H, T-M, FP: as DBA	DBA + failure of CSS	100	~890	100[a]	~5 10^{13} at 80000

	Partner - SSTC-NRS Initial inventory: Fuel designer data, 4th year EOC. T-H, T-M, FP: as DBA	DBA + failure of CSS	104	~880	100[a]	~6.1 10^{13} at 86400
	Partner VTT. Initial inventory: SSTC-NRS input file + Serpent code. T-H: APROS as DBA T-M: FRAPCON, FRAPTRAN-GENFLO FP: not performed.	DEGB in CL; LOOP Failure of CSS	104	~890 (APROS), ~650 (FRAPTRAN-GENFLO)	no damage[c]	–
PWR 900	Partner IRSN Initial inventory: VESTA code, EOC, averaged inventory T-H, T-M, FP: as DBA	SB in HL; no ECCS operating, Delay of SIS start by operators (33 min).	1	~1000	67[c]	~1.05 10^{14} at 172800
PWR 900 generic	Partner ENEA Initial inventory: provided by IRSN T-H, T-M, FP: as DBA	SB in HL; no ECCS operating, Delay of SIS start by operators (36.5 min).	1	~2250 at 2nd ring; between ~1250 and ~780 in others	67[c]	~8.6 10^{13} at 172800
PWR Konvoi	Partner HZDR Initial inventory: ATHLET-CD module (OREST/FIPISO) T-H, T-M, FP: as DBA	DBA Additional failure in ECCS	106	~1160	10[a]	~5.84 10^{14} at 86400
BWR-4 generic	Partner LEI Initial inventory: SCALE, averaged burnup T-H, T-M, FP: ASTEC	DEGB in main recirculation pipe; Failure of ECCS, except LPCI	100	~830	55[c]	~5.3 10^{14} at 200000

i: Operational power at beginning of the transient in % of nominal power P_N

ii: % of burst Fuel Assemblies: [a]: assumed & [c]: calculated

Table 5. LOCA analysed scenarios and main calculation results (DEC-A conditions).

2.4.2 SGTR calculation results

In total 9 partners analysed VVER (440 and 1000), PWR (900, 1000 and 1300) type reactors. SGTR transients under DBA and DEC-A conditions were simulated. However, the initiator was not the same for all partners (double-ended break of one or several SG tube(s) (with different break diameters) and SG cover lift-up in VVERs, double-ended break of one or several SG tube(s) on top or bottom U-tube bundle in PWRs. Due to some technology differences and provided individual assumptions for the initial and boundary conditions (additional single/multiple

failure(s), realistic/penalized parameters), individual results were slightly different from each other (Table 6 and Table 7):

- For PWR reactor types, the calculated integral activity released to the environment is in the range from ~1.166E+9 Bq to 4.7E+13 Bq. The lowest value was reached by CIEMAT PWR-1000 DEC-A analysis in which the secondary to the environment discharge is limited by considering an isolable SLBOUT.
- For PWR-1000 reactor type, DBA calculations, discrepancies between the partners are mainly explained by the differences on the iodine spiking model and intensity, but also due to FP transport assumptions with CIEMAT only modelling releases through gas phase.
- For PWR-1000 reactor type, DEC-A calculations, TRACTEBEL and Bel V results are close and are in the same order of magnitude. CIEMAT, however, calculated releases two order of magnitudes below the ones from TRACTEBEL and Bel V. Indeed, as CIEMAT modelled a transient with MSLB after MSIV, closure of the MSIV at the beginning of the transient stops the main part of the releases and only releases occurring at the SG PORV are accounted.
- For VVER-440 reactor type, the calculated integral activity released to the environment is in the range from ~2.0e+13 Bq to 4.6E+13 Bq depending on the initiator (break size)
- For VVER-1000 reactor type, the calculated integral activity released to the environment is in the range from ~3E+12 Bq to 2.23E+15 Bq.
- For VVER-1000 reactor type, DBA calculations, UJV-NRI provides a vastly greater source term in the environment due to the consideration of a conservative (conservative mass release and highest possible initial FP concentration) and simplified methodology. BOKU, on the contrary, provides a source term at least one order of magnitude lower than ARB and SSTC-NRS because the initial RCS activity is one order of magnitude lower for BOKU and also because BOKU assumed realistic initial conditions.
- For VVER-1000 reactor type, DEC-A and DBA calculations, both ARB and SSTC-NRS assumed that all RCS coolant activity released in the affected SG is released in the environment (for scenarios where liquid water is mostly released for ARB). For the other ARB scenarios, the total activity released into the environment depends on the amount of water released through the BRU-A, and SV SG for DEC-A. However, even if initial activity in the RCS is very close between both partners, ARB do not consider any dilution of the primary coolant due to water injection by the HPIS, LPIS pumps and from the HA ECCS. Therefore, in the end, releases calculated by ARB are 3 times higher than the releases calculated by SSTC-NRS. Besides, BOKU, for DEC-A, calculated a source term 7 times lower than SSTC-NRS because the initial RCS activity is one order of magnitude lower for BOKU.

The calculation results show that the results may differ up to 4 orders of magnitude. These differences could be caused by many reasons issued from differences in initiators, scenarios (considered failures), modelling, accident management procedures and assumptions for initial and boundary conditions. More especially, they can be explained by:

- The differences in the SGTR break sizes (for VVER only), the SIS duration, automatic procedures and operator actions, differences in the secondary to environment discharge capacities (considering or not) isolable/non isolable SLB, SG relief and SV discharge capacities, setpoints, failures, etc).
- Pressure evolution in the primary side which is impacted by considering (or not) some assumptions (reactor scram signals, decay heat, reactor coolant pumps trip, cooling of the primary by the intact SG Relief valves, HPIS and LPIS failure/flowrate characteristics, etc.).
- Pressure in the affected SG which is also impacted by considering (or not) some assumptions (additional isolable/non isolable SLB, failure of the affected SG RV and/or SV to close, failure of intact SG RV to open, closure of the MSIV, isolation of the main/auxiliary feedwater, etc.).
- Realistic/Conservative initial conditions, for example initial reactor power of 104% was assumed by some partners for DBA case.
- Difference in initial fuel inventory, FP gap inventory (i.e. fuel history), in the postulated number of defective fuel rods and/or in the primary circuit activity in normal operation conditions (some of the partners used for iodine the max. allowable activity form technical specifications as others used the data issued from reactor feedbacks.

- The list of isotopes considered: some partners calculated activity of only the most important isotopes in terms of activity (iodine, noble gases for instance), while others gave total activity values.
- Modelling (or not) of the spiking, pre-spiking, atomisation, flashing, pool-scrubbing and partitioning phenomena.
- Considering (or not) the deposition/filtration and dilution of isotopes in the primary circuit and in the affected SG.

Eventually, for PWR cases only, releases are higher for the DEC-A cases compared to the equivalent (reactor type and partner) DBA cases. When conservative assumptions on the releases into the environment are considered (for instance ARB and SSTC-NRS), there is not much difference on the releases between DBA and DEC-A cases. For other partners analysing PWRs (such as TRACTEBEL, BOKU and Bel V), the consideration of additional failure with the DEC-A case (MSLB before MSIV and 3 tubes SGTR instead of 1) induces more releases in the environment compared to the DBA case. For CIEMAT, because in the DEC-A case, the MSLB is isolated early in the accident and because the SG PORV is not stuck open (contrary to the DBA case), releases for DEC-A are smaller than for DBA.

Reactor type	**Partner. Used simulation tools Main assumptions**	**Scenario (Initial event + failures)**	**Cumulative steam/liquid water released in environment (tons)**	**Activity in environment (Bq) at time (s)**
VVER 440	Partner ARB T-H: ATHLET 3.2 FP: COCOSYS Realistic initial primary coolant activity + spiking from NPP measurements	SG SV stuck open +LOOP		
		SG collector lift up 107 mm	440 (mostly liquid)	4.6E+13 at 2500
		SG collector lift up 60 mm	300 (mostly liquid)	4.6E+13 at 3000
		SG collector lift up 40 mm	200 (80% liquid)	4.6E+13 at 10000
		SG collector lift up 20 mm	70 (70% steam)	3.1E+13 at 18000
		SGTR 1 tube (2*13.2 mm)	50 (steam only)	2.0E+13 at 18000
		SGTR 2 tubes (2*2*13.2 mm)	70 (70% steam)	3.4E+13 at 16000
		SGTR 3 tubes (3*2*13.2 mm)	110 (60% liquid)	4.3E+13 at 11000
	Partner EK TH: RELAP5 Mod 3.3 FP: RING Maximum allowable activity concentration in the RCS considered + spiking using conservative data derived for NPP measurements	Break of 3 SG tubes	0.218	3.1E+12 at 10000
		SG Collector cover opening (Equivalent to the break of a 37 mm diameter tube)	0.218	3.1E+12 at 10000
VVER 1000	Partner ARB TH: ATHLET 3.2 FP: COCOSYS	SG RV stuck open+LOOP		
		SG collector lift up 100 mm	760 (mostly liquid)	2.4E+14 at 5000
		SG collector lift up 60 mm	460 (80% liquid)	2.4E+14 at

	Same assumptions as for VVER 440			5000
		SG collector lift up 40 mm	300 (2/3 liquid)	2.4E+14 at 6000
		SG collector lift up 20 mm	130 (steam only)	1.1E+14 at 7000
		SGTR 1 tube (2*13 mm)	90 (steam only)	3.9E+13 at 9000
		SGTR 2 tubes (2*2*13 mm)	130 (steam only)	1.2E+14 at 9000
		SGTR 3 tubes (3*2*13 mm)	130 (steam only)	1.7E+14 at 7000
	Partner SSTC-NRS TH: RELAP5 Mod 3.2 FP: Not performed, Assumed Realistic initial primary coolant activity + spiking (same as ARB)	SG collector lift up (100 mm) LOOP+failure of 1/3 HPIS and LPIS, BRU-A1 closed after 15min	135 (steam 23%, water 77%)	7.79E+13 at 10000
	Partner UJV-NRI TH: ATHLET 3.1 FP: Maximum allowable activity concentration in the RCS considered	DEGB (1 tube) SG RV stuck open +LOOP	590	2.23E+15 at 22000
	Partner BOKU TH: RELAP5-3D 4.0.3 FP: Realistic initial primary coolant activity + spiking coming from international reference, only I131 considered	SG hot collector lift up (100 mm) +all active safety systems of one loop (HPIS, LPIS, Auxiliary Feedwater) are not available	178.8 steam/ 120.6 liq.	2.2E+10 at 4000
PWR 900	Partner IRSN TH, FP: ASTEC2.2 & MER Primary circuit activity in normal operations & transient conditions from French NPP measurement feedbacks considered for primary contamination and spike, noble gases I, Cs mainly considered.	1 tube break, top of U-tube bundle Failed SG RV blocked open after first opening (closed after 50 minutes)	188 (mostly steam)	4.7E+13 through gaseous pathway 3.3E+10 through liquid pathway from failed SG at 3240 seconds
PWR 1000	Partner TRACTEBEL TH, FP: RELAP5 Mod 2.5 Normalized initial activity contamination in the RCS +	DEGB (1 tube) SG RV stuck open	105	2.18E+10 at 3250

	spiking (confidential model), only I131 considered.			
	Partner Bel V TH: CATHARE2/V2.5_3/mod8.1 FP: VBA script Maximum allowable activity concentration in the RCS from the technical specifications considered + spiking from utility experience, only I131 considered.	DEGB (1 tube) SG RV stuck open	~95-100	1.90E+11 at 5000
	Partner CIEMAT TH, FP: MELCOR2.2 Maximum allowable activity concentration in the RCS from the technical specifications considered + conservative model of spiking	DEGB (1 tube) SG RV stuck open (closed after 30 minutes)	74.76	1.50E+9 at 1800
PWR 1300	Partner BOKU TH: RELAP5-3D 4.0.3 FP: Same as VVER	DEGB (1 tube) Failure of 2/4 HPIS/LPIS pumps and 2/4 EFW	171.7 steam/4. liq.	1.0E+10 at 8000

Table 6. SGTR analysed scenarios and main calculation results (DBA conditions).

Reactor type	**Partner. Used simulation tools Main assumptions**	**Scenario (Initial event + failures)**	**Cumulative steam/liquid water released in environment (tons)**	**Activity in environment (Bq) at time (s)**
VVER 440	Partner ARB TH: ATHLET 3.2 FP: COCOSYS Assumptions: same as DBA	SG SV+ RV stuck open +LOOP		
		SG collector lift up 107 mm	450 (mostly liquid)	4.6E+13 at 5000
		SG collector lift up 60 mm	330 (mostly liquid)	4.6E+13 at 6000
		SG collector lift up 40 mm	190 (80% liquid)	4.6E+13 at 10000
		SG collector lift up 20 mm	80 (70% steam)	3.1E+13 at 16000
		SGTR 1 tube (2*13.2 mm)	60 (steam only)	2.0E+13 at 16000
		SGTR 2 tubes (2*2*13.2 mm)	85 (70% steam)	3.4E+13 at 16000
		SGTR 3 tubes (3*2*13.2 mm)	100 (55% liquid)	4.4E+13 at 12000
VVER 1000	Partner ARB TH: ATHLET 3.2	SG RV + SV stuck open +LOOP		

Reactor type	Partner. Used simulation tools Main assumptions	Scenario (Initial event + failures)	Cumulative steam/liquid water released in environment (tons)	Activity in environment (Bq) at time (s)
	FP: COCOSYS Assumptions: same as DBA/VVER-440	SG collector lift up 100 mm	850 (90% liquid)	2.4E+14 at 5000
		SG collector lift up 60 mm	470 (80% liquid)	2.4E+14 at 7000
		SG collector lift up 40 mm	320 (60% liquid)	2.4E+14 at 7000
		SG collector lift up 20 mm	130 (steam only)	1.1E+14 at 7000
		SGTR 1 tube (2*13 mm)	90 (steam only)	4.0E+13 at 8000
		SGTR 2 tubes (2*2*13 mm)	140 (steam only)	1.2E+14 at 8000
		SGTR 3 tubes (3*2*13 mm)	140 (steam only)	1.7E+14 at 7000
	Partner SSTC-NRS TH: RELAP5 Mod 3.2 FP: Not performed, Assumptions: same as DBA	SG collector lift up (100 mm)+BRU-A1 stuck open +LOOP +failure of 1/3HPIS/LPIS	490 (steam 20%, water 80%)	7.79E+13 at 9000
	Partner BOKU TH: RELAP5-3D 4.0.3 FP: same as DBA	SGTR + MSLB+Failure of HPIS	283.4 steam/1.3 liq.	1.6E+10 at 40000
		SG hot collector lift up (100 mm) +SG RV stuck open+Failure of LPIS	145.9 steam/445.2 liq.	2.7E+12 at 4250
PWR 1000	Partner TRACTEBEL TH, FP: MELCOR2.2 Assumptions: same as DBA but all set of FP considered	DEGB (3 tubes) and simultaneous SLB out of containment (non-isolable) +LOOP	170 steam/130 liquid	2.19E+11 molecular iodine 1.09E+11 Noble gases 6.90E+11 in total at 4300
	Partner Bel V TH: CATHARE2 V2.5_3/mod8.1 FP: VBA script Assumptions: as DBA	DEGB (3 tubes) and simultaneous SLB out of containment (non-isolable) +LOOP	170 steam/130 liquid	5.0E+11 at 5000
	Partner CIEMAT TH, FP: MELCOR2.2 Assumptions: as DBA	DEGB (3 tubes) and simultaneous isolable SLB+LOOP	4.0	6.0E+8 at 3000
PWR 1300	Partner BOKU TH: RELAP5-3D 4.0.3 FP: Assumptions: as DBA	DEGB (1 tube) +SG RV stuck open +Failure of LPIS/EFW of affected SG	385.5 steam/2.9 liq.	3.0E+11 at 20000

Table 7. SGTR analysed scenarios and main calculation results (DEC-A conditions).

2.5 Main remarks and needed improvements

The initial set of calculation results enabled the identification of areas where enhancements in simulation tools and modelling approaches could be made. This will improve the estimation of environmental releases during evaluated transients, subsequently refining the decision-making processes. Improvements, which were made during the project can be roughly divided into four main categories:

1. Improvements of plant models (i.e. by updating approach of core modelling, upgrading nodalization, etc.).
2. Improvements of calculation chains and methodologies (i.e. by coupling of more mechanistic simulation tools, using statistical approaches for evaluating the number of fuel clad bursts, etc.).
3. Improvement of computational models at different levels of details (i.e. by developing new cladding burst models better corresponding to the experimental data, by refining clad burst criteria, including user-driven correlations (like iodine spiking modelling).
4. Developments/improvements of mechanistic modelling for a detailed modelling of important processes (i.e. fuel rod clad deformation and rupture, clad secondary hydriding, high burn-up structure growth and associated FP releases, FP releases from fuel rod gaps, atomisation, flashing processes in failed SG).

3 Reassessment (second set) of reactor test case simulations

The second set of simulations of the reactor cases were performed using improvements which is shortly described in the sections below. Simulations were performed using the same scenarios, which were selected by the SEG and were performed in the first set of the calculations. This was done with the purpose to compare calculation results of the first and second set of calculations and to determine through the RC evaluations the benefits of improvements, which were made during the project.
In the second set of calculations, the same group of organizations participated (in total 13 organizations). These organizations provided reassessments (second set) of reactor test case simulations and comparisons to first set of results. All first set calculations (Table 1) were reassessed with some exceptions:

- For DBA case, SGTR scenario in PWR-1000 TRACTEBEL did not foresee any improvement to the calculation scheme or modelling because it was already considered as sufficiently close to state-of-the-art.
- For DEC-A case, LOCA scenario in VVER-1000 (VTT) and Konvoi (HZDR). VTT provided FRAPTRAN simulations done in first set did not show any fuel failures for the VVER-1000 DEC-A scenario studied and therefore those simulations were not repeated in the second set of calculations. HZDR improved the calculation scheme and modelled the core in a very detailed manner, which increased calculation time very significantly. Thus, no more computational resources were available for reassessment of the DEC-A scenario.

3.1 Improved simulation approaches

As already mentioned, the results of the first set of simulations served as a reference point for a second set of simulations of the same LOCA and SGTR transients. First set of the calculations indicated needs of the improvements to reduce the conservatisms used in the initial calculation results. In this paragraph are presented improvements provided by each partner to reduce these conservatisms in terms of model/correlation improvements and/or developments. The improvements made were of two kinds:

1. Modelling improvements. For LOCA transient calculations, partners improved thermomechanical models for clad ballooning and burst, and new clad burst criteria were built. In addition, core nodalization was improved (made in more details or reorganized based on best practice and results of parametric analysis). For SGTR transient calculations partners dedicated improvements on the fission product modelling: initial

primary contamination and spiking, dilution in RCS, transport, scrubbing, partitioning, atomisation, speciation etc. Partners also improved their thermo-hydraulic model using refined model for the relief/safety valves of the SG or by applying enhanced EOPs.

2. Improvements in the calculation chains. Detailed (mechanistic) computer codes were involved in the partner's calculation chain as a support of less detailed codes for most of the part. For LOCA transient calculations, detailed codes were used to reflect the processes in the fuel during the transient. As well as coupling of T-H and T-M models to have more detailed prescription of the processes during the transient at the subchannel level. For SGTR transient calculations, detailed codes were used for spiking, FP transport and dilution thanks to CVCS operation.

Some of the partners used different calculation methodologies comparing to what was used in the first set of the calculations.

3.1.1 LOCA calculations

VVER-440 DBA case. Calculations were provided by ARB and EK.

- ARB improved the methodology for assessment of the activity release from primary circuit to the containment. More realistic simulation of the behaviour of radionuclides in the coolant of the primary circuit were provided comparing to the first set of the calculation where very conservative assumptions (instantaneous releases of 100% of the gap content from the whole core) were made. To do so, the BORON model of the ATHLET code which simulates the transport, mixing, dilution and deposition of equivalent particles of isotopes was used. A thermomechanical criterion for the release of gas gap activity was also considered. The release fraction of gas gap activity, in relation to the total content, was indirectly estimated. This estimation was achieved through an analytical evaluation of the maximum temperature criterion for the fuel rod cladding. Detailed modelling of the core's energy release non-uniformity using the ATHLET code facilitated this process. A more detailed particle size class spectrum was also considered in the containment model of COCOSYS code.
- EK implemented a new cladding failure criterion in FRAPTRAN code, and the failure strains were corrected through re-assessments of some experiments included in the database for E110 ballooning and burst. The parameters of plastic deformation of the code FRAPTRAN were then refitted using the new criterion and considering the corrected failure strain data. The failure strain is the average hoop strain of the cladding at the middle of the burst. Fitting the parameters of the plastic deformation using this strain means that the code calculations will give best-estimate results on the failure time and pressure with this failure limit. The uncertainty of the measurements was also considered, and a lower strain value was used for the evaluation of the failed rod number. Applying this new modelling resulted in reducing the conservatism used in the first set of calculation where 100% of fuel rod bursts were assumed.

VVER-440 DEC-A case. Calculations were provided by ARB. The same improvements were provided for DBA case calculations.

VVER-1000 DBA case. Calculations were provided by ARB, SSTC-NRS and UJV-NRI.

- ARB make the same improvements as for the VVER-440 DBA case.
- SSTC-NRS improved the core model in RELAP5 code. In addition, the calculation chain was improved. The core model in RELAP5 code was changed to represent the different fuel type groups based on the heat generated. The division of fuel pins in the core depending on the fuel pin energy ratio Kr was chosen for the start of cycle. It was done in the same model because preliminary analyses have shown that sequential calculations with one hot channel with different heat load can give deviations in sequence behaviour thus slightly changing the TH conditions outside the fuel. The new multichannel core model thus allowed to analyse all fuel groups behaviour at the same time.

The resulting data on the cladding temperatures and outside TH conditions were transferred to the fuel thermo-mechanical code TRANSURANUS to calculate the cladding behaviour. The number of ruptured fuel pins was then estimated based on the pin distribution. Conservatively assumed, if no fuel pins ruptured in the analysis the upper fuel pins group was assumed to be ruptured (corresponding to 1856 fuel pins) and the corresponding amount of gap activity was used for the FP and activity release analysis. The MELCOR code was then used for analysis of FP transport and behaviour in the containment.

- UJV-NRI used the same calculation chain as in initial calculations and provided improvements only for the containment part. The existing iodine dry paint deposition model was fine tuned to the Ameron Amerlock paint, which is present in the Temelin VVER-1000/V-320 NPP containment. Several minor improvements were also done within the model to improve modelling of heat structures and ventilation systems. Significant improvements were done for the initial and boundary conditions through extensive best estimate and sensitivity study.
  In the calculations, the fission product transport was conducted in the containment only with limited relation to previous steps. Two sources of fission products were considered: one from the primary coolant and the second one from the fuel. For the coolant inventory, it was assumed that the concentration of all fission products reaches the highest possible concentration including iodine spiking. The timing of this release was considered to start at t = 0 s and to ends at 12.22 s. Injection of the isotopes in the containment was done both to the water and gas phase, where the distinguishment between both phases was based on the ratio of primary coolant phases (steam, water) through the break. The in-containment source term was defined in accordance to R.G. 1.183, i.e. chemical composition, timing of the release and fraction of released FPs from fuels rods. The number of the failed fuel rods was based on statistical simulations conducted with TRANSURANUS, where the proposed 33 % of failed fuel rods provide a realistic envelope still keeping appropriate level of conservatism.

VVER-1000 DEC-A case. Calculations were provided by ARB and SSTC-NRS.

- ARB make the same improvements as for the DBA case.
- SSTC-NRS make the same improvements as for the DBA case.

PWR-900 DBA case. Calculations were provided by IRSN and ENEA.

- IRSN proposed a specific methodology able to predict the number of failed rods more accurately during a LOCA and the associated FP activity releases into the environment. This methodology is based on the DRACCAR simulation tool and the newly developed FORECAST (FOster the REactor Coolant Accident and Source Term) calculation chain interfacing the ASTEC FP modules with DRACCAR. The improvements of the modelling of clad burst failure models were also performed within the project where several models were embedded in the DRACCAR code.
- ENEA used the same simulation tool as in the first set of reactor calculations but with a new modelling approach for the reactor core. A more detailed model was developed by defining a higher number of representative rods to simulate the FAs contained in each radial fluid channels. With collaboration of IRSN new fuel cladding burst models/criteria (based on IRSN made reassessment of cladding burst criteria in the frame of this project) implemented in ASTEC code were also used. In the updated calculation, a recently implemented model for clad burst (namely the BE-exponential model) was used instead of the EDGAR model together with the maximum allowed hoop strain (25%).

PWR-900 DEC-A case. Calculations were provided by IRSN and ENEA.

- IRSN used same improvements as for DBA case.
- ENEA used the same improvements as for DBA case, but the maximum allowed hoop strain has been set to 40% (default value of the code) as in first set of calculations.

PWR-Konvoj DBA case Calculations were provided by HZDR. The second set of the calculations were performed with a developer's version of the ATHLET-CD code (similar to the official release of version 3.3). Some of the

modifications in the code were provided to extend some computational limits and disable some of the calculation modules, which are not used in the calculation (e.g. melting of core material). This allowed to decrease the computational times. A new core modelling approach was developed coupling a 3D thermal hydraulic model of the RPV with the fuel rod model of ATHLET-CD and allowing fuel rod model feedback to the thermal-hydraulic model. Core was modelled by 772 representative fuel rods (4 representative rods per fuel assembly). Four different calculations varying the rod internal pressure and the power axial profile were provided. Compared to the first set of calculations where 10% of the fuel rods were assumed to be failed, in the second set of calculations, the failed fuel rod fraction has been calculated dependent on the local thermal-hydraulic (local coolant mass flow rate, heat transfer coefficients, etc.) and local rod conditions (power distribution, rod internal pressure, material properties, etc.). The code still has several limitations. One significant limitation is that only one initial value for rod internal pressure can be defined (for cold state conditions), which is applied for the whole core. In the plant, rod internal pressure depends on the amount of gas substance accumulated in the fuel rod gap (which increases with increasing burn-up). Therefore, for each scenario two limiting case have been calculated, one with low initial value and one with conservatively high rod internal pressure. As a result, a range is estimated for the failed rod fraction.

EPR-1600 DBA case. Calculations were provided by VTT. The chain of simulations codes was modified by replacing CASMO with Serpent for the generation of cross section libraries for Apros. This change facilitated the use of new software tools developed within VTT's new reactor simulation framework called Kraken. GRS's SUSA uncertainty and sensitivity analysis software was also replaced by in-house sampling tools that make use of open-source scripts. New cladding creep and phase transformation laws as well as new fuel clad failure criteria (based on IRSN new models) were implemented in FRAPTRAN code.

BWR DEC-A case. Calculations were provided by LEI. The same calculation chain as for the first set of calculations was used. However, additionally the TRANSURANUS code was used to verify ASTEC calculation results. Uncertainty and sensitivity analysis was applied for TRANSURANUS calculation results to evaluate result uncertainty. Based on the TRANSURANUS calculation results, the ASTEC nodalization of BWR active core was modified. Different relative power distributions across the modelled concentric rings were provided.

All these improvements are summarized in the table below and further detailed in the following sections.

Partner	Applied calculation chain	Modelling improvements
ARB	Calculation chain was improved. An analytical approach in combination with a more detailed fuel model for the ATHLET code was used to estimate FP release.	Combined analytical and calculation (ATHLET code) assessment of FP activity release. Equivalent modelling of isotopes transport from primary circuit into containment with using of the ATHLET BORON model. More accuracy modelling of isotopes transport in containment (COCOSYS code).
EK	/	New criteria for clad burst strain and improvements of plastic deformation model in FRAPTRAN code.
SSTC-NRS	Calculation chain was improved. TRANSURANUS code was used to calculate the cladding behaviour. The MELCOR code is used for analysis of FP transport and behaviour in the containment.	Improved core model in RELAP5 code.

UJV-NRI	/	Improvement of the FP activity transfer with the use of a new methodology and computational approach.
IRSN	Improvement of the calculation chain using the DRACCAR code and development of the FORECAST chain	Improvements of clad burst failure models further embedded in DRACCAR code.
ENEA	/	With collaboration of IRSN new fuel cladding burst criteria implemented in ASTEC code. New modelling approach for the reactor core.
HZDR	New version of ATHLET-CD (developer version based on version 3.3)	• New 3D modelling approach for the reactor core (including 3D thermal-hydraulic model and significantly larger number of representative fuel rods) • Application of 3D power distribution derived from core simulator results, • Application of alternative creep correlation Source term evaluation on the basis of FP isotopes
VTT	Modelling approach was changed. CASMO was replaced by Serpent code for generating cross section libraries for Apros code.	New fuel clad failure criteria implemented in FRAPTRAN code based on IRSN new developed criteria.
LEI	TRANSURANUS code was used to verify ASTEC calculation results.	New modelling approach for the reactor core.

Table 8. Improvements made in the second set of calculations for LOCA transients.

3.1.2 SGTR calculations

VVER-440 DBA case. Calculations were provided by ARB and EK.

- ARB improved their calculation chain by using the BORON model for the ATHLET code which simulates the transport, mixing, dilution and deposition of equivalent particles of isotopes. ARB also modified the DRIFT FLUX model for ATHLET code to estimate fluid (liquid, vapor or liquid-vapor mixture) discharge more realistically through steam dump valves of secondary circuit (SG SV or BRU A). Several sensitivities on the BORON model or the DRIFT FLUX model were studied.
- EK improved their spiking model with the use of the RING code. The new RING calculations used refitted data based on new NPP measurements for the power, pressure and boric acid histories and provide different results for the two selected scenarios. The new spiking model allowed for time-dependent simulation of transient conditions, the sensitivity to simulated scenarios and is also able to model Cs-134 and CS-137 species in addition to iodine.
  Additionally, EK also updated their initial primary coolant activity for other species than iodine or caesium, taking into account other fission products, transuranium elements, corrosion and activation products. Most recent data were now used to assess the initial primary coolant activity and as the NPP fuel cycle has been extended to 15 months, new core inventory was also considered. In the first set of calculations, it was supposed that maximum 1% of fission products can be released from the fuel pellets. In reassessment calculations, thanks to new NPP data, this limit was increased to 2% to better simulate

high burnup fuel. In the end, 87 isotopes are now considered compared to 55 for the first set of calculations.

VVER-440 DEC A case. Calculations were provided by ARB.

- ARB made the same improvements as for the DBA case.

VVER-1000 DBA case. Calculations were provided by ARB, SSTC-NRS, BOKU and UJV-NRI.

- ARB made the same improvements as for the VVER-440 DBA case.
- SSTC NRS improved the modelling of the RCS coolant dilution and FP transport. The overall approach of activity transport was based on tracing the RCS water dimensionless concentration via RELAP5 code boron tracing model (boron in the model plays role of the tracer). This allowed to account for the dilution and mixing in RCS (including fresh ECCS water with tracer concentration) and SG volume. SSTC NRS implemented several transport equations in RELAP code via control variables.
- UJV-NRI improved their activity transport model with the use of a new methodology and computational/analytical approach that have been developed within the project [12]. The proposed approach distinguished between two groups of fission products. The first group was represented by noble gases. The second group represented other fission products like iodine or caesium. The newly developed computational tool handled140 isotopes which are relevant for further radiological consequence analysis by JRODOS code.
- BOKU improved and developed their own iodine spiking model based on empirical data found in the literature. Their model was extended by not only considering power as a variable but also current position (amount of days) of the fuel cycle as a proxy variable (see more details in [8][9]). In the calculation chain a postprocessing function was also included, which improve the fission product transport simulation. This postprocessing function considered the clean-up system (Chemical and Volume Control System) of the RCS and the pool scrubbing effect (see more details in [9]).

VVER-1000 DEC A case. Calculations were provided by ARB, SSTC-NRS and BOKU.

- ARB made the same improvements as for the VVER-440 DBA case.
- SSTC-NRS made the same improvements as for the DBA case.
- BOKU made the same improvements as for the DBA case.

PWR-1000 DBA case. Calculations were provided by Bel V and CIEMAT.

- CIEMAT used the same calculation chain as in the first set of calculations. In the reassessment of the DBA simulation two major improvements were included. First, to reduce the conservatism in iodine spiking modelling. Given that the in-code models in MELCOR 2.2 (CORSOR-Booth) should not be applied in the conditions prevailing during iodine spike in a SGTR scenario, an external MELCOR function was built to model it. The enhanced-diffusional release during reactor shutdown and any forced-convective release driven by temperature and pressure changes, were considered to estimate the iodine release rate [11]. The second improvement referred to iodine transport from primary-to-secondary side of the failed SG through the break. By using the capabilities and models in MELCOR, several mechanisms have been considered: RCS water flashing, atomization and partition between liquid and vapor states. Finally, the iodine gas accumulated in the failed SG gas phase was considered to be carried by steam into the environment (the retention on the SG upper structures was not considered).
- Bel V improved their calculation chain with the use of the CATHARE transport model of radionuclides. This feature allowed specifying the initial Iodine 131 concentration in the primary side and a better representation of the fuel radioactivity release following the spiking phenomenon. The improvement also lied in a more accurate assessment of transported radionuclide from the primary to the secondary side.

PWR-1000 DEC A case. Calculations were provided by TRACTEBEL, Bel V and CIEMAT.

- CIEMAT enhancements for DEC A were the same as the ones described for DBA.
- Bel V enhancements for DEC A were the same as the ones described for DBA.
- TRACTEBEL used the same calculation chain as in the first set of calculations, except that the new version of MELCOR 2.2 (2.2.18019 instead of 2.2.9541) was used. In the reassessment of the DEC-A calculation, TRACTEBEL improved their iodine partitioning model in the SG by considering the temperature effect on the partitioning coefficient instead of the constant coefficient of 100 in the first set of calculations. Then, in a second step, the iodine partitioning model has been further improved by considering the model dependence on evaporating conditions based on SISYPHE experiments [15]. The new model should speed up mass transfer kinetics from the liquid to the gas.
  Furthermore, in an effort to reduce the radiological consequences, new EOPs for operator's actions have been considered speeding up the implementation of important actions. These actions concerned the stop of the HPSI pumps as soon as possible to limit the flowrate inside the RCS and thus at the SGTR break. Furthermore, depressurization of the primary circuit is included to reduce the SGTR flowrate but also to depressurize RCS as fast as possible in order to reach pressure equilibrium between primary and secondary and cancellation of the break-flow.

PWR-1300 DBA case. Calculations were provided by BOKU. The same improvements were provided as for VVER type rector calculations.

PWR-1300 DEC-A case. Calculations were provided by BOKU. The same improvements were provided as for VVER type rector calculations.

PWR 900 DBA case: Calculations were provided by IRSN. A new calculation chain was provided using the SAFARI module and the DROPLET model of the ASTEC code along with the thermohydraulic module of ASTEC (CESAR) already used in the first set of calculations. This allowed to better account for the FP activity transfer in the primary circuit and in the failed steam generator. More especially thanks to the droplet model, the thermal/mechanical fragmentation of the under-relaxed jet at the SG tube rupture due to flashing could be calculated and the corresponding iodine transfer from the liquid to the gaseous phase estimated. Others ASTEC modules were also used and especially SOPHAEROS to calculate the FP speciation in the primary circuit of which iodine speciation is then used to evaluate its flashing rate at the break.
These improvements are summarized below in Table 9.

Partner.	Applied calculation chain	Modelling improvements
ARB	ATHLET 3.2 + COCOSYS (no improvement in the 2nd set of calculations)	Use of the BORON (for dilution) and DRIFT FLUX models for the ATHLET code.
EK	RELAP5 Mod 3.3 / Updated version of the RING code to simulate spiking phenomenon for I and Cs	Update of primary initial contamination for other isotopes not impacted by spiking. Updated correlations for Cs and I spiking.
SSTC-NRS	RELAP5 Mod 3.2 (no improvement in the 2nd set of calculations)	Improvement of the RCS coolant dilution and FP transport.
UJV-NRI	ATHLET 3.1 / Analytical new calculation methodology	Improvement of the FP activity transfer with the use of a new methodology and computational approach.

BOKU	RELAP5-3D 4.0.3 (no improvement in the 2nd set of calculations)	Improvement of the radiological model (iodine spiking and transport for I131). Dilution and pool scrubbing taken into account.
IRSN	Use if a new calculation chain using the SAFARI, SOPHAEROS modules and DROPLET model of ASTEC code for FP activity transfer	FP speciation in primary circuit and iodine activity transfer from primary to secondary during the flashing process, jet atomization in droplets at the break location.
TRACTEBEL	MELCOR2.2 (no improvement in the 2nd set of calculations)	Improvement of the iodine partitioning model in the SG with the consideration of the dependence on temperature and of evaporating conditions based on SISYPHE experiments. Consideration of new EOPs for operator's actions to depressurize RCS as fast as possible.
Bel V	Use of the CATHARE transport model of radionuclides.	A more accurate assessment of transported radionuclide from the primary to the secondary side. Improvement of the iodine spiking model.
CIEMAT	MELCOR2.2 (no improvement in the 2nd set of calculations)	Improvement of the iodine spiking model through the development of a, analytical external function Improvements of the iodine transport from the RCS to environment (including flashing, atomization and partition between liquid and vapor states)

Table 9. Improvements of the simulation approach in the 2nd set of calculations for SGTR transients.

3.2 Results of reassessment (second set) calculations

Results of the reassessment (second set) calculations are provided in this section. The main improvements made by partners are presented in this section, as well as the main calculation results:

- For LOCA scenarios, peak cladding temperature, percentage of the fuel rod burst in all core and calculated activity in the environment.
- For SGTR scenarios, cumulative steam/liquid water released in environment as well as calculated activity in the environment.

3.2.1 LOCA calculations

VVER-440 DBA case. Calculations were provided by ARB and EK.

- ARB studied several scenarios for DBA case (same as first set of calculations): a) guillotine rupture of cooling loop 4 at the reactor entrance with an equivalent size 2×500 mm; b) rupture of cooling loop 4 at the reactor entrance with an equivalent size 250 mm; c) rupture of cooling loop 4 at the reactor entrance with an equivalent size 100 mm; d) rupture of cooling loop 4 at the reactor entrance with an equivalent size 50 mm. The second set (with applied improvements) of the calculation results showed very similar thermal hydraulic results, the biggest different is regarding FP release and its transportation. The NPP model for the ATHLET code, for both sets of calculations showed that the entire activity of the primary circuit into the containment is released due to the rupture, which is characteristic of all considered

scenarios of large and medium leakages with significant dynamics of coolant loss. Improved modelling of the behaviour and transport of isotopes in the coolant system of the primary circuit within the second set of calculations provided, a significant reduction of the activity released to the primary coolant and, accordingly, its emission into the containment, due to considering thermomechanical criteria (strain criterion) that leads to a lower number of failed rods compared to the assumption of 100% in the first set of calculations. In the case of guillotine rupture, it was considered deduced around ~0.3% burst fuel rods in the core. Together with the fission product releases from the fuel rod (failed fuel rod gap inventory), the activity in the primary circuit was calculated considering the dilution. Calculated activity in the environment is ~1.8 10^{11} Bq at 80000 s for the double ended guillotine break. For other analysed break sizes, as no clad bursts were predicted only the primary circuit contamination was considered. Calculated activity in the environment for 250 mm break is ~1.85 10^{10} Bq at 80000 s, for 100 mm break is ~1.3 10^{10} Bq at 80000 s, for 50 mm break is ~8.2 10^{9} at 80000 s.

- EK studied the same scenario for DBA case as in the first set of calculations. The studies were concentrated on fuel thermo-mechanics. EK implemented a new cladding failure criterion in FRAPTRAN code and changed the very conservative fission product release assumption of 100 % of failed fuel rods into a prediction of the failed fuel rods. This approach is more realistic, however applying new cladding failure criterion still contains some conservatism. The second set calculations estimated the clad bursts in the highest burnup rods, that corresponds to 26% of the fuel rods in the core. As in the first set of the calculations activity in environment was calculated very conservatively – considering instant release from the bust fuel to environment and ~1.5 10^{13} Bq of total environmental activity was calculated.

VVER-440 DEC A case. Calculations were provided by ARB. Analogical analysis made were as for DBA case. The same scenarios were used for DBA and DEC-A (no additional failure considered), but for the DEC-A case more realistic assumptions were selected. Thus, for all analyzed scenarios the PCTs were lower than 800°C and consequently for activity release no burst of the cladding was observed. Only the primary circuit contamination was considered. Calculated activity in the environment for DEGB is ~7.6 10^{10} Bq at 80000 s, for 250 mm break is ~4.4 10^{10} Bq at 80000 s, for 100 mm break is ~2.4 10^{10} Bq at 80000 s, for 50 mm break is ~2.1 10^{10} at 80000 s.

VVER-1000 DBA case. Calculations were provided by ARB, SSTC-NRS and UJV-NRI.

- ARB studied several scenarios for DBA case (same as first set of calculations): a) guillotine rupture of cooling loop 1 at the reactor entrance with an equivalent size 2×850 mm; b) rupture of cooling loop 1 at the reactor entrance with an equivalent size 350 mm; c) rupture of cooling loop 1 at the reactor entrance with an equivalent size 100 mm; d) rupture of cooling loop 1 at the reactor entrance with an equivalent size 50 mm. The second set (with applied improvements) of the calculation results showed very similar thermal hydraulic results, the biggest difference is regarding FP release and its transportation. The NPP model for the ATHLET code, for both sets of calculations showed that the entire activity of the primary circuit into the containment is released due to the rupture, which is characteristic of all considered scenarios of large and medium leakages with significant dynamics of coolant loss. Improved modelling of the clad thermomechanical behaviour and transport of isotopes in the coolant system of the primary circuit within the second set of calculations provided, a significant reduction of the activity released to the primary coolant and, accordingly, its emission into the containment, due to considering thermomechanical criteria (strain criterion) that leads to a lower number of failed rods compared to the assumption of 100% in the first set of calculations. In the case of guillotine rupture, it was estimated that around 18.1% of the fuel rods in the core burst. Together with released fission products from the fuel, the activity in the primary circuit was considered. Calculated activity in the environment is ~8 10^{11} Bq at 30000 s. For the 350 mm break, it was estimated that only one fuel pin burst corresponding to ~0.002 % from all core fuel rods. Calculated activity in the environment is ~8.2 10^{8} Bq at 30000 s. For other analyzed break sizes, no cladding bursts were predicted and then only activity in the primary circuit was considered. Calculated

activity in the environment for 100 mm break is ~5.6 10^8 Bq at 30000 s, for 50 mm break is ~4.6 10^8 at 30000 s.

- SSTC NRS studied one scenario for DBA case, the same scenario as in the first set of calculations. According to the improved approach, the RELAP5 core model was changed as it is described before. Other model features correspond to the first set of calculations. No changes in the MELCOR model were performed. RELAP5 calculation results were transferred to TRANSURANUS code as boundary conditions to perform thermo-mechanical analysis and evaluate the fuel clad ruptures. This reduced the conservative assumptions taken in the first run of calculations. Provided TRANSURANUS analyses showed that there is no cladding rupture. Thus, in the second set of calculations it was conservatively assumed that rupture could accrue in the fuel rods, which have highest power: 1856 fuel rods corresponding to ~3.7% of all fuel rods. Calculated activity in the environment is ~7.9 10^{11} Bq at 86400 s.
- UJV-NRI studied one scenario for DBA case. Improvements in the containment part were performed where UJV-NRI used an improved iodine dry paint deposition model in COCOSYS code. Also, realistic values as the boundary conditions for fission product transport were used. Based on statistical calculations with TRANSURANUS an enveloping fraction of 33 % fuel rods is assumed to rupture during the postulated accident (less conservative value compared to previous calculations where 100% was assumed). According to the R.G. 1.183 5 % of the core inventory of selected fission products was injected in the containment. Calculated total activity released to the environment is ~3.1 10^{10} Bq at 30000 s.

VVER-1000 DEC A case. Calculations were provided by ARB and SSTC-NRS.

- ARB studied several scenarios for DBA case (same as first set of calculations): a) guillotine rupture of cooling loop 1 at the reactor entrance with an equivalent size 2×850 mm; b) rupture of cooling loop 1 at the reactor entrance with an equivalent size 350 mm; c) rupture of cooling loop 1 at the reactor entrance with an equivalent size 100 mm; d) rupture of cooling loop 1 at the reactor entrance with an equivalent size 50 mm. The second set (with applied improvements) of the calculation results showed very similar thermal hydraulic results, the biggest different is regarding FP release and its transportation. The NPP model for the ATHLET code, for both sets of calculations showed that the entire activity of the primary circuit into the containment is released due to the rupture, which is characteristic of all considered scenarios of large and medium leakages with significant dynamics of coolant loss. Improved modelling of the release and transport of isotopes in the coolant system of the primary circuit within the second set of calculations provides, a significant reduction of the activity released to the primary coolant and, accordingly, its emission into the containment, due to taking into account a thermomechanical criterion for fuel rod clad failure. In the case of guillotine rupture, it was then estimated that around 5.84% of the fuel rods from all core burst. This value is smaller compared to the results of DBA. This is because for the DEC-A analysis, a nominal initial reactor power of 100% was considered instead of 104% as for DBA. It significantly reduces the number of fuel rods which PCT higher than 800°C. Together with fission product release from the fuel the activity in the primary circuit was considered. Calculated activity in the environment is ~4 10^{11} Bq at 30000 s. For other analysed break sizes as no clad burst was predicted only activity in the primary circuit was considered. Calculated activity in the environment for 350 mm break is ~5.8 10^8 Bq at 30000 s for 100 mm break is ~5.7 10^8 Bq at 30000 s, for 50 mm break is ~4.5 10^8 at 30000 s.
- SSTC NRS studied one scenario for DEC-A case, the same scenario as in the first set of the calculations. According to the improved approach, the RELAP5 core model was changed as it is described before. Other model features correspond to the first set of calculations. No changes to the MELCOR model were performed. RELAP5 calculation results were transferred to TRANSURANUS code as boundary conditions to perform thermo-mechanical analyses and evaluate the fuel clad ruptures. This reduced the conservative assumptions taken in the first run of calculations. However, from the TRANSURANUS analyses, it was conservatively assumed that 1856 of the fuel rods failed corresponding to ~3.7% of all the fuel rods in the core. Calculated activity in the environment is ~2.4 10^{12} Bq at 86400 s. The difference in activity release into environment compared to DBA case, despite the same number of failed rods

considered, is explained by the failure of CSS considering in the case of DEC-A and thus higher containment pressure.

PWR-900 DBA case. Calculations were provided by IRSN and ENEA using slightly different model of PWR-900.

- IRSN studied one scenario for DBA case (same as first set of calculations). IRSN used a new modelling approach based on the DRACCAR simulation tool (instead of ASTEC/ICARE) and developed FORECAST calculation chain. Also, clad burst failure models were improved. In updated calculations, two different DRACCAR modelling nodalizations were used for the core. Used modelling nodalizations were: 1- "DRACCAR 5 groups" – corresponding to ASTEC nodalization scheme (same ring channel defined in the core) used for the first run; 2- "DRACCAR realistic" – using a 3D meshing describing of 1/8th of the core with one representative fuel rod per fuel assembly, allowing a better consideration of the different fuel rod parameters and thermomechanical behaviour. Using "realistic" nodalization, PCT of ~750°C was calculated leading to 10.2% of failed fuel rods in the core. Using "5 groups" nodalization, PCT of ~690°C was calculated leading to 33.1% of failed fuel rods in the core (same as the first set of ASTEC calculation results). This also influenced the activity releases in the environment. Using "realistic" nodalization ~6.4 10^{12} Bq at 172800 s was calculated while using "5 groups" nodalization it was ~1.9 10^{13} Bq at 172800.
- ENEA studied one scenario for DBA case. They used new modelling approach for the reactor core increasing the number of equivalent rods per fluid channel and then the total number of equivalent rods in the core from 5 to 20. For the thermomechanical calculations, the best-estimate exponential clad burst criterion developed by IRSN within the project was used. A new version of the ASTEC code (v2.2.0.1) was also used. Applied improvements had minor or negligible effect on thermo-hydraulic and thermo-mechanical results. Computed PCT was ~866°C (vs ~859°C in first calculation set) and 12.7% of total fuel rods were predicted to fail as in the first set of calculations. In both calculation sets, the cladding failed when the maximum allowed hoop strain was reached (25%), which occurred before other criteria are met (i.e. respectively for the second and first calculation sets the best-estimate exponential and the EDGAR criterion). The higher number of representative fuel rods per ring channel in new core modelling led however to a more precise estimation of the cladding burst timing and in turn of the FP gap inventory release kinetics. This aspect, together with the minor differences on thermal hydraulic results in the primary circuit, influenced at least in part the FPs retention (except noble gasses not retained at all) in primary loops which was lower than the one computed in first set calculations, leading in turn to higher FPs release in containment then in environment (e.g., Cs mass released in environment is 7.1 10^{-7} of initial inventory against 3.3 10^{-7} in the first set of calculations). The total activity released in the environment at 180000 s, being mainly determined by noble gasses and especially of Xe, is however very close to the one calculated inf the initial set of calculations (6.17 10^{12} Bq instead of 6.13 10^{12} Bq).

PWR-900 DEC-A case. Calculations were provided by IRSN and ENEA using slightly different model of PWR-900.

- IRSN studied one scenario for DEC-A case (same as first set of calculations). IRSN used a new modelling approach based on the DRACCAR simulation tool and developed FORECAST calculation chain that interfaces DRACCAR and the SOPHAEROS module of ASTEC. In addition, improvements of the clad burst failure models were performed and included in DRACCAR. For this study two different DRACCAR modelling nodalizations for the core were used: 1- "DRACCAR 5 groups" –in the core) used for the first run and 2- "DRACCAR realistic" –using a 3D meshing describing 1/8th of the core with one representative fuel rod per fuel assembly, thus, accounting for fuel rod parameters with more details. Thermal-hydraulic results were similar to first run calculations, but calculated thermomechanical behaviour of fuel rods was different from the ASTEC calculation results provided in the first run. Furthermore, the two DRACCAR calculations provided different thermomechanical results. Using "realistic" nodalization PCT reached ~1030°C and 87.3% of total fuel rods were predicted to fail while using "5 groups" nodalization PCT reached ~1010°C and 100% of total fuel rods were predicted to fail. The corresponding released activity

in the environment was ~9.2 10^{13} Bq and ~9.8 10^{13} Bq at 172800 s respectively for "realistic" and "5 groups" nodalization.

- ENEA studied one scenario for DEC-A case. A new modelling approach for the reactor core was used to increase the number of equivalent rods per fluid channel from 5 to 20. For the thermomechanical calculations the new best-estimate exponential burst criterion was used). A new version of ASTEC (v2.2.0.1) was also used. Computed PCT was ~1065°C much lower than in the previous set where locally (at the top of the 2nd group of fuel assemblies representing 12.7% of the total fuel rods in the core) a very high cladding temperature (~2250°C) was predicted. Such a difference was not imputable to the improved core modelling, but to the used new ASTEC version. Despite the lower cladding temperatures predicted, the number of calculated failed rods was as in the first set of calculations (67%). This is because, the cladding burst was triggered by the maximum allowed hoop strain (40% in DEC-A) in both calculations for cladding temperature of approximately 850° C. A total activity of ~7.5 10^{13} Bq at 172800 s was calculated to be released in the environment slightly lower compared to initial set (~8.7 10^{13} Bq).

PWR Konvoi DBA case. Calculations were provided by HZDR. One LB LOCA scenario was studied, for which thermohydraulic and thermomechanical analyses were provided. A new core modelling approach has been developed which combines a 3D thermal hydraulic model of the RPV with the fuel rod model of ATHLET-CD and feedback from the fuel rod model back to the thermal-hydraulic model (based on calculation of reduction of the flow cross sectional areas). Four calculations were provided, which includes a variation of the power profile and limiting cases for the rod internal pressure (RIP). In particular, a conservative calculation with a top-peaked power profile was performed (i.e. the most unfavourable power distribution with a maximum linear heat generation rate of 455 W/cm) and a second calculation with a realistic power profile (with maximum linear heat generation rate of 350 W/cm). For both power profiles, two limiting cases were calculated, corresponding to different values of RIP found in the literature (one with lower initial RIP value, 2.25 MPa, and one with upper initial RIP value, 3.6 MPa).
For conservative initial and boundary conditions with top-peaked power profile, the burst rod percentage ranged from 12.6% to 29.1%, as for a realistic power profile burst rod percentage ranged from 3.4% to 11.7% of all fuel rods. For burst rods, the release of eight fission products is considered (Xe, Kr, Cs, I, Te, Ba, Sr, Sb) with burst release fractions taken from the CORSOR burst release model. Simulations did not include a detailed containment model, so the release to environment was not calculated in a detailed manner. Instead, the design leakage rate (0.25% vol./day) was applied to estimate the source term to environment. However, scaling factors for airborne fraction of fission products in containment as well as filter efficiencies have been taken into account (values taken from German guidelines for PWR).
The total in-containment source term 24 h after transient onset ranged from $2.04 \cdot 10^{17}$ to $4.71 \cdot 10^{17}$ Bq for a top-peaked power profile. The corresponding source term to environment ranged from $4.66 \cdot 10^{14}$ to $1.08 \cdot 10^{15}$ Bq. For the realistic power profile, the estimated in-containment source term ranged from $5.7 \cdot 10^{16}$ to $1.9 \cdot 10^{17}$ and the environmental source term from $1.30 \cdot 10^{14}$ to 4.35 10^{14} Bq. This study revealed that with best-estimate power profile significantly lower number of failed rods as well as lower source term is observed.
The new approach must be considered as an experimental approach, which need further research. Additional analyses where the feedback from mechanical rod model to thermal hydraulic model has been switched off, show that the feedback model (ATHLET-CD's blockage model) has significant impact to the results (peak cladding temperature is reduced by up to 200 K, when feedback is not applied). Furthermore, several code issues were identified at the end of the project that might lead to too high cladding temperature.

EPR-1600 DBA case. Calculations were provided by VTT. One scenario for DBA case was studied with a new cladding creep and phase transformation laws and new fuel failure criteria (based on IRSN newly developed models) that were implemented in the FRAPTRAN code. Analysis was only made for the thermomechanical part. Results showed that when using the IRSN minimum stress limit, the number of fuel failures per 1000 simulated rods increased by 0.7 percentage points compared with both the original plastic deformation model and the implemented Kaddour et al. creep model. The fraction of failing rods in the worst scenario was 2.1%. Furthermore, for all the rods that had been in reactor for two cycles before the LOCA event simulated using the Kaddour et al.

creep model (+ phase transformation) and IRSN minimum stress limit, the number of fuel failures increased from 1.96% to 3.4%.

BWR-4 DEC-A case. Calculations were provided by LEI. One scenario for DEC-A case was studied. TRANSURANUS code was used to verify ASTEC calculation results. Uncertainty and sensitivity analyses were also applied for TRANSURANUS calculation results. Based on the TRANSURANUS calculation results, the ASTEC nodalization of BWR active core was modified. Different relative power distribution across the modelled concentric rings were provided. PCT temperature reached ~830°C. The number of calculated failed rods was around 42% of the total fuel rods, lower than in the first calculation set (55%). A total activity of ~4.6 10^{14} Bq at 200000 s was calculated to be released in the environment.

Summarized information and results regarding the second set of calculations are displayed in the tables below.

Reactor type	Partner	Improvements		PCT (°C)	Burst from total core (%)	Activity in environment (Bq) at time (s)
VVER 440	ARB	Analytical methodology used FP activity release assessments –from thermomechanical criterion triggering the fuel rod clad failures. Use of BORON models from ATHLET code for equivalent isotopes transport modelling. A more detailed particle size classes spectrum considered for COCOSYS analysis	DEGB	~900	~0.3	~1.8 10^{11} at 80000
			250 mm	<800	0	~1.85 10^{10} at 80000
			100 mm	<800	0	~1.3 10^{10} at 80000
			50 mm	<800	0	~8.2 10^{9} at 80000
	EK	Implementation of new cladding failure criterion in FRAPTRAN	DEGB	~900	26 (conservatively considering clad bursts of the highest burn-up rods)	~1.5 10^{13} instant release
VVER 1000	ARB	Analytical methodology used for FP activity release assessment	DEGB	>800	18.1	~8 10^{11} at 30000
			350 mm	~800	~0.002 (one rod)	~8.2 10^{8} at 30000

		from thermomechanical criterion triggering the f fuel rod clad failures. Use of BORON models from ATHLET code for equivalent isotopes transport modelling. A more detailed particle size classes spectrum considered for COCOSYS analysis	100 mm	<800	0	~5.6 10^{8} at 30000
			50 mm	<800	0	~4.6 10^{8} at 30000
	SSTC-NRS	Improved RELAP5 nodalization for modelling of the reactor core and calculation chain	DEGB	~900	3.7	7.93 10^{11} at 86400
	UJV-NRI	Improved iodine dry paint deposition model for VVER paints and use of more realistic values as the boundary conditions for fission product transport	DEGB	~860	33% (enveloped value)	3.12 10^{10} at 30000
PWR 900	IRSN	New modelling approach based on DRACCAR simulation and developed FORECAST calculation chain. Improvements of clad burst failure models and criteria.	IB	~750 (DRACCAR realistic)	10.2	6.2 10^{12} at 172800
			IB	~690 (DRACCAR 5 groups)	33.1	1.9 10^{13} at 172800
PWR 900 generic	ENEA	New modelling approach for the reactor core considering more equivalent rods per fluid channel. Application of IRSN developed BE-exponential fuel	IB	~866	12.7	~6.17 10^{12} at 180000

		cladding burst criterion in ASTEC				
PWR Konvoi	HZDR	New core modelling approach coupling a 3D thermal hydraulic model of RPV with the fuel rod thermomechanical model of ATHLET-CD.	DEGB	~958 (for realistic power profile and 2.25 MPa RIP)	3.4 (for realistic power profile and 2.25 MPa RIP)	~1.3 10^{14} at 86400 (for realistic power profile and 2.25 MPa RIP)
EPR-1600	VTT	Chain of simulations codes was modified. New cladding creep and phase transformation laws and new fuel failure criteria (based on IRSN developed models) implemented in FRAPTRAN code.	DEGB	~900	2.1	Not evaluated

Table 10. Improvements and main results (LOCA scenario, DBA conditions) of the second set of calculations.

Reactor type	**Partner**	**Improvements**		**PCT (°C)**	**Burst Fail (%)**	**Activity in environment at time**
VVER 440	ARB	Analytical methodology for FP activity release assessments from thermomechanical criterion triggering the fuel rod clad failures. Use of BORON models from ATHLET code for equivalent isotopes transport modelling. More detailed particle size classes spectrum considered for COCOSYS	DEGB	<800	0	~7.6 10^{10} at 80000
			250 mm	<800	0	~4.4 10^{10} at 80000
			100 mm	<800	0	~2.4 10^{10} at 80000
			50 mm	<800	0	~2.1 10^{10} at 80000

VVER 1000	ARB	Analytical methodology for FP activity release assessments from thermomechanical criterion triggering the fuel rod clad failures. Use of BORON models of e ATHLET code for equivalent isotope transport modelling. More detailed particle size classes spectrum considered in COCOSYS	DEGB	>800	5.84	~4 10^{11} at 30000
			350 mm	<800	0	~5.8 10^{8} at 30000
			100 mm	<800	0	~5.7 10^{8} at 30000
			50 mm	<800	0	~4.5 10^{8} at 30000
	SSTC-NRS	Improved RELAP5 nodalization for modelling of the reactor core and calculation chain	DEGB	~900	3.7	~2.4 10^{12} at 86400
PWR 900	IRSN	New modelling approach based on DRACCAR simulation tool and developed FORECAST calculation chain. Improvements of clad burst failure models.	IB	~1030 (DRACCAR realistic)	87.3	~9.2 10^{13} at 172800
			IB	~1010 (DRACCAR 5 groups)	100	~9.8 10^{13} at 172800
PWR 900 generic	ENEA	New modelling approach for reactor core considering more equivalent fuel rods per fluid channel. Application of IRSN BE-exponential cladding burst criterion + sensitivity calculations with the other burst criteria proposed by IRSN.	IB	~1065	67	~7.5 10^{13} at 172800
BWR-4 generic	LEI	Improved ASTEC nodalization for reactor core modelling	DEGB	~830	42	~4.6 10^{14} Bq at 200000 s

Table 11. Improvements and main results (LOCA scenario, DEC-A conditions) of the second set of calculations.

3.2.2 SGTR calculations

VVER-440 DBA case. Calculations were provided by ARB and EK.

- ARB studied several scenarios for DBA case: Steam generator collector cover lift-up (leak size – 107 mm, 60 mm, 40 mm, 20 mm) and guillotine rupture of 1, 2 or 3 SG tube (s). The calculation results showed that with the reassessments of the reactor test case simulations the mass of the coolant flowing through the break from the primary circuit to the secondary circuit for the different scenarios was reduced by 3 to 30 tons compared to first set of calculations, except for 2 cases where there is an increase of cumulated mass transferred from the primary to the secondary of 5 tons. ARB calculated that the primary circuit activity including spiking equals 4.6 10^{13} Bq.

  The presence of a postulated single failure (failure to close one control SG SV of affected SG after its opening) strongly increases the release from the affected SG to the environment and leads to the unhindered outflow of the primary coolant and its mixture with the boiling water from the SG to the environment. The release from the affected SG to the environment through the failed control SG SV for the different scenarios varies from approx. 50 to 428.5 t. Modelling improvements in second set of calculations are allowing to reduce the releases of water to the environment between 2.1 % to 7.6 % for the different scenarios due to reduction of coolant flowing at the SGTR break, except for two cases (collector cover lift up of 60 mm and guillotine rupture of 2 tubes) where the releases of water are slightly increasing. The new realistic models used in the reassessment of the simulations lead to a decrease of the releases of fission products into the environment of between 50.2 % to 71.5 %. In the end, the releases of fission products into the environment vary from 5.73 10^{12} Bq to 2.29 10^{13} Bq for the different scenarios.
- EK studied 2 scenarios for DBA case: Steam generator collector cover lift-up and 3 SG broken tubes. In both scenarios, the primary pressure decreased to the secondary pressure. It took 4000 s in case of tube rupture and 2000 s for collector cover opening. The break flow started with 50 kg/s flowrate for the SG tube break event, while the initial break flow was about 100 kg/s for the collector cover opening. The lost coolant was compensated by the operation of HPIS. At the end of the simulation both scenarios reached stable conditions with equal pressures in the primary and secondary circuits.
  EK did not modify their thermal-hydraulic calculation, instead they focused on the update of the initial primary contamination and on the spiking model. As a matter of fact, the calculated new ^{131}I, ^{134}Cs and ^{137}Cs activities in the primary circuit are higher compared to the results of the first set calculations. In the reference calculation the water purification rate was lower, and the spiking of caesium isotopes were not taken into account. In primary circuit, the iodine isotopes inventory considered in the first set calculation was in average two order of magnitude more important compared to the inventory considered in the reassessment calculations (except for iodine 131 for which the inventory is around 6-7 times higher in the reassessment calculations). As iodine species are the main FP contributing to release of activity in the environment, activity releases are lower for reassessment calculations. EK calculated the activity releases to be in the range 1.6 10^{12} to 2.4$10^{12}$ Bq for the two reassessment calculations, whereas activity releases for the reference calculation are of 3.1$10^{12}$ Bq.

VVER-440 DEC A case. Calculations were provided by ARB.

- For DEC A case, ARB added another failure on BRU-A1 (Steam dump valve to-atmosphere stuck open) of the accidented SG to the studied DBA scenarios (the lower frequency of emergency event with a single failure of the BRU-A corresponds to DEC A category). The calculation results show that with the reassessment of the reactor test case simulations the mass of the coolant flowing through the break from the primary circuit to the secondary circuit for a majority of the scenarios is increased by 1 to 8 tons (in 6000s to 17000s) compared to first set calculation results, except for 2 cases where there is a reduction of cumulated mass transferred from the primary to the secondary of 8 to 23 tons. ARB calculated that the primary circuit activity including spiking equals 4.6$10^{+13}$ Bq.

The presence of a postulated single failure (failure to close of control SG SV of affected SG after its opening) and additional failure (failure to close BRU-A1) slightly increases the release from the affected SG to the environment compared to the DBA case and leads to the unhindered outflow of the primary coolant and its mixture with the boiling water of the SG to the environment. The release from the affected SG to the environment through the failed control SG SV and BRU-A1 for the different scenarios varies from approx. 60 to around 430 t. In contrast to the SGTR DBA, the presence of an additional failure to close the BRU-A1 leads to an increase in the activity release rate into the environment. Modelling improvements allow to reduce the releases of water to the environment between 2.6 % to 5.3 % for a majority of the scenarios, except for three cases where the releases of water are slightly increasing (between 1.2 to 3.1 %). The new realistic models used in the reassessment of the simulations lead to a decrease of the releases of fission products into the environment of between 46 % to 70.8 %. In the end, the releases of fission products into the environment vary from 5.80 10^{12} Bq to 2.48 10^{13} Bq for the different scenarios.

VVER-1000 DBA case. Calculations were provided by ARB, SSTC-NRS, BOKU and UJV-NRI.

- ARB studied several scenarios for DBA case: Steam generator collector cover lift-up (leak size – 100 mm, 60 mm, 40 mm, 20 mm) and guillotine rupture of 1, 2 or 3 SG tube (s). The calculation results showed that with the reassessment of the reactor test case simulations the mass of the coolant flowing through the break from the primary circuit to the secondary circuit for the different scenarios is reduced by 2 to 30 tons (in 6000s to 9000s) compared to first set of calculation results, except for one case where there is an increase of cumulated mass transferred from the primary to the secondary of 13 tons. ARB calculated that the primary circuit activity including spiking equals 2.4110^{14} Bq.

  The presence of a postulated single failure (failure to close the BRU-A of affected SG after its opening) strongly increases the release from the affected SG to the environment and leads to the unhindered outflow of the primary coolant and its mixture with the boiling water from the SG to the environment. The releases from the affected SG to the environment through the failed BRU-A for the different scenarios vary from approx. 90 to around 730 t. Modelling improvements were allowing to reduce the releases of water to the environment between 1.0 % to 4.9 % for all the scenarios. The new realistic models used in the reassessment of the simulations lead to a decrease of the releases of fission products into the environment of between 34.8 % to 71.4 %. In the end, the releases of fission products into the environment vary from 1.81 10^{13} Bq to 1.57 10^{14} Bq for the different scenarios.

- SSTC NRS studied one scenario for DBA case: The SG-1 cold collector cover lift-up is assumed. This results in a primary to secondary break of 100mm diameter. Because of operator response delays and since the opening setpoints of SG safety relief valves (SG SRV) and of steam dump valves (BRU-A) are lower than the head of the HPIS pumps injecting into primary circuit, the initiating event results in release of radioactive primary coolant to the environment. The break mass flow rate at the very beginning of accident reaches its maximum value. Loss of coolant causes a sharp decrease in primary pressure and coolant boiling in the vessel. The loss of normal power supply is postulated at the beginning of the initiating event (IE)and leads to Diesel Generator start-up. The single failure was assumed on Diesel Generator-1 leading to corresponding failures of 1/3 HPIS and 1/3 LPIS. After closure of turbine stop valves the steam dump to atmosphere valves BRU-As open at 2 s on all SGs. At the same time the short-term opening of control SG SRV was observed. SI signal is activated by loop subcooling less than 10°C at 35s followed by HPSI-1,2 trains injection. Because of the break flow the secondary side of broken SG-1 is filled with water at 350 s and water release through BRU-A into environment begins. 15 minutes after IE occurrence the forced closure of the feed water valves and BRU-A of broken SG by operator is modelled that temporarily terminates the release, but HPIS operation and coolant heat-up causes an increase of RCS pressure and at 1350 s periodic opening of control SG SRV of broken SG begins. At 1800s the HPSI is fully stopped by operator, all MSIVs are closed and cooling of RCS through SG-2,3,4 is initiated to the target SG pressure 35kgf/cm^2. This eventually causes gradual decrease of RCS and broken SG pressure.

By 2500 s the last opening cycle of SG-1 SRV occurs, and leak flow decreases to zero. From that time the break is isolated. The total mass loss from the primary circuit to the broken SG secondary side is 210 ton. The total mass of coolant released to the environment is 135 tons through BRU-A1 and SG-SV-1. The maximum fuel cladding temperature of 351°C is reached at the beginning of the Initiating Event. No challenge to the cooling of the fuel cladding is observed in the accident.
SSTC NRS did not modify the thermal-hydraulic behaviour of the accident compared to the first set of calculations. Only radiological activity transfer model has been improved (see §**Erreur ! Source du renvoi introuvable.**). In second set of calculations, SSTC NRS was doing a sensitivity analysis on the gas transfer coefficient K_g which is the fraction of activity transferred from the liquid phase to the gas/vapor phase in SG-1. From this analysis, it was seen that the fraction of RCS activity transferred to SG in case of such break is about 0.64 and depends on the timing of operator's actions on break isolation and ECCS throttling (assumed in EOPs). The total amount of activity coming to environment (gas+liquid) depends on the transfer coefficient from liquid to gas phase and corresponds to the value 0.345 for K_g=0 and to 0.64 for K_g=1 (as for non-condensable gases).
SSTC NRS modelled an initial primary activity of 2.24 10^{14} Bq. In the end, the integral activity released into the environment in the gas phase is equal to about 4.52 10^{13} Bq in the second set of calculations for the main case studied while it was 7.79 10^{13} Bq in the first set of calculations.

- UJV-NRI studied one scenario for DBA case: Guillotine rupture of a single steam generator tube was assumed. The single failure was assumed on the Steam Dump to Atmosphere (BRU-A) of the affected SG (BRU-A stuck open). The pressure in the secondary circuit rises at initiating event due to the turbine stop valves. At the same time the reactor was shut down and remaining BRU-A were opened. The pressure then decreases significantly, mainly for the affected SG. In general, the temperature decreases throughout the accident. The water mass in affected SG drops significantly due to closure of the feedwater line. In the later phase, the water mass rises thanks to the leak from the primary circuit and the SG becomes flooded. Thanks to the activation of safety injection systems and reactor SCRAM, the primary circuit remains subcooled throughout the accident. The calculation results showed that the mass of the coolant flowing through the break from the primary circuit to the secondary circuit is approximately 260 t (in 22000 s).
  UJV-NRI did not modify the thermal-hydraulic behaviour of the accident compared to first set of calculations. Only radiological model has been improved (see §**Erreur ! Source du renvoi introuvable.**). The fission products release starts when the BRU-A open at 1667 s. The dominant way is through the BRU-A4, which belongs to the affected SG and remains opened throughout the accident. UJV-NRI calculated activity in the primary coolant equals 5.99 10^{15} Bq. The integral activity of noble gases released into the environment is 1.13 10^{15} Bq for second set calculations while it was 1.43x10^{15} Bq for first set calculation results. For I-131, the decrease is even higher in second set calculations compared to first with a reduction of nearly 55% of the releases which accounts to 2.32x10^{14} Bq. With a transfer to the gas phase of 100% when the FP are transported thanks to flashing phenomenon, the flashing remains the main release mechanism for iodine in the SG (contributing to more than ¾ of the releases). Overall, releases of fission products in the environment are of 1.50x10^{15} Bq for second set calculation results while it was 2.23x10^{15} Bq for first set. The current approach provides more realistic radiological releases compared to the first set of calculations.
- BOKU studied one scenario for DBA case: A hot header break was assumed; this means a leakage (equivalent diameter of 100 mm) from the primary to the secondary side of the reactor occurs in loop No. 2. This constitutes a primary to secondary system leak (PRISE). Due to the closing of the turbine stop valve the emergency power mode is initiated. It is assumed that one diesel generator (DG) failed (single failure case). Therefore, all active safety systems of one loop (HPIS, LPIS, Auxiliary Feedwater) were not available. Operator actions are the depressurization of the secondary side (60 K/h) via the BRU-A valves in the intact loops and the deactivation of the HPIS after 1800s to limit the loss of coolant through the break. During the first seconds of the accident, the break mass flow rate reaches its maximum value of 500 kg/s. Due to the SCRAM and the pressure reduction at the Primary System, the mass flow rate

through the break decreases rapidly until 400s. After the activation of the HPIS the break mass flow rate stabilizes at about 100 kg/s. After 1900s, the HPIS stopped and the break mass flow rate decreases. Due to the activation of the Accumulators the break mass flow rate is shortly increased again. At 2000s the flow through the break is reversed for about 2000s. As the MSIV closes, the pressure in SG 2 deviates in comparison to the unaffected loops. Between 300s and 1900s the PS – pressure and the pressure in SG 2 are affected by the opening/closure of the BRU-A in the isolated SG. The HPIS and the Accumulators are very important in this accident. Those systems prevent a dry out of the core. The HPIS is switched on automatically and is deactivated by the operator at 1900s. The LPIS are activated at about 6000s, when the pressure threshold of 25 bar abs in the primary side is reached. During the transient the core was never at risk of running empty due to the injection of the HPIS, the Accumulators and later the LPIS. The PRZ runs empty early in the transient and is filled up again at about 3000s due to the HPIS and Accumulators injection, as well as the reverse mass flow rate through the break.
BOKU did not modify the thermal-hydraulic behaviour of the accident compared to the first set calculations. Only radiological model (iodine spiking and transport) has been improved (see §**Erreur ! Source du renvoi introuvable.** and §**Erreur ! Source du renvoi introuvable.**). Three sensitivities have been studied in the second set calculations: the accident occurs at a time position in the fuel cycle of 6, 12 or 18 months. It is assumed that I131 is released in the primary vessel within the first 300s of the transient. Fission products can only reach the environment through the BRU-A valve in the affected loop. The maximum I131 concentration reached in the primary system is between 2.2 10^{13} Bq to 3.2 10^{13} Bq at about 400s after transient initiation while it was 4.2 10^{13} Bq in first set of calculation results. The released I131 activity to the environment has been evaluated to be between 1.2 10^{10} to 1.7 10^{10} Bq for the 3 sensitivities studied in second set calculations while it was 2.2 10^{10} Bq in first set. The current approach provides more realistic radiological releases compared to the first set calculations.

VVER-1000 DEC A case. Calculations were provided by ARB, SSTC-NRS and BOKU.

- ARB studied several scenarios for DEC A case: Steam generator collector cover lift-up (leak size – 100 mm, 60 mm, 40 mm, 20 mm) and Guillotine rupture of 1, 2 or 3 SG tube (s). The calculation results showed that with the reassessment of the reactor test case simulations the mass of the coolant flowing through the break from the primary circuit to the secondary circuit for the different scenarios was reduced by 0.2 to 23 tons (in 6000s to 8500s) compared to first set calculation results, except for one case where there is an increase of cumulated mass transferred from the primary to the secondary of 9 tons. ARB calculated that the primary circuit activity including spiking equals 2.4110^{14} Bq.

  The presence of failures to close BRU-A and control SG SV of affected SG after their opening increases the release from the affected SG to the environment and leads to the unhindered outflow of the primary coolant and its mixture with the boiling water from the SG to the environment. The releases from the affected SG to the environment through the failed BRU-A and control SG SV for different scenarios varies from approx. 90 to around 820 t. Compared to the SGTR DBA, the presence of an additional failure to close the control SG SV leads to an increase in the activity release rate into the environment. Modelling improvements in reassessment calculations were allowing to reduce the releases of water to the environment between 1.7 % to 4.6 % for almost all scenarios, except for one case (guillotine rupture of one tube) where the releases of water are slightly increasing. The new realistic models used in the reassessment of the simulations lead to a decrease of the releases of fission products into the environment of between 31.1 % to 70.5 %. In the end, the releases of fission products into the environment vary from 1.86 10^{13} Bq to 1.66 10^{14} Bq for the different scenarios.
- SSTC NRS studied one scenario for DEC A case: The SG-1 cold collector cover lift-up was assumed. This results in a primary to secondary break of 100mm diameter. Because of operator response delays and since the opening setpoints of SG safety relief valves (SG SRV) and of steam dump valves (BRU-A) are lower than the head of the HPIS pumps injecting into primary circuit, the initiating event results in release of radioactive primary coolant to the environment. In DEC-A scenario an additional failure of SG-1 BRU-A was postulated assuming that this valve stuck in open position after the first opening. The break

mass flow rate at the very beginning of accident reaches its maximum value. Loss of coolant causes sharp decrease in primary pressure and coolant boiling in the reactor core. The loss of normal power supply is postulated at the beginning of IE and leads to Diesel Generator startup. The single failure was assumed on Diesel Generator-1 leading to corresponding failure of 1/3 HPIS (High pressure Injection System) and 1/3 LPIS (Low Pressure Injection System). After closure of turbine stop valves the steam dump to atmosphere valves BRU-As open at 2 s on all SGs. The BRU-A valve at SG-1 is stuck open according to calculation scenario. SI is activated at 35 s followed by HPIS-1,2 trains injection. Rapid decrease of RCS pressure down to LPIS shut-off head (24 bar) causes start of LPIS injection to the primary circuit at 610 s. Because of the primary-to-secondary break flow the secondary side of broken SG-1 is completely filled with water at 850 s and water release through stuck BRU-A to environment begins. 15 minutes after IE occurrence the operator actions on broken SG feedwater lines isolation, termination of injection from 1 out of 2 operating HPIS pumps, closure of all main steam isolation valves, switching of BRU-As of intact SGs into cool-down mode, and opening of gas removal valves from PRZ top are modelled. The latter causes an increase of PRZ level and at 1260 s (when PRZ level reaches 8 m and coolant subcooling is greater than 10°C) the operator switches off LPIS pumps. 30 min after the IE started operator aligns RCS residual heat removal system. At 4100 s the sump water is completely exhausted and injection from the last operating HPIS stops. Close to 8000 s the leak rate stabilizes around zero value. The total mass loss from the primary circuit to the broken SG secondary side is 545 tons. The total mass of coolant released to the environment is 490 tons through BRU-A1. The maximum fuel cladding temperature of ~340°C is reached at the beginning of the Initiating Event. No challenge to the cooling of the fuel cladding is observed in the accident.

SSTC NRS did not modify the thermal-hydraulic behaviour of the accident compared to the first set calculations. Only radiological model has been improved (see §**Erreur ! Source du renvoi introuvable.**).

In the second set of the calculations, SSTC NRS has done a sensitivity analysis on the gas transfer coefficient K_g which is the fraction of activity transferred from the liquid phase to the gas/vapor phase in SG-1. From this analysis, it was seen that the fraction of RCS activity transferred to SG in case of such break was about 0.91 and depends on the timing of operator's actions on break isolation and ECCS throttling (assumed in EOPs). The total amount of activity coming to environment (gas+liquid) depends on the transfer coefficient from liquid to gas phase and corresponds to the value 0.74 for K_g=0 and to 0.91 for K_g=1 (as for non-condensable gases). This calculation supports the idea of SG volume containing some FP in liquid phase.

SSTC NRS modelled an initial primary activity of 2.2410^{14} Bq. In the end, the integral activity released into the environment in the gas phase is equal to about 6.4210^{13} Bq in the second set of calculations for the main case studied while it was 7.79 10^{13} Bq in first set of calculations.

- BOKU studied two scenarios for DEC A. In the first scenario the initiating event of was a double-ended break of one SG tube with an equivalent break area of 13 mm² (2 times). This allows coolant of the Primary System to reach the Secondary System. In addition, a simultaneous guillotine break of the main steam line with an equivalent break area of 0.283 m² occurs. Failure of all HPIS trains and Hydro - accumulators was assumed, while the LPIS is available. Operator actions are the depressurization of the secondary side (60 K/h) via the BRU-A valves in the intact loops and the opening of the power operated relief valve (PORV) after 1800s. During the first seconds of the accident the break mass flow rate reaches its maximum value of 24 kg/s. Due to the SCRAM and the pressure reduction at the Primary System, the mass flow rate through the break decreases slowly until 1800s. At 1800s, the secondary side cooling via the BRU-A valves is initiated. After the LPIS is activated the primary inventory and the primary mass flow rate is increased considerably, which leads to an increase of the mass flow through the break at about 5700s. The maximum value (about 1900 kg/s) of the mass flow in the main steam line is reached within the first 100s. The Primary mass inventory is reduced in the first 5100s of the transient due to the loss of coolant through the primary break. The level of the PRZ decreases due to the SCRAM and the depressurization of the Primary System, until it is empty at about 1000s. After 1800s the PRZ level begins to fill in again, when the depressurization of the secondary system is initiated. This is caused by the boiler-

condenser phenomenon where steam flow of the Primary System is redirected to the PRZ. In accordance with the decline of the primary mass inventory, the PRZ level starts to decrease again after 2500s. This development is reversed after 5100s when the LPIS is activated and starts injecting into the Primary System. The operator initiates the opening of the PRZ PORV at 1800s. This leads to an increase in the pressure drop at the Primary System. The simultaneous depressurization of the secondary side enhances this effect. At about 5600s the PORV reacts to the injection of the LPIS and a greater amount of coolant is ejected. The BRU-A valves of the intact loops are opened by the operator at 1800s. This action is primarily intended to depressurize the secondary side, which eventually results in a decrease of the primary side pressure.

BOKU did not modify the thermal-hydraulic behaviour of the accident compared to first set of calculations. Only radiological model (iodine spiking and transport) has been improved (see §**Erreur ! Source du renvoi introuvable.** and §**Erreur ! Source du renvoi introuvable.**). Three sensitivities have been studied in second set calculations: the accident occurs at a time position in the fuel cycle of 6, 12 or 18 months. Within 300s after the SCRAM, an iodine spike is developed which is caused by the fast loss of reactor power that is associated with a pressure decrease. The maximum I131 concentration reached in the primary system is between 2.3 10^{13} Bq to 3.4 10^{13} Bq at about 400s after transient initiation while it was 4.4 10^{13} Bq in first set of calculations. The I131 activity released into the environment through the MSLB is highly dependent on the break flow of the SGTR (PRISE). It is expected that the whole iodine concentration, which reaches the secondary side is ejected through the MSLB into the environment. The released activity to the environment has been evaluated to be between 0.8 10^{10} to 1.2 10^{10} Bq for the 3 sensitivities studied in second set of calculations while it was 1.6 10^{10} Bq in first. The current approach provides more realistic radiological releases compared to first set calculations.

In the second scenario a hot header break is assumed, this means a leakage (equivalent diameter of 100 mm) from the primary to the secondary side of the reactor occurs in loop No. 4. This constitutes a primary to secondary system leak (PRISE). It is assumed that the BRU-A valve in the affected loop is stuck in an open position after the first opening. Due to the closing of the turbine valve the emergency power mode is initiated. It is assumed that all HPIS and ACCs are available, but the LPIS cannot be used. Operator actions are the depressurization of the secondary side (60 K/h) via the BRU-A valves in the intact loops and the deactivation of the HPIS/ACCs after 1800s to limit the loss of coolant through the break. During the first seconds of the accident the break mass flow rate reaches its maximum value of 450 kg/s. Due to the SCRAM and the pressure reduction at the Primary System, the mass flow rate through the break decreases rapidly until 200s. After the activation of the HPIS and the ACCs the break mass flow rate stabilizes again but decreases steadily until 1800s. After 1800s, the HPIS are stopped, and the break mass flow rate gets negative for a short time until it steadies at about 40 kg/s. As the MSIV close, the pressure in SG 4 deviates in comparison to the unaffected loops. The pressure in the affected SG is reduced rapidly due to the break. The three intact SGs display a pressure increase in the first phase of the transient, because they have to take on a higher load. Depressurization of the intact SGs starts only when the BRU-A valves are activated by the operator after 1800s The HPIS and the Accumulators are very important in this accident. Those systems prevent a dry out of the core. The HPIS is switched on automatically due to the pressure threshold and is deactivated by the operator in the 1800s. The PRZ runs empty early in the transient.

BOKU did not modify the thermal-hydraulic behaviour of the accident compared to the first set of calculations. Only radiological model (iodine spiking and transport) has been improved (see §**Erreur ! Source du renvoi introuvable.** and §**Erreur ! Source du renvoi introuvable.**). Three sensitivities have been studied in the second set of calculations: the accident occurs at a time position in the fuel cycle of 6, 12 or 18 months. Fission products can only reach the environment through the BRU-A valve in the affected loop. The maximum I131 concentration reached in the primary system is between 0.9 10^{13} Bq to 1.3 10^{13} Bq at about 3000s after transient initiation while it was 1.7 10^{13} Bq in first set calculations. The I131 integral activity released into the environment is between 1.5 10^{12} Bq to 2.2 10^{12} Bq for the 3 sensitivities studied in second set calculations while it was 2.8+10^{12} Bq in first set calculation results. The

current approach provides more realistic radiological releases compared to the first set calculation results for I-131.

PWR-900 DBA case

IRSN analyzed a DBA scenario with a break of a single steam generator tube at the hot leg side located at the top of the U-tube bundle on loop 3 (without pressurizer). In addition, the atmospheric by-pass steam relief valve of the failed steam generator was assumed to remain open after its first opening occurring 330 seconds after the tube rupture. No operator's actions were assumed before 20 minutes while automatic reactor management procedures triggered on set point/threshold values started very early due to the sharp primary circuit depressurization (320 s after SG tube rupture on reactor shutdown signal) leading to safety water injection (HPIS) in primary circuit. At transient onset, the calculated break mass flow rate is about 42kg/s, quickly then decreasing to about 25-30 kg/s. Primary pressure and pressurizer level quickly decrease leading to an automatic isolation of primary circuit heaters and let-down circuit, and to reactor shutdown. Subsequent sharpening of primary circuit depressurization and secondary pressure increase lead to first vapour releases to environment at 330 s. Safety water injection in primary circuit automatically starting on low primary circuit pressure leads to a re-increase of the SGTR mass flow rate from about 8 kg/s to about 27 kg/s and slows down the primary circuit depressurization. Secondary pressure in all SGs decreases until the first operator actions, the aim of which is the failed SG isolation, and the break mass flow rate cancellation. They consist of closing the steam line, the blow-down (purge) circuit and the water injection supply (normal then auxiliary) after 1500 s.

Liquid/steam inventories in SGs evolve according to cooling automatic management procedures and to by-pass atmospheric steam relief valve (SRV) successive opening/closure. Steam is continuously released from the failed SG up to the end of calculation at 3250 s. Liquid is also released, but the lost amount remains negligible during the period of SI occurrence. Once the SI is fully stopped, no significant mass of liquid is released but only vapour. The by-pass atmospheric SRV was assumed to be closed by operators at about 3200 seconds i.e. well before the SG overflowing, occurring at about 150000 s. During all the transient the core remains properly cooled and the primary circuit under saturation.

Updated calculations used the ASTEC/SAFARI module (in a coupled mode) instead of the MER software for activity transport up to the environment while the thermohydraulic data are provided by ASTEC/CESAR calculations as in the first set of calculations. The specific DROPLET model of ASTEC used in updated calculations allowed to model the flashing phenomena in the failed SG (droplet mechanical and thermal fragmentation) and the associated transfer of iodine from the liquid to the gaseous phase. For the spiking phenomena modelling (onset, duration, height, etc.), the same assumptions as in MER were used (based on French PWR measurement feedback). Cumulated gaseous activity releases in environment calculated by SAFARI exceed those obtained with MER for every element by a factor 2 to 8 depending on the elements. The difference is the strongest in the case of iodine (factor 8), partially explained by the additional flashing modelling (30%). Although not all the phenomena have yet been considered (such as i.e. the retention in the upper parts of the failed SG, in the steam lines…), the progress made in the simulation of the flashing mechanism, associated to the calculation of the iodine speciation in the primary circuit, allowed to sharpen the assessment of the iodine transfer towards the secondary coolant system then to the environment. The improved calculations, despite shortcomings, highlighted thus the importance, for a better estimation of the radiological consequences of SGTR scenarios with uncovered SG tube breaks, of the modelling of the thermodynamic iodine flashing, as well as the consideration of the iodine chemical speciation.

PWR-1000 DBA case. Calculations were provided by Bel V and CIEMAT.

- CIEMAT analysed the total amount of released activity due to I-131 at the end of the transient (1800 s) is equal to 2.7810^{8} Bq in the reassessed calculation i.e. much lower than calculated in the first calculation

set (1.4710^9 Bq). Most of the difference comes from the updated iodine spike model, but the models describing the iodine transfer to the SG-failed secondary side also play a significant role. In other words, the new models released approximately 50 times less iodine in the RCS but considering the partitioning of iodine (dominating transfer mechanism) from the water phase in the failed SG, also increases the released fraction to its gas phase. Even so, the activity released to the environment is about 5 times less than in WP 2.3. The main mechanism contributing to the radiological term in the calculation is then the iodine partition between liquid and vapor states in the affected SG.

- At Bel V, the DBA scenario is considered to occur in a reference 3-loop Pressurized nuclear Water Reactor (PWR) of 1000 MWe reactor. The transient starts at the occurrence of a double-ended break located in the apex of the longest U-tube of the three simulated U-tubes. The objective was to maximize the radioactivity release as the break remains uncovered for a longer period with respect to the lower part of the U-tubes. When the break is uncovered the release is larger (droplets and steam) the primary discharged water is not diluted with clean water of the feedwater.
  The scenario was numerically simulated using the advanced best-estimate fully implicit thermal-hydraulic system code CATHARE2 developed by CEA, EDF, AREVA, and IRSN. The adopted nodalization was based on a fully 1-D model, including all the 3 primary cooling loops and their associated safety injection systems as well as detailed representation of the RPV and the secondary side systems. Particular attention was given to the SG nodalization where three U-tubes lengths (short, medium and long) with detailed ascending and descending nodes were considered. This kind of nodalization is more suitable for the current study since the break is supposed to take place at the apex of the longest U-tubes. The goal was to maximize the time period of the break uncovery.
  The radioactivity transport was simulated using the CATHARE code transport model coupled with the TH calculations. This constitutes the main difference with respect to the previous calculations. Also, an enhanced spiking model was considered together with the former following assumptions:
    - Radioactivity release mechanisms due to flashing, partitioning and atomization are considered.
    - Only the Iodine 131 is considered for the current calculations even though other isotopes could be handled by the code together with the 131I.
    - No radioactivity is considered in the affected SG at the beginning of the accident.
    - The flow through the SG tube break is considered isenthalpic.
    - The radioactivity release through the partitioning effect is considered using a constant partitioning coefficient (PC = 100) and the steam released through the stuck open relief valve by partitioning calculated by subtracting the steam released by flashing.
    - The radioactivity release by atomization and flashing is assumed to be 100% released into environment, independently of the SG relief valve flow rate.

  The transient calculations were performed for a time period of 3500 s starting from break time occurrence and ending shortly after the closure of the stuck open Relief Valve (RV) by the operator.
  After the opening of the break, the primary coolant inventory, the pressure and the pressurizer water level decrease. The control systems automatically try to restore and maintain both the pressurizer pressure and level. However, due to the continuous primary inventory loss, the makeup system is not able to compensate the primary to secondary break flow, and therefore the pressurizer pressure and level continue to decrease. These conditions I lead, shortly after, to the isolation of the Chemical and Volume Control System (CVCS) letdown line and the pressurizer heaters due to the low pressurizer level. In the calculation, the SCRAM setpoint by low primary pressure was not reached before 30 min after the beginning of the transient, and therefore a manual SCRAM is activated by the operator. After the reactor trip, both the CVCS charge line and the Main Feedwater (MFW) systems are isolated. The turbine is tripped, the Main Steam Isolation Valves (MSIVs) are closed, and the Auxiliary feedwater (AFW) system is activated. The accident scenario also assumes that the condenser steam dump was not available. This causes a rise of the secondary pressure and the opening of the Relief Valves (RVs) in all the SGs. For the current DBA scenario, it was assumed, as a single failure, that the RV in the affected SG remains stuck fully open until it is manually closed by the operator.

The primary side pressure decrease stops due to the activation of the high-pressure safety injection system (HPSI). This leads to a stabilization of the primary pressure around the maximum head of the HPSI. The secondary pressure, after a short rise at the beginning of the transient, decreases and resumes later after the closure of the stuck open RV. The abrupt power change together with the primary pressure decrease, following the SCRAM, lead to the spiking phenomenon, which results into a significant increase of the primary side activity. This leads to a faster increase of activity in the secondary side of the faulted SG-3. The total predicted radioactivity release (considered that all the radioactivity in the steam line is released to the environment) by the three airborne mechanisms amounts to 190 GBq, of the three contributions, the radioactive release by atomization appears to be the dominant mechanism (70%), followed by the flashing (17%) and partitioning (13%) mechanisms.
Generally, the current results obtained using enhanced radionuclide transport and spiking model, are close to the previous calculations. Indeed, both the previous and the current calculations are based upon the same influent key parameters that govern the release to the environment i.e. the atomization phenomena. Nevertheless, the improved models allowed getting more reliable assessment of the radioactivity release.

PWR-1000 DEC A case. Calculations were provided by TRACTEBEL, Bel V and CIEMAT.

- CIEMAT analysed the DEC-A scenario with a concurrent isolable main steam line break (MSLB) with the double ended rupture of three steam generator tubes at the cold leg side tube sheet. The MSLB occurs outside the containment downstream MSIV. The analysis considers operator actions according to EOPs. The main operator actions modelled include those related to isolation of the affected SG and cooldown and depressurization of the RCS to the pressure of the affected SG to terminate the primary to secondary leak. The MSLB concurrent with the rupture of three tubes of the SG-C is postulated to occur at time t=0 s. This transient causes a rapid depressurization in the steam line and in the affected SG-C and, therefore, a rapid decrease in the pressurizer pressure and pressurizer level. The reactor trip occurs after the beginning of the transient and is followed by the activation of the safety injection system on low primary pressure. After the initiation of the high safety injection, the flow injected in the RCS becomes sufficient to compensate the coolant loses through the SG tubes rupture. With the beginning of the cooldown operations (by the opening of the PORV in the intact SGs) the primary pressure decreases to the point where the plant operator initiates the RCS depressurization to equalize the pressure with the pressure in the affected SG. The calculation chain considered in the reassessment calculation is similar to calculation scheme used in the first set of calculations. There are not substantial differences in the thermal-hydraulic results between both calculations. It is worth highlighting though that even in the modelled DEC-A scenario, core does not undergo any damage because the water level was at no time below the top of active fuel The described above improvements (iodine spiking model and iodine transport model) did not have substantial effects on these results.
  According to the results of both calculations, the total amount of released activity due to I-131 at the end of the transient (3000 s) is equal to 1.7910^{7} Bq in the updated calculations and was 7.37108 Bq in the initial calculations. Most of the difference (80%) comes from the updated iodine spike model, but the models describing the iodine transfer to the SG-failed secondary side also play a significant role (20%). In other words, the new models released 50 times less iodine in the RCS, but the partitioning of iodine (dominating transfer mechanism) from the water phase in the failed SG) contributes to slightly increase its fraction in the SG gas phase, then into the environment. Even so, the activity released to the environment is about 40 times less in the updated calculations compared to the initial ones.
  The main mechanism contributing (100 %) to the radiological term in iodine in the environment is its partitioning in the affected SG as the break is discharging in the water phase of the SG.
- TRACTEBEL studied one scenario for DEC A case: The simulated scenario was a Steam Generator Tube Rupture (SGTR) where a double-ended break on 3 tubes with Steam Line Break Outside Containment (SLBOUT) before Main Steam Isolation Valve (MSIV) were assumed. The tube break is located in the

SG-1 (SG on the same loop as the pressurizer), at the bottom of the U-tubes bundle on the cold leg side (exit of the SG). The break was assumed to be happening on the shortest tubes. The reactor was assumed to be at hot full power (HFP) before the transient and a spiking phenomenon was assumed to occur at SCRAM. The location of the SGTR break (bottom of the U-tubes) aimed at maximizing the overfilling phenomenon for the affected SG.

At transient initiation, 2 events were postulated: a non-isolable SLBOUT before MSIV and a double-ended break of 3 U-tubes at the bottom (cold leg side) of the bundle of SG 1. The initiator leads to a rapid steam pressure decrease. Safety Injection Signal (Signal S) is triggered. This results in the reactor trip (t = 0.75 s), the isolation of the MSIV, the start of all SI pumps, the isolation of the MFW and the start of the AFW (t = SCRAM + 110 s = 110.7 s). The reactor cooling pumps are assumed to be lost at reactor trip due to the LOOP. The depressurization of the affected SG takes about 1200 s. The total (both hot leg and cold leg sides) primary-to-secondary break flow rate initially increases from about 90 kg/s to around 110 kg/s between t = 0 and t = 500 s. The HPSI flow rate compensates for the loss of primary coolant through the SG's broken U-tubes resulting in a stabilization of the primary pressure around 95 bar abs. The primary-to-secondary break flow stabilizes around 110 kg/s. On the secondary side, the reactor trip leads to the level collapse in all SGs. After the isolation of the MFW and the closure of the MSIVs, the pressure increases in the intact SGs but stays under the pressure setpoint of the relief valves. The affected SG dries out due to the steam line double-ended break.

First impact from the new EOPs used in the second set of calculations is witnessed around 1000 s when at t = 1070.7 s the operators isolate the affected SG which includes the stop of AFW towards the affected SG 1, while in the 1st set of calculations, the isolation was occurring 140 s after. From this point on, the break flow rate becomes the only source of mass to the affected SG 1 adding about 110 kg/s of contaminated primary coolant. This results in a slightly slower increase of the mass inventory of the affected SG 1. At t = 1900-1950 s for the reassessed calculation, the affected SG starts overfilling: liquid water starts being spilled through the secondary break toward the environment.

Operators start opening 1 PORV at 2080.7 s in the 2nd set of calculations, 320 s before the 1st set of calculations. In the 2nd set of calculations, operators also stop the last HPSI pump at 2438 s, more than 1000 s before than the 1st set of calculations. Furthermore, in the 2nd set of calculations operators are controlling the PZR level between 50 and 76% according to EOPs while in the 1st set of calculations, the level of the PZR is kept stable around 29%. All these aspects combined are contributing to the faster depressurization of the RCS in the 2nd set of calculations compared to the 1st one. In the end, primary pressure is already below 20 bar abs. after 2500 s for the 2nd set of calculations while in the 1st set, the same threshold is only reached after 3600 s.

Reducing the RCS pressure allows to reduce the difference of pressure between primary and secondary circuits and therefore the SGTR break mass flow rate. At 3000 s, the total SGTR break mass flowrate (hot side + cold side) is around 26 kg/s for the 2nd set of calculations whereas for 1st one, the flowrate is still around 93 kg/s (more than 3 times more). By having lower SGTR break mass flowrate, lower quantities of FP are going from the RCS to SG 1 and in the end, the SLB will release less liquid water thus less FP (especially true for low volatile or non-volatile species). Accordingly, total liquid mass released from SG 1 through SLB is at least 3 times lower for the 2nd set of calculations (40 tons) compared to the 1st one (130 tons). Total releases of steam + liquid water is also lower for the 2nd set of calculations (210 tons) compared to the 1st set of calculations (around 305 tons). Main differences on the total quantity of water released is then coming from the liquid mass released difference.

At t = 2858.0 s in the 2nd set of calculations, 800 s earlier than the 1st set of calculations, the operators are allowed to connect the RHRS thanks to a RCS pressure lower than 28 bar abs. The connection of the RHRS was not simulated. The calculation ends 10 minutes after the connection time of RHRS. The timing difference on the connection with the RHRS also contributes to the fact that releases from the SLB are lower in the updated calculation compared to the initial ones.

Activities presented by TRACTEBEL are normalized activities and for each class, the initial specific activity in the RCS is set to 1 GBq/ton of water. The primary-to-secondary break opening is immediately assumed to be followed by iodine spiking. Due to the large release of molecular iodine (FP class 4) from the fuel, the inventory of class 4 in the RCS/vessel increases.

During the transient, the affected SG 1 is responsible for the radiological releases to the environment. Before liquid discharge through the SLB, the partitioning phenomenon was the main contributor to the radiological releases to the environment for molecular iodine. As expected, before first liquid discharges, releases of molecular iodine with the partitioning phenomenon are of $70*10^9$ Bq for the 2nd set of calculations while they are of $1.67*10^9$ Bq for the 1st set of calculations. Indeed, the new partitioning model developed for the 2nd set of calculations which consider evaporating conditions is more realistic than the model used in the 1st set of calculations which was not conservative enough and was based on old data from the 70s. By also considering the evaporation rate, the current model proposed in the 2nd set of calculations for the partitioning of the molecular iodine in SG 1 represents what is the closest to reality.

Then, when the SG 1 is full of liquid water, releases of molecular iodine with liquid water are happening provoking a much more increase of releases to the environment. The situation is reversed compared to the releases due to partitioning as due to lower SGTR break mass flowrate for the 2nd set of calculations, the SG 1 is filled slower and there are fewer liquid discharges through SLB. In the end, releases of molecular iodine from the 1st set of calculations are higher ($2.19*10^{11}$ Bq) compared to the 2nd set of calculations ($1.75*10^{11}$ Bq). The contribution of the partitioning phenomenon becomes important for the 2nd set of calculations with more than 40 % of the releases due to partitioning (releases of iodine in gas phase) while for the reference calculation it was around 1 %.

At the end of the transient, considering an initial specific activity of 1 GBq/ton of primary water, the radiological releases to the environment are of $4.2*10^{11}$ Bq for the 2nd set of calculations mainly constituted by 1.0e+11 Bq released for the noble gases and $1.75*10^{11}$ Bq released for the molecular iodine while they were of $6.9*10^{11}$ Bq for the 1st set of calculations with $1.1*10^{11}$ Bq for the noble gases and $2.19*10^{11}$ Bq for the molecular iodine.

- Bel V addressed the DEC-A scenario using the same tools and models as in the DBA case. The DEC-A scenario considered a concurrent three SGTR plus a non-isolable steam line break SLB. The rupture was assumed to take place in the bottom of the shortest cold side of the U-tube. The objective was to maximize the overfilling phenomenon in the affected SG. On the other hand, the SLB is located upstream the MSIV in order to maximize the release to the environment. After the break, the SCRAM set point is reached rapidly, leading to a loss of offsite power. The charging and the main feedwater are isolated. This is followed by the closure of the MSIV, the turbine trip, and the start of the auxiliary feedwater (AFW). Due to the rapid depressurization of the system, the high-pressure safety injection system set point is reached soon. This also activates the operator actions according to the prescribed emergency operating procedures EOPs. Subsequently, after a certain time, the operator identifies the faulted SG and stops the AFW towards the faulted SG-3 and starts the cooldown via the intact SGs at a cooldown rate of 56K/h. However, since the primary pressure remains high, the operator starts opening the PORV for a certain period of time in order to recover the pressurizer level. This is followed by a sequential stopping of the HPSI pumps. After that, the conditions for connecting the decay heat removal system are reached. The primary pressure decrease to low level and this ends the release to the environment.
  The radioactivity transport was simulated using the CATHARE code transport model coupled with the TH calculations. This constitutes the main difference with respect to the previous calculations. On the other hand, for the radioactivity release into the primary circuit an enhanced spiking model was considered.

  The transient calculations were performed for a time period of 5000 s. The calculation results showed that at the early phase of the transient (0-2000 s) the main mechanism of the iodine release is due to partitioning. After that (2000-5000 s), the dominant release mechanism becomes the liquid flow through the steam line break.

At the end of the transient, the cumulative discharged water and steam through the SLB is around 300 tons corresponding to a radiological release to the environment of $3.6*10^{12}$ Bq.
Unlike the DBA case, the updated calculations using enhanced radionuclide transport and spiking models, result in a larger difference in results with respect to the former calculations. Indeed, in the DEC-A case the calculations are only based on the CATHARE transport model of radioelements. No consideration was given to the atomization, partitioning and flashing phenomena since the SGTR break is almost all the time flooded.
The impact of using the CATHARE radio- isotope transport model instead of the simplified model shows a large difference for the DEC-A SGTR/SLB scenario. This impact is even larger than the impact of the spiking model. The total amount of released radioactivity is larger by a factor of 9 with respect to the former calculations. This difference is lower at earlier period of the transient when only steam is discharged through the SLB. Indeed, in this period the new results are larger by a factor of 2.5 only.

PWR-1300 DBA case. Calculations were provided by BOKU.

- BOKU studied one scenario for DBA case: A leakage from the primary to the secondary side of the reactor occurs in loop 4 with an equivalent break area of 600 mm² (2 times the tube area). The rupture is located at the bottom of the SG. A single failure is assumed (the HPIS/LPIS trains and the EFW are not available in the affected loop (L3/4)). Operator actions are the depressurization of the secondary side (100 K/h) via the relief valves (RV) in the intact loops and the deactivation of the HPIS after 2100s to limit the loss of coolant through the break. During the first seconds of the accident the break mass flow rate reaches its maximum value of 45 kg/s. Due to the SCRAM and the pressure reduction at the Primary System, the mass flow rate through the break decreases fast until 1000s, when the HPIS pumps are activated. At 2100s, the secondary side cooling via the SG relief valves is initiated. The Primary System and Secondary System pressure are affected by the break and the following power reduction. The Primary System pressure is decreasing linearly in the first 240s after the break due to the gradual power reduction system. At about 1000s, the pressure starts increasing again due to activation of the HPIS. The pressure in the intact loops decreases after 2100s due to depressurization of the secondary side via the relief valves. The PRZ level decreases due to the SCRAM and depressurization of the primary system. However, the PRZ level begins to rise again, after the HPIS has been activated. After about 3000s the PRZ level starts to steadily decline again. The level in all intact SGs decreases after 2100s, when the secondary depressurization system is activated by the operator. This affects loop 3 differently than loop 1 and 2 because a repair case is assumed, and no diesel generator is available for loop 3. The level in the affected SG (loop 4) slowly and steadily decreases after 2100s. All 4 RVs are opened automatically at the beginning of the transient and closed again before 2100s. The operator opened again the RV valves of the intact loops at 2100s. This action is primarily intended to depressurize the secondary side, which eventually results in a decrease of the primary side pressure. The RV in the affected loop is not opened by the operator to prevent emitting Fission Products to the environment.
  BOKU did not modify the thermal-hydraulic behaviour of the accident compared to the first set calculations. Only radiological model (iodine spiking and transport) has been improved (see §**Erreur ! Source du renvoi introuvable.** and §**Erreur ! Source du renvoi introuvable.**). 3 sensitivities have been studied in the second set of calculations: the accident occurs at a time position in the fuel cycle of 6, 12 or 18 months. Fission products can only reach the environment through the relief valve. The maximum I131 concentration reached in the primary system is between 1.8 10^{14} Bq to 2.6 10^{14} Bq while it was 3.510^{14} Bq in the first set calculations. The released activity to the environment has been evaluated to be between 0.55 10^{10} to 0.8 10^{10} Bq for the 3 sensitivities studied in second set while it was 1.05 10^{10} Bq in first set calculation results. The current approach provides more realistic radiological releases compared to the first set calculation results for I^{131}.

PWR-1300 DEC A case. Calculations were provided by BOKU.

- BOKU studied one scenario for DEC A case. The initiating event of this transient simulation was a double-ended break of one SG tube in loop 4 with an equivalent break area of 600 mm² (2 times the tube area).

This constitutes a primary to secondary system leak (PRISE). It is assumed that the relief valve in the affected loop is stuck in an open position after the first opening. All HPIS trains and all hydro accumulators (ACCs) are available at this scenario. However, the LPIS and the emergency feed water in the affected SG (due to isolation) are not available. Operator actions are the depressurization of the secondary side (100 K/h) via the relief valves (RV) in the intact SGs and the deactivation of the HPIS after 1800s to limit the loss of coolant through the break.
During the first seconds of the accident the break mass flow rate reaches its maximum value of 46 kg/s and drops down rapidly as the pressure in the Primary System falls. Due to the SGTR, at 300 s the primary system pressure declines but stabilizes due to the injection of the available HPIS system at around 700 s. On the secondary side the pressure in the intact SGs (loops 1-3) rises quickly before the closure of the MSIV due to the affected SG pressure increase, but finally declines as well after the SCRAM is initiated at 589 s on low Primary System Pressure (setpoint 132.5 bar abs). The Secondary System pressure rises before the SCRAM initiation initiates the opening of the relief valve of SG 4 (loop 4). It was assumed that the relief valve of the affected SG is stuck open and does not close again throughout the simulation. This assumption penalizes the emission of Fission Products into the environment. The PRZ level decreases due to the break and finally rises and stabilizes due to HPIS operation.
BOKU did not modify the thermal-hydraulic behaviour of the accident compared to the first set calculations. Only radiological model (iodine spiking and transport) has been improved. 3 sensitivities have been studied in the second set calculations: the accident occurs at a time position in the fuel cycle of 6, 12 or 18 months. Fission products can reach the environment through the relief valve in the affected loop. The maximum I131 concentration reached in the primary system is between 1.5 10^{14} Bq to 2.2 10^{14} Bq while it was 2.8 10^{14} Bq in first set calculation results. The released activity to the environment has been evaluated to be between 1.6 10^{11} to 2.5$10^{11}$ Bq for the 3 sensitivities studied in second set calculation results while it was 3.0 10^{11} Bq in first set calculation results. The current approach provides more realistic radiological releases compared to the first set calculations.

Reactor type	Partner	Improvements	Scenario	Cumulative steam/liquid water released in environment (tons)	Activity in environment at time
VVER 440	ARB	Use of the BORON (for dilution) and DRIFT FLUX models for the ATHLET code (20 isotopes considered)	SG collector lift up 107 mm	428.5 (almost all liquid) (12 tons less than 1st set of calc.)	2.3E+13 Bq at 6000 s
			SG collector lift up 60 mm	302.3 (almost all liquid) (2 tons more than 1st set of calc.)	1.9E+13 Bq at 7000 s
			SG collector lift up 40 mm	188.5 (90% liquid) (12 tons less than 1st set of calc.)	1.5E+13 Bq at 15000 s
			SG collector lift up 20 mm	69.4 (70% steam) (same as in 1st set of calc.)	9.74E+12 Bq at 17000 s
			1 tube 2*13.2 mm	50.1 (steam only) (1 ton less than 1st set of calc.)	5.73E+12 Bq at 17000 s

Reactor type	Partner	Improvements	Scenario	Cumulative steam/liquid water released in environment (tons)	Activity in environment at time
			2 tubes 2*2*13.2 mm	71.1 (majority steam) (1 tons more than 1st set of calc.)	1.1E+13 Bq at 13000 s
			3 tubes 3*2*13.2 mm	100.9 (majority liquid) (8 tons less than 1st set of calc.)	1.5E+13 Bq at 11000 s
	EK	Use of an updated version of the RING code to simulate spiking phenomenon for I and Cs and update of primary initial contamination for other isotopes not impacted by spiking (87 isotopes considered)	Break of 3 SG tubes	0.218 (same as in 1st set of calc.)	2.4e12 Bq at 10000s
			Collector cover opening (Equivalent to the break of a 37 mm diameter tube)		1.6e12 Bq at 10000 s
VVER 1000	ARB	Use of the BORON and DRIFT FLUX models for the ATHLET code (20 isotopes considered)	SG collector lift up 100 mm	730 (almost all liquid) (32 tons less than 1st set of calc.)	1.57E+14 Bq at 6000s
			SG collector lift up 60 mm	447 (80% liquid) (13 tons less than 1st set of calc.)	1.43E+14 Bq at 7000 s
			SG collector lift up 40 mm	286 (70% liquid) (14 tons less than 1st set of calc.)	9.73E+13 Bq at 8000 s
			SG collector lift up 20 mm	120 (steam only) (10 tons less than 1st set of calc.)	3.49E+13 Bq at 9000 s
			SGTR 1 tube (2*13 mm)	91 (steam only) (same as in 1st set of calc.)	1.82E+13 Bq at 10000 s
			SGTR 2 tubes (2*2*13 mm)	120 (steam only) (10 tons less than 1st set of calc.)	3.59E+13 Bq at 10000 s
			SGTR 3 tubes (3*2*13 mm)	123 (steam only) (7 tons less than 1st set of calc.)	4.73E+13 Bq at 10000 s

Reactor type	Partner	Improvements	Scenario	Cumulative steam/liquid water released in environment (tons)	Activity in environment at time
	SSTC NRS	Improvement of the RCS coolant dilution and FP transport (20 isotopes considered)	SG collector lift up (100 mm) LOOP+failure of 1/3 HPIS and LPIS	135 (steam 23%, water 77%) (same as in 1st set of calc.)	4.52E+13 Bq at 10000 s
	UJV-NRI	Improvement of the FP activity transfer with the use of a new methodology and computational approach (6 isotopes considered)	DEGB (1 T) + LOOP + failed SG RV stuck open	590 (same as in 1st set of calc.)	1.50E+15 Bq at 22000 s
	BOKU	Improvement of the radiological model (iodine spiking and transport for I131). Dilution and pool scrubbing taken into account (I-131 only considered).	SG hot collector lift-up (100 mm) +all active safety systems of one loop (HPIS, LPIS, Auxiliary Feedwater)	178.8 steam/ 120.6 liq. (same as in 1st set of calc.)	1.2e10 to 1.7e10 Bq (from 6 months to 18 months fuel cycle duration) at 4000 s
PWR 900	IRSN	Use of ASTEC/SAFARI module and DROPLET model for FP activity transfer, flashing/atomization and iodine partitioning (20 isotopes considered)	1 T break at U-bundle top + failed SG RV stuck open (closed after 54 min)	95.3 (92% from the failed SG) /0.7 (62% from the failed SG)	9.5e13 at 3240 seconds
PWR 1000	CIEMAT	Improvement of the iodine spiking and iodine transport from the RCS to environment (5 iodine isotopes and 6 xenon isotopes considered)	DEGB (1 T) at top of U-bundle +failed SG RV stuck open (closed after 30 min)	74.76 (same as in 1st set of calc.)	2.78E+08 Bq at 1800 s 2.69 E+06 Bq Noble gases at at 1800 s

Reactor type	Partner	Improvements	Scenario	Cumulative steam/liquid water released in environment (tons)	Activity in environment at time
	Bel V	Improvement of the iodine spiking model and of RN transport model from primary to secondary side. (I-131 only considered)	DEGB (1 Tube) at top of U-bundle + failed SG RV stuck open (closed after 30 min)	~95-100 (same as in 1st set of calc.)	1.9E11 Bq at 3500 s
PWR 1300	BOKU	Improvement of the radiological model (iodine spiking and transport for I131) Dilution and pool scrubbing taken into account (I-131 only considered)	DEGB (1 tube) at bottom Failure of 2/4 HPIS/LPIS pumps and 2/4 EFW	171.7 steam/4. liq. (same as in 1st set of calc.)	0.55e10 to 0.8e10 Bq (from 6 months to 18 months fuel cycle duration) at 8000s

Table 12. Improvements and main results (SGTR scenario, DBA conditions) of the second set of calculations.

Reactor type	Partner	Improvements	Scenario	Cumulative steam/liquid water released in environment (tons)	Activity in environment (Bq) at time (s)
VVER 440	ARB	Use of the BORON and DRIFT FLUX models for the ATHLET code (20 isotopes considered)	SG collector lift up 107 mm	430 (almost all liquid) (20 tons less than 1st set of calc.)	2.48E+13 Bq at 6000 s
			SG collector lift up 60 mm	316 (almost all liquid) (14 tons less than 1st set of calc.)	2.22E+13 Bq at 7000 s
			SG collector lift up 40 mm	196 (80% liquid) (6 tons more than 1st set of calc.)	1.73E+13 Bq at 15000 s
			SG collector lift up 20 mm	79 (majority steam) (same as in 1st set of calc.)	9.91E+12 Bq at 17000 s
			SGTR 1 tube (2*13.2 mm)	61 (steam only) (same as in 1st set of calc.)	5.80E+12 Bq at 17000 s
			SGTR 2 tubes (2*2*13.2 mm)	86 (majority steam) (1 ton more than 1st set of calc.)	1.22E+13 Bq at 15000 s
			SGTR 3 tubes (3*2*13.2 mm)	100 (half liquid/half steam) (3 tons more than 1st set of calc.)	1.52E+13 Bq at 11000 s
VVER 1000	ARB	Use of the BORON and DRIFT FLUX models for the ATHLET code (20 isotopes considered)	SG collector lift up 100 mm	820 (almost all liquid) (25 tons less than 1st set of calc.)	1.66E+14 Bq at 6000s
			SG collector lift up 60 mm	450 (80% liquid) (15 tons less than 1st set of calc.)	1.46E+14 Bq at 7000s

			SG collector lift up 40 mm	302 (60% liquid) (20 tons less than 1st set of calc.)	1.06E+14 Bq at 8000s
			SG collector lift up 20 mm	132 (steam only) (same as in 1st set of calc.)	3.61E+13 Bq at 8500s
			SGTR 1 tube (2*13 mm)	93 (steam only) (same as in 1st set of calc.)	1.86E+13 Bq at 8500 s
			SGTR 2 tubes (2*2*13 mm)	132 (steam only) (8 tons less than 1st set of calc.)	3.75E+13 Bq at 8500s
			SGTR 3 tubes (3*2*13 mm)	135 (steam only) (5 tons less than 1st set of calc.)	4.94E+13 Bq at 8500s
	SSTC NRS	Improvement of the RCS coolant dilution and FP transport (20 isotopes considered)	SG collector lift up SG RV (BRU-A1) stuck open +LOOP +failure of 1/3HPIS/LPIS	490 (steam 20%, water 80%) (same as in 1st set of calc.)	6.42E+13 Bq at 8000s
	BOKU	Improvement of the radiological model (I131 spiking and transport) (1 isotope considered)	SGTR + MSLB	283.4 steam/1.3 liq. (same as in 1st set of calc.)	0.8e10 Bq to 1.2e+10 Bq (from 6 months to 18 months fuel cycle duration) at 40000s
			Hot header break + BRU-A stuck open	145.9 steam/445.2 liq. (same as in 1st set of calc.)	1.5e12 Bq to 2.2e+12 Bq (from 6 months to 18 months fuel cycle duration) at 4250s
PWR 1000	CIEMAT	Improvement of the iodine spiking and iodine transport from the RCS to environment (5 iodine isotopes and 6 xenon isotopes considered)	DEGB (3 tubes) and simultaneous isolable SLB+LOOP	4.0 (same as in 1st set of calc.)	1.79E+07 Bq at 3000 s 2.11E+06 E+06 Bq Noble gases at 3000 s

	TRACTEBEL	Improvement of the iodine partitioning model infailed SGand consideration of new EOPs for operators actions to depressurize RCS as fast as possible (80 isotopes considered)	DEGB (3 tubes) and simultaneous SLB out of containment (non-isolable) +LOOP	170 steam/40 liquid (90 tons of liquid less than 1st set of calc.)	4.2E+11 in total 1.75E+11 molecular iodine 1.0E+11 Noble gases at 3500
	Bel V	Improvement of the iodine spiking model and of RN transport model from primary to secondary (I-131 only considered)	DEGB (3 tubes) and simultaneous SLB out of containment (non-isolable) +LOOP	170 steam/130 liquid (same as in 1st set of calc.)	3.6E12 Bq at 5000 s
PWR 1300	BOKU	Improvement of the radiological model (iodine spiking and transport) (1 isotope considered)	DEGB (1 tube) +SG RV stuck open +Failure of LPIS	385.5 steam/2.9 liq. (same as in 1st set of calc.)	1.6e11 Bq to 2.5e11 Bq (from 6 months to 18 months fuel cycle duration) at 20000s

Table 13. Improvements and main results (SGTR scenario, DEC-A conditions) of the second set of calculations.

3.3 Impact of the new modelling approach for radiological consequences evaluations

In this section is provided a comparison of radiological consequences calculated in the first set of the calculations and second set calculations where improvements were applied.
For the evaluation of the radiological consequences the simplified method developed in the frame of the R2CA project and the associated excel file were used considering the event effective dose due to external exposure and inhalation as well as the equivalent thyroid dose. Doses were evaluated for six different categories of ages. Calculations considered height for the releases from NPP, distance from the emission point (function of NPP design and location) and time period for the evaluation. Each partner could use their own values of height, distance and time period that are more representative of the NPP and the transients they analysed.

3.3.1 LOCA calculations

VVER-440 DBA case. Calculations were provided by ARB and EK.

- ARB modelled the height of the release point correspondent to the top of the BRU A discharge pipe (40 m) and the doses were determined for a distance of 2.5 km from the NP. 48 h time period for the evaluation was selected.
  Thyroid equivalent doses in second set calculations range from 1.7E-4 mSv to 0.0116 mSv for the different calculations for all kind of population age groups. It is much lower than the first set calculation results where range is from 1.6 mSv to 12.6 mSv. The total effective doses calculated in the second set calculations range from 1.03E-5 mSv to 3.4E-3 mSv for the different calculations for all kinds of population age groups. Also, it is much lower than the first set calculation results where the range is from 9.3E-2 to 2.4 mSv. For example, thyroid equivalent dose for the adults in the case of the double ended guillotine break is 0.00311 mSv in the second set of the calculations while the first set calculations showed 2.63 mSv. For the total effective doses for adults in the case of the double ended guillotine break is 0.00315 mSv in the second set of the calculations while the first set calculations showed 2.18 mSv.
  In the second set of the calculations the activity in the environment at the end of the investigated period of time decreased around 99.9 % compared to the first set of calculation results. This is mostly due to the very conservative assumptions taken in the first set calculations (including the 100% failed rod assumption). This result leads to decreased radiological consequences to humans. For the thyroid equivalent dose, the reduction of the radiological consequences is around 99.9 % compared to first set calculation results. The same result is also applicable for the total effective dose.
- EK did not provide evaluation of radiological consequences, it is because the fission product transport was not analysed in their work. However, performed improvements providing a thermomechanical analysis of the fuel rods enabled to estimate than reduce the number of the failed fuel rods considered where in the first calculation set conservative 100% failed rod assumption was used. This was expressed in the reduction of activity. Activity was reduced ~16 % compared to the results of the first set calculations (1.5E+13 Bq instead of 9.5E+13 Bq).

VVER-440 DEC A case. Calculations are provided only by ARB. Results of the received results is very close to the DBA case, due to the very conservative assumptions taken in the first set calculations. Thyroid equivalent doses in second set calculations are ranging from 3.4E-4 mSv to 3.5E-3 mSv for the different calculations for all kind of population age groups. It is much lower than the first set calculation results where range is from 1.9 mSv to 17.7 mSv. The total effective doses calculated in second set calculations are ranging from 2.3E-5 mSv to 3.9E-4 mSv for the different calculations for all kind of population age groups. As well, it is much lower than first set calculation results where range is from 0.113 mSv to 1.57 mSv. For example, thyroid equivalent dose for the adults in second set calculations for the case of the double ended guillotine break is 0.00072 mSv in while the first set calculations showed 3.24 mSv. The total effective doses for adults in the case of the double ended guillotine break is 0.000375 mSv in the second set of the calculations while the first set calculations showed 1.4 mSv.

VVER-1000 DBA case. Calculations were provided by ARB, SSTC-NRS and UJV-NRI.

- ARB modelled the height of the release point correspondent to the top of the BRU A discharge pipe (48 m) and the doses were determined for a distance of 2.5 km from the NPP. 48 h time period for the evaluation was selected.
  Thyroid equivalent doses in second set calculations are ranging from 3.9E-5 mSv to 7.9E-2 mSv for the different calculations for all kind of population age groups. It is much lower than the first set calculation results where the range is from 0.195 mSv to 3.43 mSv. The total effective doses calculated in the second set calculations range from 2.3E-6 mSv to 3.5E-2 mSv for the different calculations for all kind of population age groups. Also, it is much lower than the first set calculation results where the range is from 3.4E-2 to 0.35 mSv. For example, the thyroid equivalent doses for adults in the case of the double ended

guillotine break is 0.0194 mSv in the second set of the calculations while the first set calculations showed 0.195 mSv. The total effective doses for adults in the case of the double ended guillotine break is 0.0324 mSv in the second set of the calculations while the first set calculations showed 0.323 mSv.
In the second set of the calculations for the case of double ended guillotine break (DEGB) the activity in the environment at the end of the investigated period of time was decreased around 90 % compared to the first set calculation results. These results also reflected the radiological consequences to humans. For the thyroid equivalent dose, the reduction of the radiological consequences is around 90 % compared to first set calculation results. The same result is also applicable for the total effective dose.
Calculation results of activity and radiological consequences for the smaller pipe break were close to 99.9 % difference compared to the first set of calculations, similar as in the case of VVER-440 calculation results.

- SSTC NRS used the default horizontal distance between the release-point and the receiver of the dose (300 m) and default height of the release point (65 m) for evaluation to calculate the radiological consequences. 48 h time period for the evaluation was selected.
  SSTC NRS in the second set of the calculations received ~61% reduced activity compared to the first calculation results. For the thyroid equivalent dose, reassessment of the reactor test case simulations allows for a reduction of the radiological consequences of about 96 % compared to first set calculations. For the total effective dose reduction of also 96% compared to first set calculation results was noticed.
  The thyroid equivalent dose for adults is 0.003 mSv in the second set of the calculations while the first set calculations showed 0.077 mSv. The total effective doses for adults in the case of the double ended guillotine break is 0.004 mSv in the second set of the calculations while the first set calculations showed 0.1 mSv.
- UJV-NRI used the default values for horizontal distance between the release-point and the receiver of the dose was 300 m and height of the release point was 65 m. 48 h time period was evaluated.
  Activity difference between first and second sets of the calculations is ~81 %. Activity after provided improvements were reduced. For the thyroid equivalent dose, reassessment of the reactor test case simulations allows for a reduction of the radiological consequences of about 93 % compared to first set calculations. For the total effective dose, was reduced around 90 % compared to first set calculation results.
  Thyroid equivalent doses for the adults in the second set calculations was received 0.17 mSv and it is 10 times lower than it was in the first set of the calculations (1.71mSv). The total effective doses for the adults in second set calculations are 0.0084 mSv and again it is ~10 lower when in the first set of calculations, 0.086 mSv.

VVER-1000 DEC A case. Calculations were provided by ARB and SSTC-NRS.

- ARB modelled the height of the release point correspondent to the top of the BRU A discharge pipe (48 m) and the doses were determined for a distance of 2.5 km from the NPP. 48 h time period for the evaluation was selected.
  Thyroid equivalent doses in second set calculations range from 7.9E-5 mSv to 0.26 mSv for the different calculations for all kind of population age groups. It is much lower than the first set calculation results where the range is from 0.86 mSv to 36.7 mSv. The total effective doses calculated in the second set calculations range from 4.6E-6 mSv to 0.1 mSv for the different calculations for all kind of population age groups. Also, it is much lower than the first set calculation results where range is from 5E-2 to 4.4 mSv. For example, thyroid equivalent doses for the adults in the second set calculations for the double ended guillotine scenario was 0.062 mSv and it is much lower than it was in the first set of the calculations – 2.63 mSv. The total effective doses for adults in the case of the double ended guillotine break is 0.1 mSv in the second set of the calculations while the first set calculations showed 4 mSv.
  In the second set of the calculations, for the case of DEGB, the activity in the environment upon completion of radioactive release from reactor plant through SG steam dump valve has decreased around 98 % compared to the first set calculation results. This also results in a decrease in the radiological

consequences to humans. For the thyroid equivalent dose, the reduction of the radiological consequences is around 98 % compared to first set calculation results. The same result is also applicable for the total effective dose.
Calculation results of activity and radiological consequences for the smaller pipe break were close to 99.9 % difference comparing to the first set of calculations, similar as in the case of VVER-440 calculation results.

- SSTC NRS used the default values for the horizontal distance between the release-point and the receiver of the dose was 300 m and height of the release point was 65 m. 48 h time period for the evaluation was selected.
  SSTC NRS in the second set of the calculations received ~96% reduced activity comparing to the first calculation results. For the thyroid equivalent dose, reassessment of the reactor test case simulations allowed for a reduction of the radiological consequences of about 96 % compared to first set calculations. For the total effective dose, was reduced also 96% compared to first set calculation results.
  The thyroid equivalent doses for adults is 0.085 mSv in the second set of the calculations while the first set calculations showed 2.13 mSv. The total effective doses for adults in the case of the double ended guillotine break is 0.04 mSv in the second set of the calculations while the first set calculations showed 1.1 mSv.

PWR-900 DBA case. Calculations were provided by IRSN and ENEA.

- IRSN modelled the height of the release point corresponding to the top of the chimney at 60 m and the doses were determined for a distance of 1 km from the NPP to calculate the radiological consequences. 48 h time period for the evaluation was selected.
  Activity difference between first and second sets of the calculations is ~80 %. Released activity after provided improvements were reduced. For the thyroid equivalent dose, reassessment of the reactor test case simulations allows for a reduction of the radiological consequences of about 90 % compared to first set calculations. The total effective dose was reduced around 91 % compared to the first set calculation results.
  Thyroid equivalent doses for the adults in second set calculations is 0.00685 mSv while in the first set of calculations was 0.066 mSv. Analogical situation is for the total effective dose for adults 0.00125 mSv in the second set of calculations while 0.0135 mSv in the first set of calculations.
- ENEA modelled the height of the release point corresponding to the top of the chimney at 60 m and the doses were determined for a distance of 1 km from the NPP to calculate the radiological consequences. 48 h time period for the evaluation was selected.
  Activity between the first and second sets of the calculations is almost the same value, increase by 0.7 %. This is due to different retention in the cooling circuit, explained by slightly different thermohydraulic calculation results. Calculated doses in both cases are small, but for the thyroid equivalent dose, reassessment of the reactor test case simulations showed ~100% increase comparing to the first set calculations. For the total effective dose in the second set of the calculations the values increased by 40% compared to the first set of calculations. This could be explained by higher inventories in iodine and caesium respectively due to lesser retention in the primary circuit itself.
  Thyroid equivalent doses for the adults in second set calculations is 0.0034 mSv while in the first set of calculations was 0.0017 mSv. The total effective dose for adults 0.0007 mSv in the second set of calculations while it was 0.0005 mSv in the first set of calculations.

PWR-900 DEC-A case. Calculations are provided by IRSN and ENEA.

- IRSN modelled the height of the release point corresponding to the top of the chimney at 60 m and the doses were determined for a distance of 1 km from the NPP to calculate the radiological consequences. 48 h time period for the evaluation was selected.
  Activity between first and second sets of the calculations is decreased by ~22 %. For the thyroid equivalent dose, reassessment of the reactor test case simulations allows for a reduction of the

radiological consequences of about 57 % compared to first set calculations. For the total effective dose, was reduced also around 56 % compared to first set calculation results.
Thyroid equivalent doses for the adults in second set calculations is 0.81 mSv while in the first set of calculations was 1.8 mSv. Analogical situation is for the total effective dose for adults 0.122 in the second set of calculations while 0.26 mSv in the first set of calculations.

- ENEA modelled the height of the release point corresponding to the top of the chimney at 60 m and the doses were determined for a distance of 1 km from the NPP to calculate the radiological consequences. 48 h time period for the evaluation was selected.
  Activity between the first and second sets of the calculations is decreased by ~15 %. For the thyroid equivalent dose, reassessment of the reactor test case simulations allows for a reduction of the radiological consequences of about 17 % compared to first set calculations. For the total effective dose, was reduced also around 16 % compared to first set calculation results.
  The thyroid equivalent doses for the adults in second set calculations is 0.55 mSv while in the first set of calculations was 0.66 mSv. The total effective dose for adults was 0.086 mSv in the second set of calculations while 0.103 mSv in the first set of calculations.

PWR-Konvoi DBA case. It was evaluated by HZDR. The total in-containment source term at 24 h after beginning of the accident ranges from $2.04 \cdot 10^{17}$–$4.71 \cdot 10^{17}$ Bq, calculated for the assumption of a top-peaked power profile (reaching most unfavourable power distribution with a maximum linear heat generation rate of 455 W/cm). The corresponding source term to environment ranges from $4.66 \cdot 10^{14}$ – $1.08 \cdot 10^{15}$ Bq. For best-estimate power profile (taken directly from core simulator results with a maximum linear heat generation rate of 350 W/cm), the estimated in-containment source term ranges from $5.7 \cdot 10^{16}$–$1.90 \cdot 10^{17}$ Bq and source term to environment is in the range between $1.3 \cdot 10^{14}$–$4.35 \cdot 10^{14}$ Bq. To be in the line with other partners results of best-estimate power profile and 2.25 MPa internal rod pressure was selected to be showed in the summarized table ($1.3 \cdot 10^{14}$ Bq).
The calculated activities were approximately in the same order of magnitude as the values reported in the first set of calculations where 10% of fuel rod failure was assumed.
Radiological consequences for the humans were not evaluated by HZDR.

EPR-1600 DBA case. It was evaluated by VTT and only the FRAPTRAN-GENFLO part was improved and recalculated. From FRAPTRAN-GENFLO analysis, the rod failure times are available, and the fractional FGR (the portion of fission gas in the gap over the total amount of generated gas during the steady-state). The fractions cover krypton and xenon, but the output files only have the FGR percentage, not the total fission gas produced, so it is not possible to determine the activity. Furthermore, the FRAPTRAN-GENFLO simulations were done only until 700 s. Thus, it was decided not to evaluate radiological consequences.

BWR-4 DEC-A case. It was evaluated by LEI. The default horizontal distance between the release-point and the receiver of the dose (300 m) and default height of the release point (65 m) were used for the evaluation to calculate the radiological consequences. 48 h time period for the evaluation was selected.
LEI in the second set of the calculations received ~13% reduced activity compared to the first calculation results. For the thyroid equivalent dose, reassessment of the reactor test case simulations allows for a reduction of the radiological consequences of about 8 % compared to first set calculations. For the total effective dose is about 10% reduction compared to the first set calculation results.
The thyroid equivalent dose for adults is 0.026 mSv in the second set of the calculations while the first set calculations showed 0.028 mSv. The total effective doses for adults in the case of the double ended guillotine break is 0.043 mSv in the second set of the calculations while the first set calculations showed 0.048 mSv.

A summary of the results obtained from the radiological evaluations is presented in the tables below.

Reactor type	Partner Scenario	Parameters of release Height (m) Distance (m) Time period (h)	Thyroid equivalent dose for adults, mSv		Total effective dose for adults, mSv	
			First set of calculations	Second set of calculations	First set of calculations	Second set of calculations
VVER 440	ARB, DEGB	Height (m) 40 Distance (m) 2500 Time period (h) 48	2.6	0.0031	2.18	0.0031
VVER 1000	ARB, DEGB	Height (m) 40 Distance (m) 2500 Time period (h) 48	1.95	0.019	0.32	0.032
	SSTC-NRS, DEGB	Height (m) 65 Distance (m) 300 Time period (h) 48	0.077	0.003	0.1	0.004
	UJV, DEGB	Height (m) 65 Distance (m) 300 Time period (h) 48	1.71	0.17	0.086	0.0084
PWR 900	IRSN, IB	Height (m) 60 Distance (m) 1000 Time period (h) 48	0.066	0.0069	0.0135	0.00125
PWR 900 generic	ENEA, IB	Height (m) 60 Distance (m) 1000 Time period (h) 48	0.0017	0.0034	0.0005	0.0007

Table 14. Thyroid equivalent doses and total effective doses evaluated for adults with the tool developed with the project for (LOCA scenario, DBA conditions).

Reactor type	Partner Scenario	Parameters of release Height (m) Distance (m) Time period (h)	Thyroid equivalent dose for adults, mSv		Total effective dose for adults, mSv	
			First set of calculations	Second set of calculations	First set of calculations	Second set of calculations
VVER 440	ARB, DEGB	Height (m) 40 Distance (m) 2500 Time period (h) 48	3.24	0.00072	1.4	0.00038
VVER 1000	ARB, DEGB	Height (m) 40 Distance (m) 2500 Time period (h) 48	2.63	0.062	4	0.1
	SSTC-NRS, DEGB	Height (m) 65 Distance (m) 300 Time period (h) 48	2.13	0.085	1.06	0.042
PWR 900	IRSN, IB	Height (m) 60 Distance (m) 1000 Time period (h) 48	1.79	0.81	0.26	0.12
PWR 900 generic	ENEA, IB	Height (m) 60 Distance (m) 1000 Time period (h) 48	0.66	0.55	0.103	0.086
BWR-4 generic	LEI, DEGB	Height (m) 65 Distance (m) 300 Time period (h) 48	0.028	0.026	0.048	0.043

Table 15. Thyroid equivalent doses and total effective doses evaluated for adults with the tool developed with the project for (LOCA scenario, DEC-A conditions).

3.3.2 SGTR calculations

BOKU and Bel V did not participate in the evaluation of radiological consequences and therefore did not perform the analysis mainly because their simulation or their improvement only concerned I-131 isotope. Due to this, their improvements made in the second set of calculations compared to the first set would directly lead to a proportionality between their radiological consequences analysis and their calculated released activity in the environment.

VVER-440 DBA case. Calculations were provided by ARB and EK.

- ARB modelled the height of the release point correspondent to the top of the BRU A discharge pipe (40 m) and the doses were determined for a distance of 2.5 km from the NPP.
  For the thyroid equivalent dose, reassessment of the reactor test case simulations allows for a reduction of the radiological consequences between 50.5 to 80 % compared to the first set of calculation results. In the end, thyroid doses in the second set of calculations are ranging from 0.58 mSv to 7.44 mSv for the different calculations for all kinds of population age groups.
  For the total effective dose, reassessment of the reactor test case simulations allows for a reduction of the radiological consequences between 50 to 67 % compared to first set calculation results. In the end, total effective doses calculated in the second set of calculations are ranging from 0.03 mSv to 0.197 mSv for the different calculations for all kinds of population age groups.

- EK modelled the height of the release point corresponding to the top of the chimney (120 m) and the doses were determined for a distance of 1 km from the NPP.
  For the thyroid equivalent dose, reassessment of the reactor test case simulations calculated the doses to be ranging from 0.16 mSv to 0.56 mSv for the two different calculations for all kinds of population age groups.
  For the total effective dose, reassessment of the reactor test case simulations allows for a reduction of the radiological consequences between 11 to 42 % compared to first set calculation. In the end, total effective doses in of the second set of calculations are ranging from 0.01 mSv to 0.031 mSv for the different calculations for all kinds of population age groups.

VVER-440 DEC A case. Calculations were provided by ARB.

- ARB modelled the height of the release point correspondent to the top of the BRU A discharge pipe (48 m) and the doses were determined for a distance of 2.5 km from the NPP.
  For the thyroid equivalent dose, reassessment of the reactor test case simulations in the second set of calculations allows for a reduction of the radiological consequences between 47 to 78 % compared to the first set of calculations. In the end, thyroid doses calculated in the second set of calculations are ranging from 0.58 mSv to 8.07 mSv for the different calculations for all kinds of population age groups.
  For the total effective dose, reassessment of the reactor test case simulations in the second set calculations allows for a reduction of the radiological consequences between 44 to 62 % compared to the first set. In the end, total effective doses calculated the second set are ranging from 0.03 mSv to 0.216 mSv for the different calculations for all kinds of population age groups.

VVER-1000 DBA case. Calculations were provided by ARB, SSTC-NRS, BOKU and UJV-NRI.

- ARB modelled the height of the release point correspondent to the top of the BRU A discharge pipe (48 m) and the doses were determined for a distance of 2.5 km from the NPP.
  For the thyroid equivalent dose, reassessment of the reactor test case simulations allows for a reduction of the radiological consequences between 29 to 83 % compared to the first set calculation results. In the

end, thyroid doses in the second set of calculation results are ranging from 1.27 mSv to 38.8 mSv for the different calculations for all kinds of population age groups.
For the total effective dose, reassessment of the reactor test case simulations allows for a reduction of the radiological consequences between 33 to 61 % compared to the first set of calculations. In the end, total effective doses calculated in the second set are ranging from 0.068 mSv to 1 mSv for the different calculations for all kinds of population age groups.

- SSTC NRS used the default horizontal distance between the release-point and the receiver of the dose (300 m) and default height of the release point (65 m) to calculate the radiological consequences.
  For the thyroid equivalent dose, reassessment of the reactor test case simulations allows for a reduction of the radiological consequences of about 89 % compared to the first set of calculations. In the end, thyroid doses calculated in the second set of calculations are ranging from 0.79 mSv to 1.65 mSv for all kinds of population age groups.
  For the total effective dose, reassessment of the reactor test case simulations allows for a reduction of the radiological consequences of about 85 to 86 % compared to the first set calculation results. In the end, total effective doses calculated in the second set are ranging from 0.063 mSv to 0.11 mSv for all kinds of population age groups.
- UJV-NRI used default height of the release point (65 m) of task 2.2 to calculate the radiological consequences and used a horizontal distance of 2 km from the release point.
  For the thyroid equivalent dose, reassessment of the reactor test case simulations allows for a reduction of the radiological consequences of about 55 % compared to the first set of calculation. In the end, thyroid doses calculated in the second set are ranging from 159 mSv to 304 mSv for all kinds of population age groups.
  For the total effective dose, reassessment of the reactor test case simulations allows for a reduction of the radiological consequences of about 55 % also compared to the first set of calculations. In the end, total effective doses calculated in the second set are ranging from 8.6 mSv to 15.5 mSv for all kinds of population age groups.
  The current approach used by UJV-NRI assumes overly conservative initial inventory.

VVER-1000 DEC A case. Calculations were provided by ARB, SSTC-NRS and BOKU.

- ARB modelled the height of the release point correspondent to the top of the BRU A discharge pipe (48 m) and the doses were determined for a distance of 2.5 km from the NPP.
  For the thyroid equivalent dose, reassessment of the reactor test case simulations allows for a reduction of the radiological consequences between 27 to 82 % compared to the first set of calculations. In the end, thyroid doses calculated in the second set are ranging from 1.31 mSv to 40.6 mSv for the different calculations for all kinds of population age groups.
  For the total effective dose, reassessment of the reactor test case simulations allows for a reduction of the radiological consequences between 28 to 62 % compared to the [f] first set of calculations. In the end, total effective doses calculated in the second set are ranging from 0.07 mSv to 1.07 mSv for the different calculations for all kinds of population age groups.
- SSTC NRS used the default horizontal distance between the release-point and the receiver of the dose (300 m) and default height of the release point (65 m) of task 2.2 to calculate the radiological consequences.
  For the thyroid equivalent dose, reassessment of the reactor test case simulations allows for a reduction of the radiological consequences of about 84 % compared to the first set of calculations. In the end, thyroid doses calculated in the second set are ranging from 1.12 mSv to 2.35 mSv for all kinds of population age groups.
  For the total effective dose, reassessment of the reactor test case simulations in allows for a reduction of the radiological consequences of about 79 to 81 % compared to the set of calculations. In the end, total

effective doses calculated in the second set are ranging from 0.089 mSv to 0.15 mSv for all kind of population age group.

PWR-900 DBA case.

- IRSN modelled the height of the release point at 60 m and the doses were determined for a distance of 1 km from the NPP to calculate the radiological consequences. Moreover, to assess a range of radiological consequences, as a first approximation, the proportions of released iodine under particle and molecular gas form were assumed to be either 50% - 50%, or 90% - 10%. These proportions are expected to vary along the transient in accordance with the significance of the different processes occurring in the failed steam generator (atomization, flashing, partitioning).
  For the thyroid equivalent doses, reassessment of the reactor test case simulations leads to a high increase of the radiological consequences (>100%) compared to the first set of calculations. In the end, thyroid doses calculated in the second set are ranging from 0.1 mSv to 0.48 mSv for all kinds of population age groups and iodine speciation distribution (iodine released was considered to be in particle and molecular form and their proportion was assumed to be 50%-50% or 90%-10% for respectively the two forms).
  For the total effective dose, reassessment of the reactor test case simulations also leads to an increase of the radiological consequences varying from about 79 % for adults to percentiles slightly higher than 100% for the most impacted age group compared to the first set of calculations, depending also on the iodine speciation distribution considered for the updated SAFARI calculations. In the end, total effective doses calculated in the second set are ranging from about 0.03 mSv to 0.045 mSv for all kinds of population age groups and iodine speciation distribution with the highest values for the proportions of released iodine under particle and molecular gas form being 50%-50%.

PWR-1000 DBA case. Calculations were provided by Bel V and CIEMAT. Only CIEMAT calculated the radiological assessments.

- CIEMAT used the height of the release point equal to 30 m (reference point of the SG PORV). The horizontal distance between the release point and the receiver of the dose was set approximately to 700 m. Concerning the thyroid equivalent dose and the total effective dose, the second reactor test case simulations a reduction of the radiological consequences of about 80% compared to the first set of calculations. The values of the thyroid doses calculated in the second set of calculations, considering the time of the modelled scenario, are ranging from 0.01 mSv to 0.021 mSv for all the population age groups considered. The values of the effective doses calculated in the second set of calculations, considering the time of the modelled scenario, are ranging from 0.0005 mSv to 0.001 mSv for all the population age groups considered.

PWR-1000 DEC A case. Calculations were provided by TRACTEBEL, Bel V and CIEMAT. Bel V did not calculate the radiological consequences.

- CIEMAT used the height of the release point equal to 30 m (reference point of the SG PORV). The horizontal distance between the release point and the receiver of the dose was set approximately to 700 m. Concerning the thyroid equivalent dose and the total effective dose, the second reactor test case simulations showed a reduction of the radiological consequences of about 97%. The values of the thyroid doses calculated in the second set of calculations, considering the time of the modelled scenario, are ranging from 0.0013 mSv to 0.0026 mSv for all the population age groups considered. The values of the effective doses calculated in the second set of calculations, considering the time of the modelled scenario, are ranging from 0.00007 mSv to 0.00014 mSv for all the population age groups considered.
- TRACTEBEL used the default horizontal distance between the release-point and the receiver of the dose (300 m) and default height of the release point (65 m) to calculate the radiological consequences.
  For the thyroid equivalent dose, reassessment of the reactor test case simulations allows for a reduction of the radiological consequences between 20 to 25 % compared to first set calculations. In the end, thyroid

doses calculated in second set calculations range from 0.83 mSv to 1.61 mSv for all kinds of population age groups.
For the total effective dose, reassessment of the reactor test case simulations allows for a reduction of the radiological consequences of about 25 % compared to first set calculation results. In the end, total effective doses calculated in second set are ranging from 0.048 mSv to 0.085 mSv for all kinds of population age groups.

Reactor type	Partner/ Scenario	Parameters of release Height (m) Distance (m) Time period (s)	Activity difference (%)	Event thyroid equivalent dose difference after improvements (%)	Total effective dose difference after improvements (%)
VVER 440	**ARB**	40 2500			
	107 mm	6000	Decrease of 50 %	Decrease of 50 %	Decrease of 50 %
	60 mm	7000	Decrease of 59 %	Decrease of 58 %	Decrease of 58 %
	40 mm	15000	Decrease of 67 %	Decrease of 67 %	Decrease of 67 %
	20 mm	17000	Decrease of 69 %	Decrease between 56 % to 72 %	Decrease of around 60 %
	2*13.2 mm	17000	Decrease of 71 %	Decrease between 51 % to 80 %	Decrease of around 58 %
	2*2*13.2 mm	13000	Decrease of 68 %	Decrease between 56 % to 71 %	Decrease of around 59 %
	3*2*13.2 mm	11000	Decrease of 65 %	Decrease between 60 % to 68 %	Decrease of around 61 %
	EK	120 1000			
	Break of 3 SG tubes	10000	Decrease of 23 %	2nd set of calculations: 0.26 mSv to 0.56 mSv	Decrease of 11 %
	Collector cover opening	10000	Decrease of 48 %	2nd set of calculations: 0.16 mSv to 0.35 mSv	Decrease of 42 %
VVER 1000	**ARB**	48 2500			
	100 mm	6000	Decrease of 35 %	Decrease between 32 % to 37 %	Decrease of 33 %
	60 mm	7000	Decrease of 40 %	Decrease between 39 % to 43 %	Decrease of 40 %
	40 mm	8000	Decrease of 59 %	Decrease between 58 % to 62 %	Decrease of 59 %
	20 mm	9000	Decrease of 68 %	Decrease between 48 % to 80 %	Decrease of around 55 %
	2*13 mm	10000	Decrease of 53 %	Decrease between 29 % to 73 %	Decrease of around 38 %

	2*2*13 mm	10000	Decrease of 70 %	Decrease between 50 % to 81 %	Decrease of around 57 %
	3*2*13 mm	10000	Decrease of 72 %	Decrease between 55 % to 83 %	Decrease of around 61 %
	SSTC NRS	65 300 10000	Decrease of 42 %	Decrease of 89 %	Decrease of 85 % to 86 %
	UJV-NRI	65 2000 22000	Decrease of 33 %	Decrease of 55 %	Decrease of 55 %
	BOKU	Not evaluated	Decrease between 23 % to 45 %	Not evaluated	Not evaluated
PWR 900	IRSN	60 1000 3240	Increase >100%	Increase >100%	Increase of 79 % to 125 %
PWR 1000	CIEMAT	30 700 1800	Decrease of 80 %	Decrease of ≈77 %	Decrease of ≈77 %
	Bel V	Not evaluated	No Change	Not evaluated	Not evaluated
PWR 1300	BOKU	Not evaluated	Decrease between 24 % to 48 %	Not evaluated	Not evaluated

Table 16. Radiological consequence differences after improvements (SGTR scenario, DBA conditions).

Reactor type	**Partner/ Scenario**	**Parameters of release Height (m) Distance (m) Time period (s)**	**Activity difference (%)**	**Event thyroid equivalent dose difference after improvements (%)**	**Total effective dose difference after improvements (%)**
VVER 440	**ARB**	48 2500			
	107 mm	6000	Decrease of 46 %	Decrease of 46 %	Decrease of 46 %
	60 mm	7000	Decrease of 52 %	Decrease of 51 %	Decrease of 51 %
	40 mm	15000	Decrease of 62 %	Decrease of 62 %	Decrease of 62 %

Reactor type	Partner/ Scenario	Parameters of release Height (m) Distance (m) Time period (s)	Activity difference (%)	Event thyroid equivalent dose difference after improvements (%)	Total effective dose difference after improvements (%)
	20 mm	17000	Decrease of 68 %	Decrease between 58 % to 73 %	Decrease of 62 %
	2*13.2 mm	17000	Decrease of 71 %	Decrease between 51 % to 79 %	Decrease of around 57 %
	2*2*13.2 mm	15000	Decrease of 64 %	Decrease between 53 % to 68 %	Decrease of around 53 %
	3*2*13.2 mm	11000	Decrease of 65 %	Decrease between 58 % to 69 %	Decrease of around 60 %
VVER 1000	**ARB**	48 2500			
	100 mm	6000	Decrease of 31 %	Decrease between 27 % to 34 %	Decrease of 29 %
	60 mm	7000	Decrease of 39 %	Decrease between 37 % to 42 %	Decrease of 38 %
	40 mm	8000	Decrease of 56 %	Decrease between 54 % to 60 %	Decrease of 55 %
	20 mm	8500	Decrease of 67 %	Decrease between 47 % to 80 %	Decrease of around 53 %
	2*13 mm	8500	Decrease of 54 %	Decrease between 28 % to 72 %	Decrease of around 37 %
	2*2*13 mm	8500	Decrease of 69 %	Decrease between 48 % to 80 %	Decrease of around 55 %
	3*2*13 mm	8500	Decrease of 71 %	Decrease between 54 % to 82 %	Decrease of around 60 %
	SSTC NRS	65 300 8000	Decrease of 17.6 %	Decrease of 84 %	Decrease of 79 % to 81 %
	BOKU	Not evaluated		Not evaluated	Not evaluated
	SGTR + MSLB		Decrease between 25 % to 50 %		
	Hot header break + BRU-A stuck open		Decrease between 21 % to 46 %		
PWR 1000	CIEMAT	30 700 3000	Decrease of ≈ 97 %	Decrease of ≈ 97 %	Decrease of ≈ 97 %

Reactor type	Partner/ Scenario	Parameters of release Height (m) Distance (m) Time period (s)	Activity difference (%)	Event thyroid equivalent dose difference after improvements (%)	Total effective dose difference after improvements (%)
	TRACTEBEL	65 300 3500	Decrease of 39 %	Decrease between 20 % to 25 %	Decrease of about 25 %
	Bel V	Not evaluated	Increase > 100%	Not evaluated	Not evaluated
PWR 1300	BOKU	Not evaluated	Decrease between 17 % to 47 %	Not evaluated	Not evaluated

Table 17. Radiological consequence differences after improvements (SGTR scenario, DEC-A conditions).

3.4 Overview and discussion

In total 34 accidental scenarios (both LOCA and SGTR) were calculated in the second set of calculations on different kinds of reactor designs (VVERs, PWRs, EPR and BWR), covering both DBA and DEC-A conditions.
Improvements mostly were applicable for the thermal mechanic phenomena in the fuel rods (LOCA) and FP release, transport and behaviour in primary and/or secondary circuit (SGTR). Thus, in the second set of calculations, no significant changes in thermos-hydraulic results were noticed, except for some partners. Biggest changes were achieved in thermo-mechanical calculation results and fission product releases.
This section presents a summary of the comparison results of the first and second set calculation results. LOCA and SGTR results are discussed in the different chapters.

3.4.1 Overview and discussion of LOCA calculation results

For LOCA scenario most of the partners achieved significant lower fuel rod burst percentage after provided improvements and considered more realistic assumptions, especially for DBA where in the first set of calculations mostly conservative ones have been used. This directly involved a significant reduction in FP release to the primary circuit then transport to containment and environment. In the DBA scenarios, the reduction of the activity in the environment was achieved from 90 % (for partners who did not use decoupling factor for fuel rod burst (i.e. IRSN or ENEA) to 100% (for partners who assumed 100% failed fuel rods). For DEC-A scenario it ranges from 7% to 54% for partners not using decoupling factor and to 100% for partners assuming 100% of failed fuel rods. Second set of the calculations showed also less scatter of results between partners, for VVER type reactors the environmental activities were found to differ by one order of magnitude for DEC-A up to two for DBA and for PWR type reactors differences ranged from a factor 1.2 to 4 respectively for DEC-A and DBA conditions.

VVER calculations, DBA scenario.
For LOCA transient in the case of the DBA scenario five calculations from four partners were provided. For the first set of the calculations all partners used very conservative assumptions for the burst of the fuel rods in the core, assuming that all fuel rods in the core have burst (Figure 3). These conservative assumptions were based on the

regulatory practices in their country. In updated calculations, all partners except one calculated the fuel rod failure, where sometimes a margin has been superimposed. In some of the cases the percentage of the burst fuel in the core were reduced almost 100 % (Figure 3). The maximum value of fuel rod burst fraction in updated calculations was 33%, assumed by one partner.

In analysed scenarios only the design leakage from the containment to the environment was considered. The activity in the environment is then constantly increasing (except one partner, who conservatively assumed instant fission product release), and the increase rate is a function of the pressure difference between containment and environment. Figure 4 presents the calculated activity in the environment after approximately 24 hours (except for one partner assuming instantaneous releases), the maximum value reaching slightly over 1E+13 Bq i.e. about one order of magnitude less compared to the initial calculations. This is mainly explained by the reduction of conservatisms (especially the use of a decoupling factor for the failed fuel rod fraction). These results were achieved by application of improved calculation strategies – i.e. using more detailed fuel rod modelling tools, updated (i.e. for clad plastic deformation) computational models and/or applying new cladding burst criteria. In the second set of calculations some partners also improved the core modelling/nodalization, the fission product release from the fuel transport mechanisms (including dilution) in reactor cooling system and behaviour in containment.

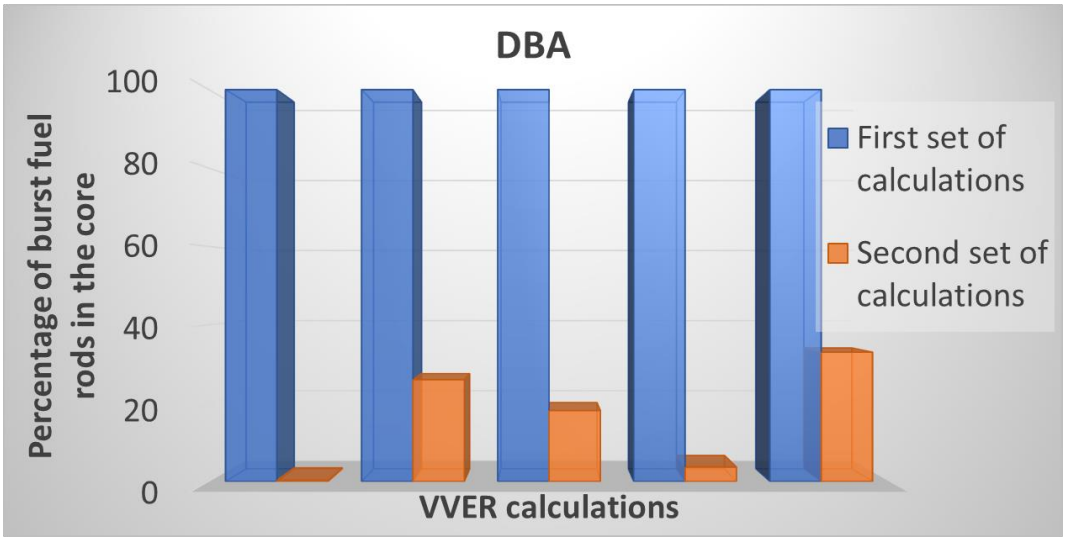

Figure 3. Percentages of burst fuel rods in LOCA DBA transients from VVER initial and final calculations.

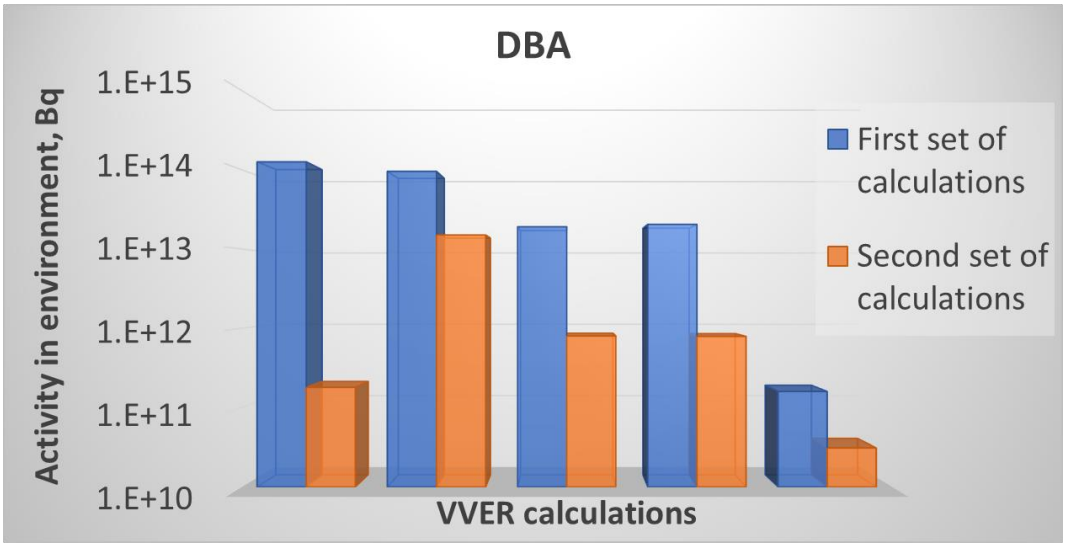

Figure 4. Activity in environment for LOCA DBA transients (DEGB) from VVER initial and final calculations.

The corresponding thyroid equivalent and total effective doses calculated by all partners (except one) for adults using the simplified radiological tool developed within the project are displayed respectively in figure 5 and 6. As expected, due to lower environmental activity calculated in the second set the radiological consequences for adults are significantly lower compared to the first set of calculations results, well below dose limits as expected for DBA transients.

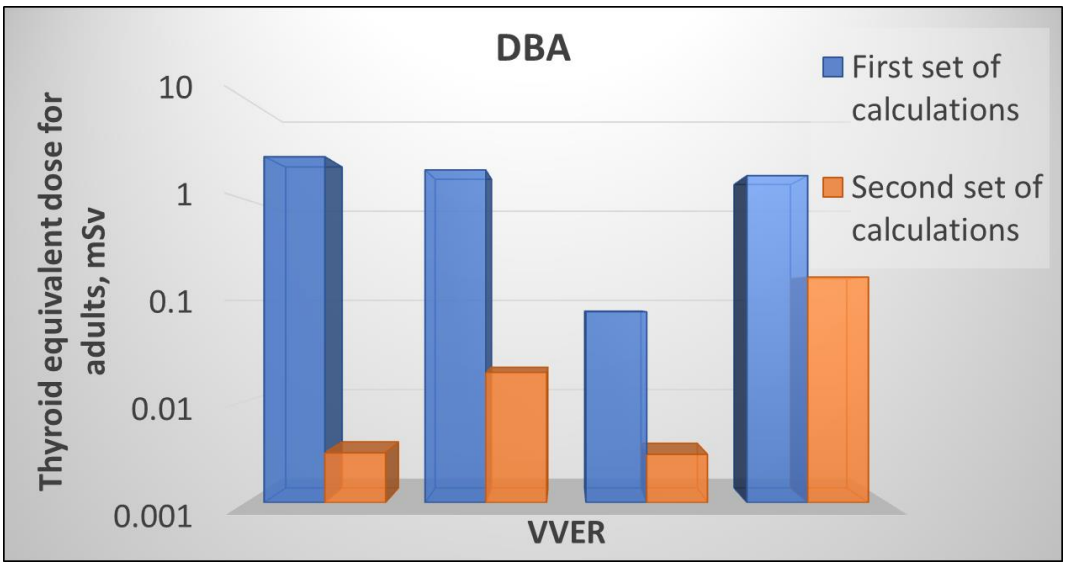

Figure 5. Thyroid equivalent doses for adults for LOCA DBA transients (DEGB) from VVER initial and final calculations.

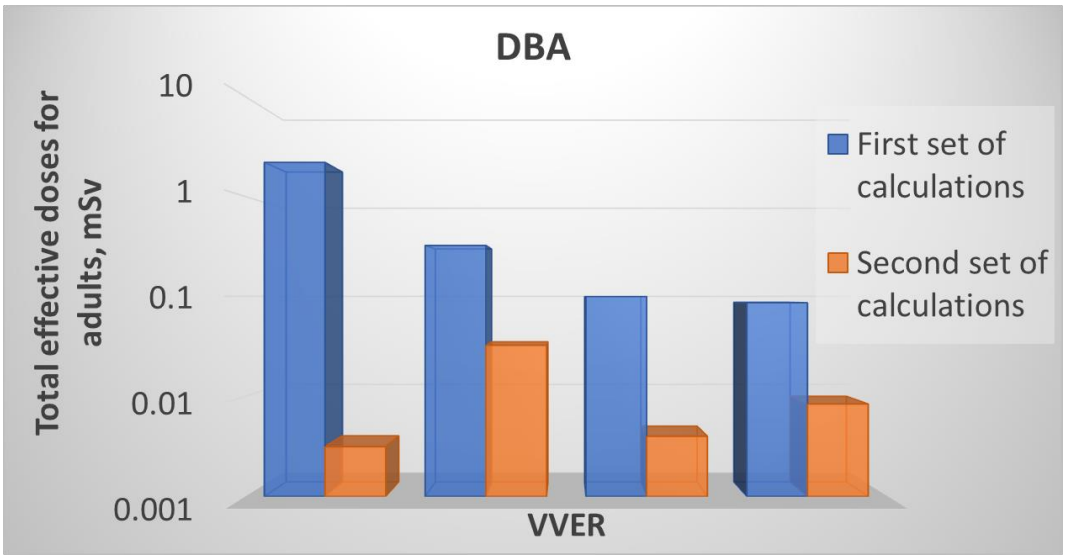

Figure 6. Total effective doses for adults for LOCA DBA transients (DEGB) form VVER initial and final calculations.

VVER calculations, DEC-A scenario.

For LOCA DEC-A transients 3 calculations from 2 partners were provided. As for DBA case, for the first set of the calculations all partners decided to use very conservative and decoupled assumptions for the burst of the fuel rods in the core. Indeed, as for DBA case, it was assumed that all fuel rods in the core have burst (Figure 7). These assumptions were based on the regulatory practices in their country. In some of the cases the percentage of the burst fuel in the core were reduced almost 100 % (Figure 7). The maximum percentage of fuel rods calculated to fail is only around 6% also taking some conservatism. It is needed to emphasize that in the case of DEC-A scenario realistic (best estimate) initial and boundary conditions were used, while in DBA scenario initial and boundary conditions were conservative. As in the case of DBA scenario, only design leakages from containment to environment were considered. The activity in the environment is then constantly increasing (except one partner, who conservatively assumed instant fission product release), and the increase rate is a function of the pressure difference between containment and environment. Figure 8 presents the results of the calculated environmental activity after approximately 24 hours. The maximum value in updated calculations is slightly over 1E+12 Bq i.e. about 2 orders of magnitude less compared to initial calculations. This is mainly explained by the non-use of the conservative and decoupled assumption related to the number of burst rods as initial and boundary conditions were kept similar as in the first set of calculations. In updated calculations, all partners calculated the fuel rod failure. In updated calculations, the fuel rod burst evaluations were improved by application of different calculation strategies (i.e. use of more detailed fuel rod modelling tools, updated core modelling/nodalization). In the second set of the calculations some of the partners also, more accurately modelled the fission product release from the fuel and its transport mechanism in reactor cooling system and behaviour in containment.

Decrease of the number of the burst fuel in the core also reduced the activity in the environment (Figure 8) by more than one order of magnitude in maximum values of second set comparing to the first set calculation results.

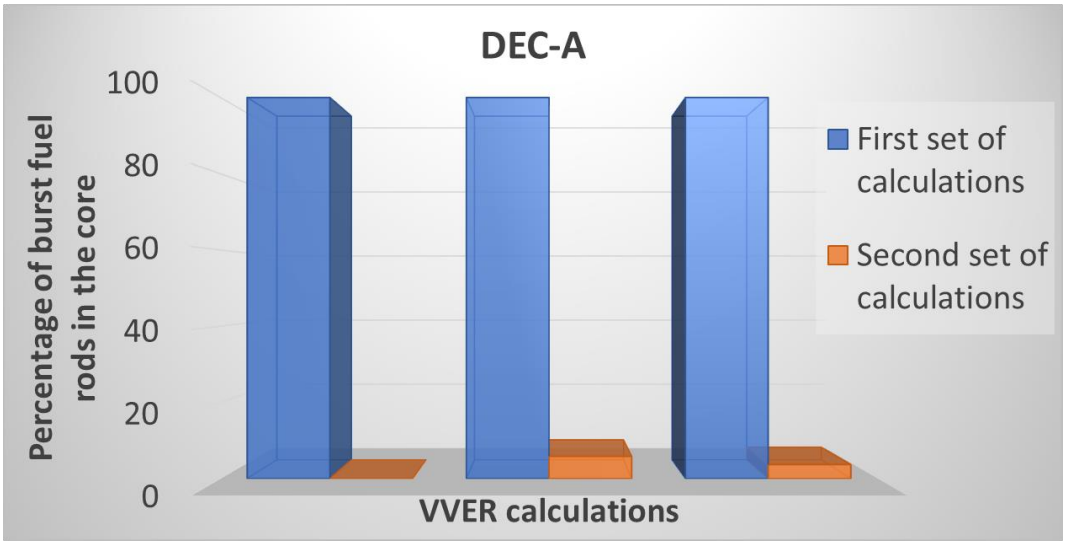

Figure 7. Percentage of burst fuel rods in the core for LOCA DEC-A transients (DEGB) from VVER initial and final calculations.

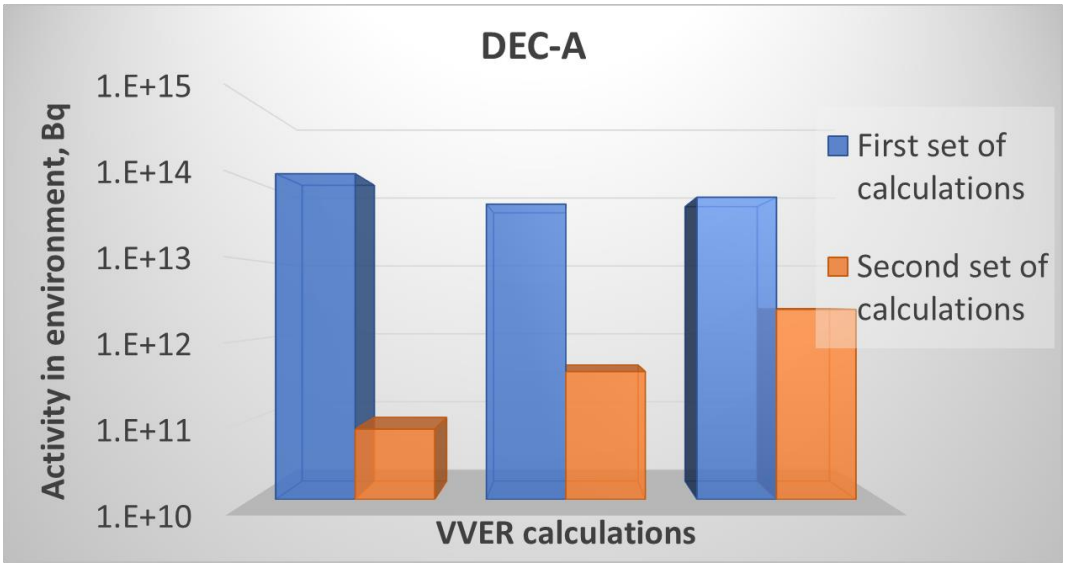

Figure 8. Activity in environment after 24 hours for LOCA DEC-A transients (DEGB) from VVER initial and final calculations.

The corresponding thyroid equivalent and total effective doses calculated by all partners for adults using the simplified radiological tool developed within the project are displayed respectively in figure 9 and 10. As expected, due to lower environmental activity calculated in the second set, the radiological consequences for adults are significantly lower comparing to the first set of calculations results. From the figures is clearly seen that due to lower activity in the second set of calculations the radiological consequence for adults is significantly lower comparing to the first set of calculations results.

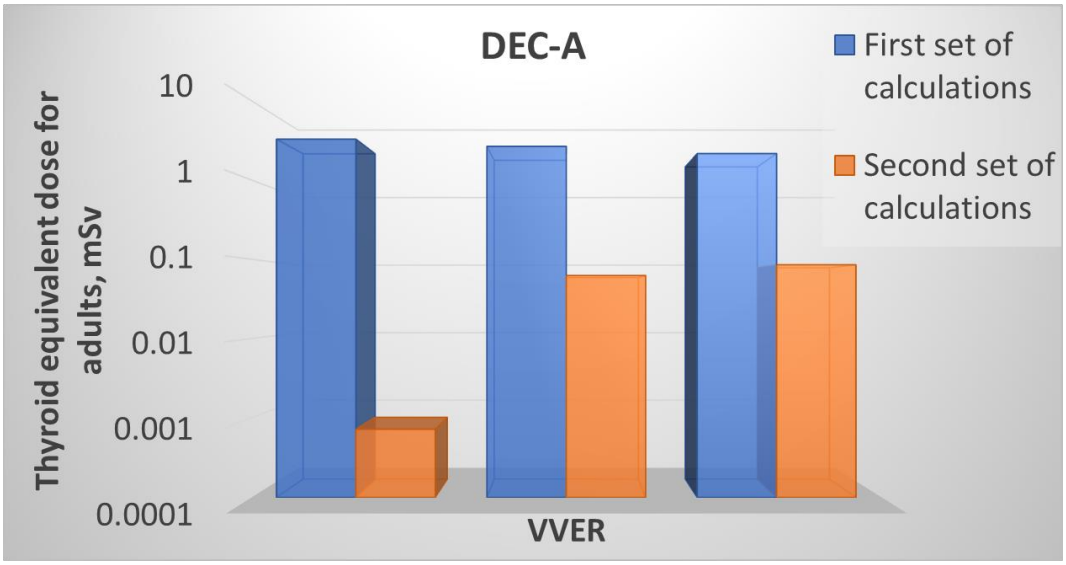

Figure 9. Thyroid equivalent doses for adults for LOCA DBA transients (DEGB) from VVER initial and final calculations.

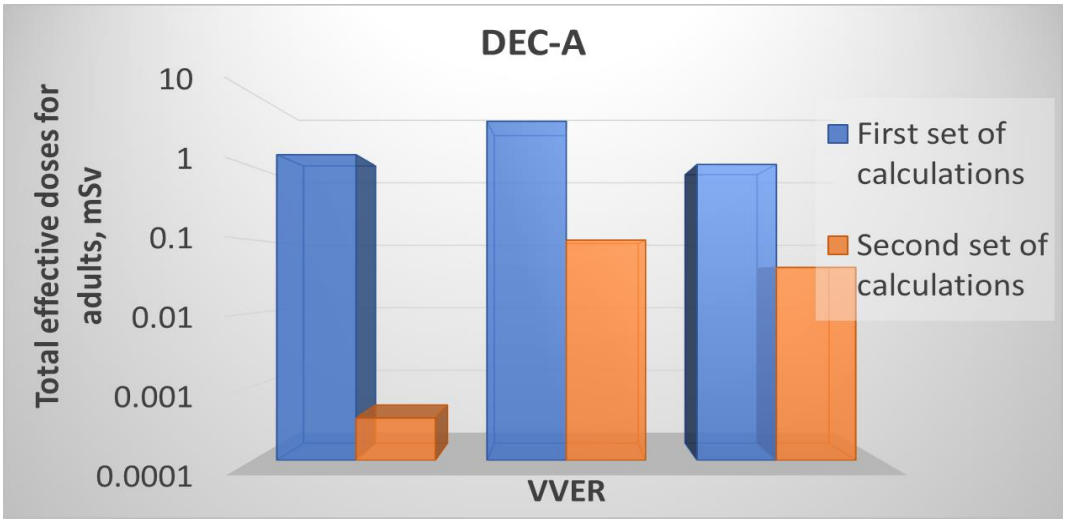

Figure 10. Total effective doses for adults for LOCA DBA transients (DEGB) from VVER initial and final calculations.

PWR calculations, DBA scenario.

For LOCA DBA transient two PWR-900, one Konvoi and one EPR reactors were analysed. For the first set of calculations, only one partner decided to use conservative assumptions for the burst of the fuel rods in the core (Figure 11), based on the regulatory practices in its country. Other partners already in the first set of the calculations decided to use more detailed codes or integral codes to evaluate the failed fuel rod number. In the second set of calculations, however improvements were performed where new calculation chain was used including a more detailed modelling of the core, updated thermomechanical models for simulating the behaviour of the fuel rods during the accident were used (or i.e. new cladding creep and phase transformation laws as well as new fuel failure criteria were implemented in calculation tools). It allowed us to slightly reduce the number of the burst fuel in the core. For EPR calculation, the new cladding creep and phase transformation laws together with the new fuel failure criteria used in the second set of calculations gave slightly higher number of fuel rod burst in the core.

The reduction of the number of burst fuel rods in the core has direct influence in the predicted environmental activity (Figure 12). For EPR reactor, no activity release was calculated, because the model improvements were focused on thermomechanical processes.

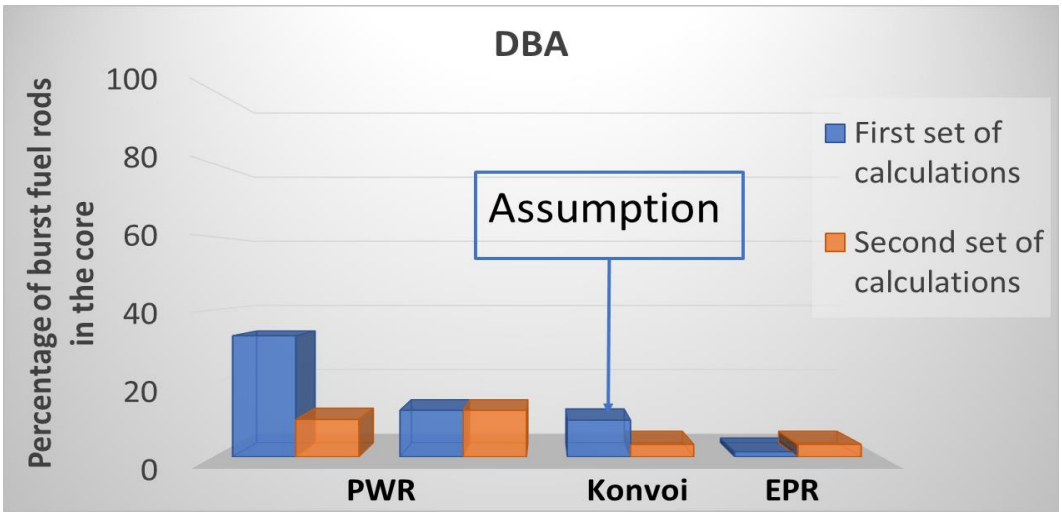

Figure 11. Percentage of burst fuel rods in the core for LOCA DBA transient from PWR initial and final calculations.

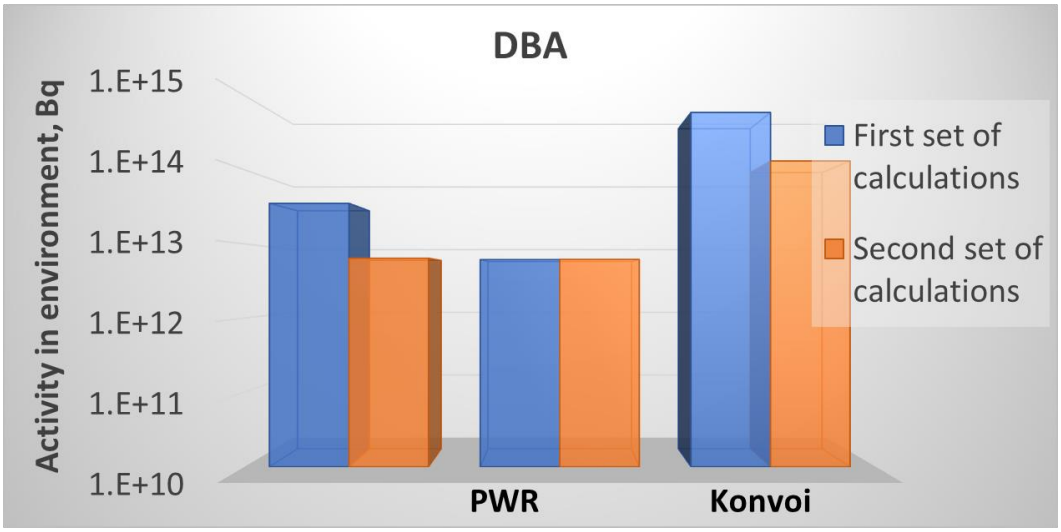

Figure 12. Activity in environment for LOCA DBA transient from PWR initial and final calculations.

The corresponding thyroid equivalent and total effective doses calculated by all partners for adults using the simplified radiological tool developed within the project are displayed respectively in figure 13 and 14. Doses are given only for the PWR-900 reactor, no radiological consequences were evaluated for the Konvoi reactor. As seen on the figures, for the case where lower environmental activity was calculated in the second set, the radiological consequences (i.e. both the thyroid equivalent and the total effective doses) for adults are significantly lower comparing to the first set of calculations results. However, for the partner who calculated similar environmental activity in both sets, the radiological consequences are slightly higher as it was in the first set of calculations. This is especially the case for the thyroid equivalent dose and was explained by a higher retention of this nuclide in the primary circuit. For all the calculations, the radiological consequences are always low (below the dose limits), especially for the updated evaluations.

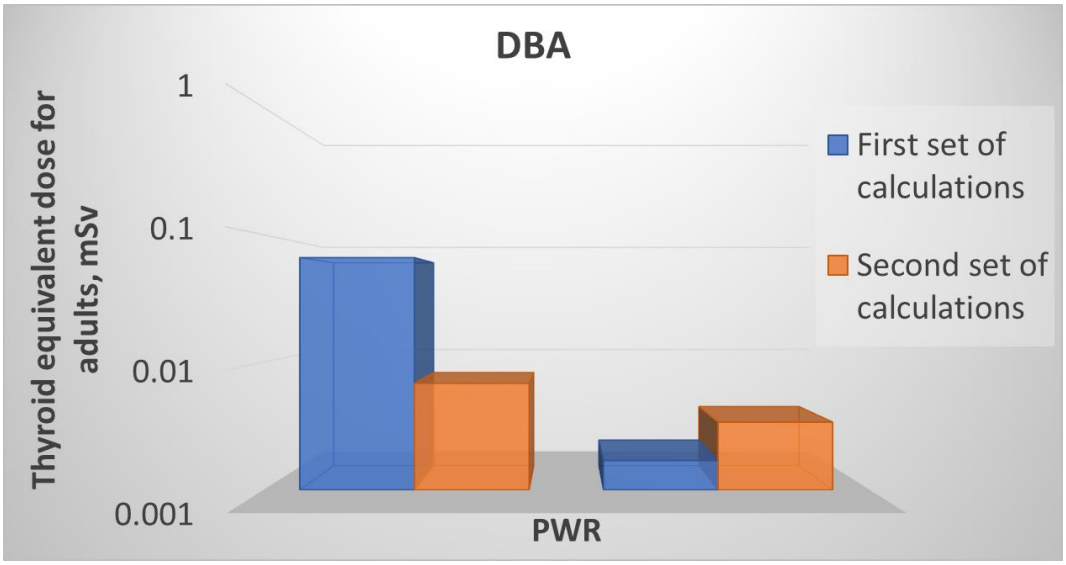

Figure 13. Thyroid equivalent doses for adults for LOCA DBA transients from PWR initial and final calculations.

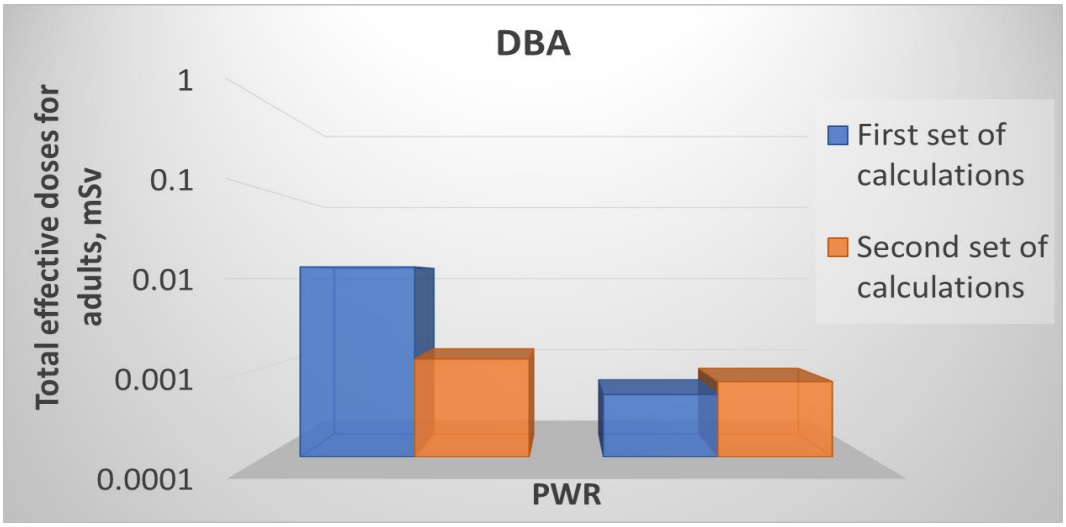

Figure 14. Total effective doses for adults for LOCA DBA transients from PWR initial and final calculations.

PWR and BWR calculations, DEC-A scenario.

For LOCA DEC-A transients, analyses for two PWR-900 and one BWR-4 reactor were provided. All partners already used in their first set of calculations integral codes with thermomechanical models to simulate the fuel rod behaviour during the transient and clad failure criteria as well as FP release and transport model in the primary circuit and containment. In the second set of calculations however, most of the partners improved their calculation chains mainly focusing on clad burst models and criteria and core modelling. The calculated percentage of burst fuel rods in the core in case of LOCA DEC-A transient is presented in Figure 15. For PWR calculations, the second set of calculations showed greater or equal percentage of the burst fuel rods in the core. Both calculations used new clad burst models/criteria, but the core modelling was different. One of them using a new calculation chain with a 3D core modelling as the other one used the same core description in five concentric rings as in the initial calculations. For BWR calculations the second set of calculations showed lower number of fuel rods burst due to a refined core nodalisation. The results showed a direct impact of the number of burst fuel rods on environmental activity only for BWR calculation (Figure 16). For PWR calculations indeed, due to the use of new code version or new calculation chain as well as, for one partner, change in the assumption regarding leaks to environment the link between failed rod number and environmental activity is not so obvious and sometimes even counter intuitive.

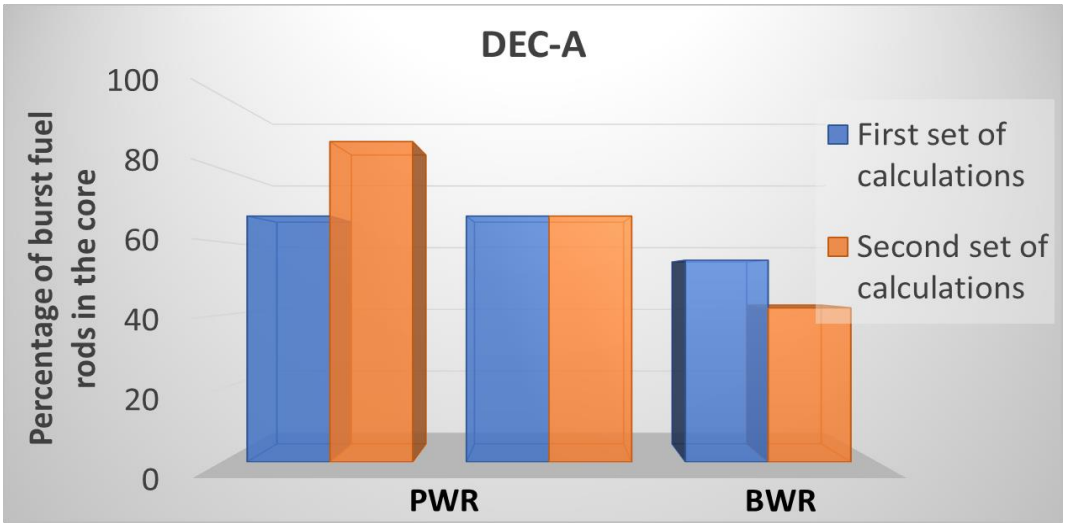

Figure 15. Percentage of the burst fuel rods in the core in the case of the LOCA DEC-A transient from PWR and BWR initial and final calculations.

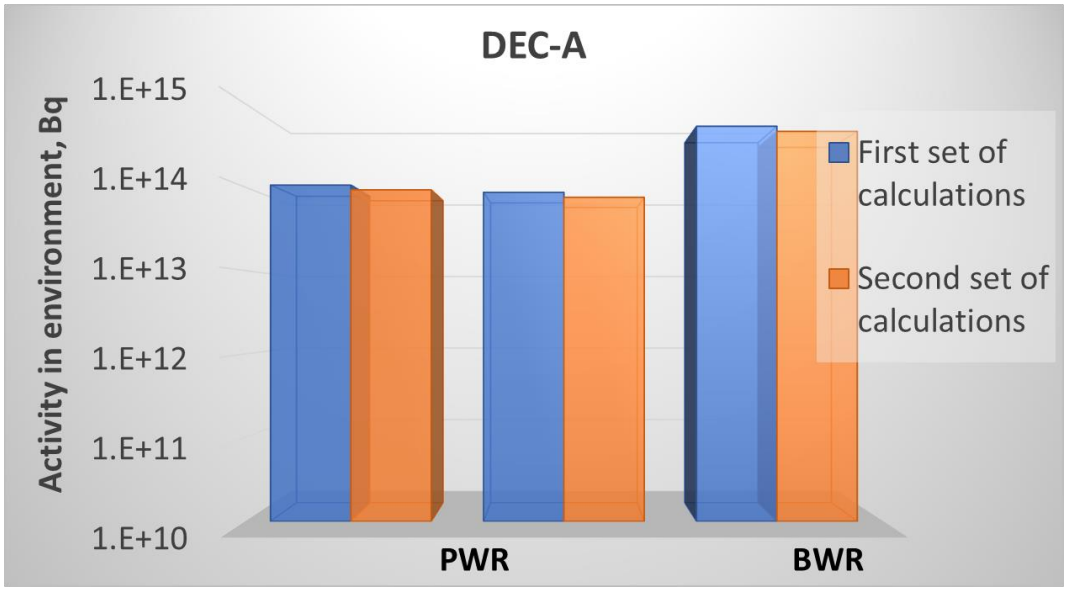

Figure 16. Environmental activity for LOCA DEC-A transient from PWR & BWR initial and final calculations.

The corresponding thyroid equivalent and total effective doses calculated by all partners for adults using the simplified radiological tool developed within the project are displayed respectively in Figure 17 and Figure 18. One of the partners calculating PWR reactor case for the second set of calculations received a higher percentage of fuel burst rate, however the activity in the environment was calculated lower comparing to the first set of calculations. This is because in the second set of calculations the partner used auxiliary buildings in to account what was not the case for the first set of calculations.

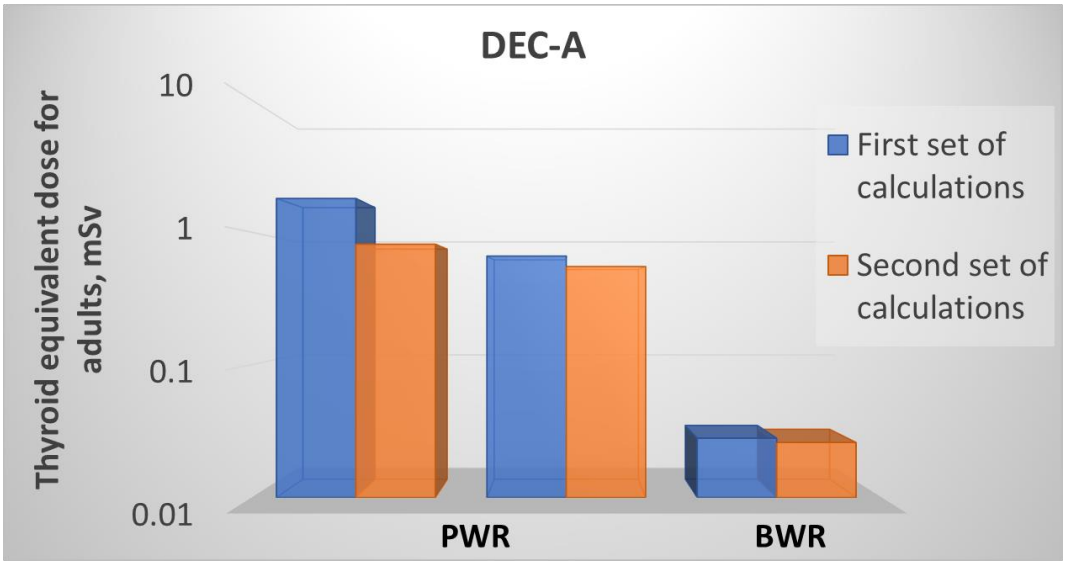

Figure 17. Thyroid equivalent doses for adults for LOCA DEC-A transients from PWR and BWR initial and final calculations.

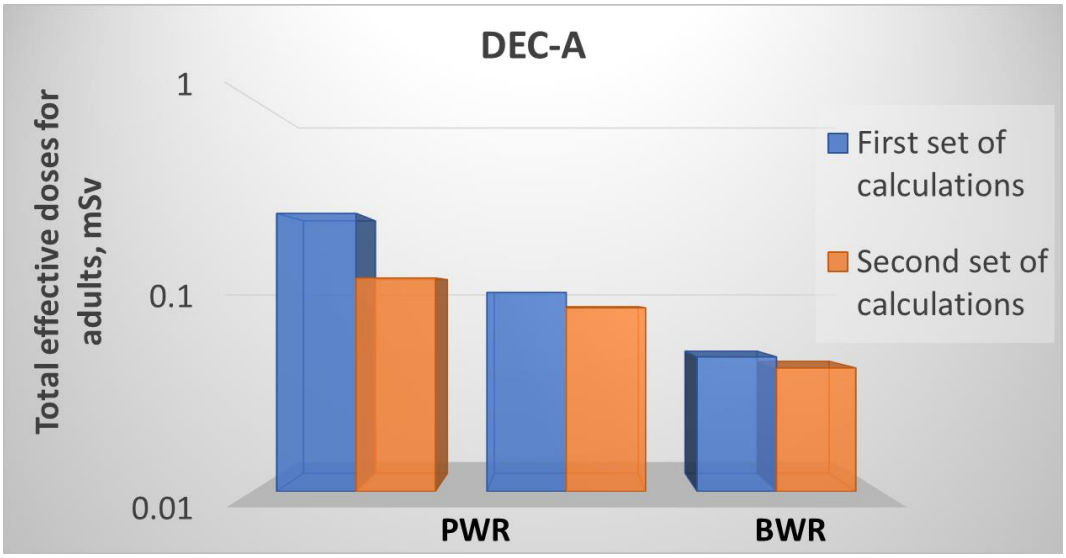

Figure 18. Total effective doses for adults for LOCA DEC-A transients from PWR and BWR initial and final calculations.

3.4.2 Overview and discussion of SGTR calculation results

As a remainder, for the 2nd set of calculations, the improvements made were of two kinds:

- Modelling improvements: For SGTR transient calculations, partners dedicated improvements on the fission product modelling: initial primary contamination and spiking, dilution in RCS, transport, scrubbing, partitioning, atomisation, speciation etc. Partners also improved their thermohydraulic model using refined model for the relief/safety valves of the SG or by applying enhanced EOP.
- Improvements in the calculation chains: Detailed (mechanistic) computer codes were involved in the partners calculation chain as a support of less detailed codes for most of the part. For SGTR transient calculations, detailed codes were used for spiking, FP transport and dilution thanks to CVCS operation. Some of the partners used different modelling approaches comparing to what was used in the first set of the calculations.

As such, for SGTR scenarios, partners improved their simulation scheme mainly on the FP inventory and transport aspects. Therefore, except for two partners who also improved their thermohydraulic transient, there is no change on the calculated cumulative steam/liquid water released in environment. Thanks to more realistic models for FP transport in the RCS and SG, partners generally achieved a reduction of the activity releases in the environment between 17 to 97 %. Nonetheless, two partners calculated higher activity releases with the second set of calculations.

Radiological consequences were evaluated for the first and second sets of calculations. The results are consistent with what is observed with the activity releases to the environment: radiological consequences are reduced in the second set of calculations compared to the first one, except for two SGTR transients.

The calculated doses for all SGTR transient conditions (DBA and DEC-A) stayed under acceptance criteria.

VVER calculations, DBA scenario.

For VVER type reactors (440 and 1000), SGTR transients in the case of the DBA scenario, 19 calculations from 5 partners were provided. The initiating event was not the same for all partners (break in the SG collector, break of SG tube(s), number/diameter of broken tubes,) but some identical initiating events may be found for different partners. The main improvements made by the partners between 1st and 2nd set of calculations are diversified: improvement of the SG relief/safety valves thermohydraulic correlation (ARB), consideration/improvement of the dilution in the RCS (ARB, SSTC NRS, BOKU), improvement of the spiking model (EK, BOKU), improvement of the

FP transport (SSTC NRS, UJV-NRI, BOKU) and improvement of the pool scrubbing model in the SG (BOKU). For the VVER reactor calculations, only ARB improved their TH with the use of a refined model for SG relief/safety valve correlations with DRIFT FLUX. Thanks to this improvement, the affected SG cumulative liquid and steam masses released to the environment was generally slightly reduced (less than 8%) for the 2nd set of calculations compared to the 1st one (see Figure 19). Overall, the cumulative liquid water and steam released to the environment is between 0.218 and 429 t for the VVER 440 calculations. EK only computes 0.218 t of water going into the environment because releases from the SG are first going in the containment and there is a lot of retention in the containment. For VVER 1000 calculations, the cumulative liquid water and steam released to the environment is between 90 and 730 t. As explained in D2.5 [16], differences observed in the primary to secondary and secondary to environment discharges could be explained mainly by the differences in the scenario, in the SGTR break sizes, the IS duration, automatic procedures and operator actions, in the secondary to environment discharge capacities (SG relief and safety valves discharge capacities, setpoints, failures, operator actions, etc.) and in the considered initial and boundary conditions (additional single/multiple failure(s), best estimate/penalized parameters). These differences may also impact the evolution of the pressure in the RCS and in the affected SG that will further influence the water and steam released.

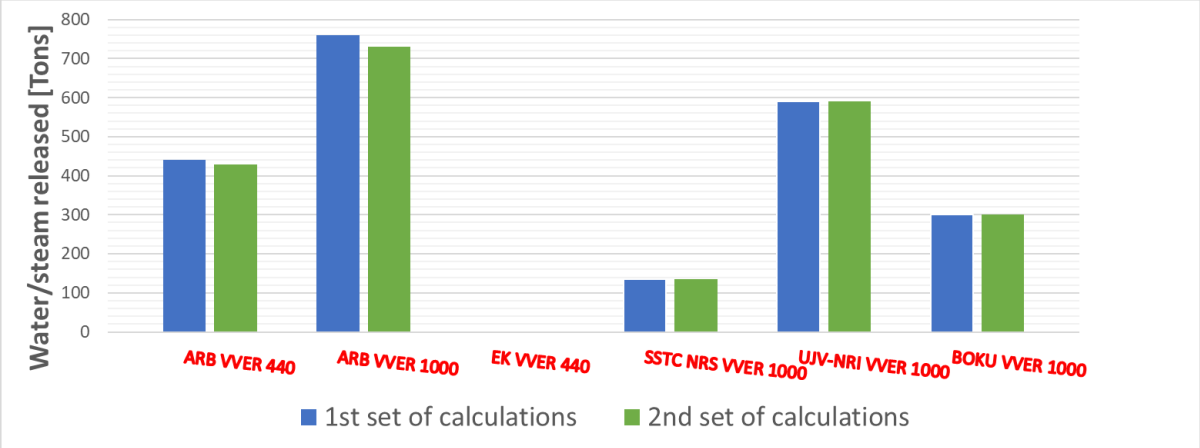

Figure 19. Cumulative liquid water and steam released to environment for VVER type SGTR DBA calculations.

Thanks to the improvements made by the partners, the calculated activity released to the environment is reduced between 23% to 72% for the 2nd set of calculations compared to the first one (see Figure 20). For VVER-440 reactor type, the calculated integral activity released to the environment in the 2nd set of calculations is ranging from 1.6e+12 Bq to 2.3e+13 Bq. For VVER-1000 reactor type, the calculated integral activity released to the environment in the 2nd set of calculations is ranging from 1.2e+10 Bq (BOKU) to 1.5e+15 Bq (UJV-NRI). The calculation results show that the results may differ up to 5 orders of magnitude. The differences may be due to several reasons: the ones already listed before for the water/steam released in the environment, differences on the initial FP inventory and spiking, differences on the isotopes considered, differences on the dilution in the RCS, differences on the transport phenomena through the SGTR break and in the SG (atomization, flashing, partitioning, scrubbing), differences in the consideration of activity releases in the steam phase only or in both liquid and steam phases etc; differences in the time period considered for releases.

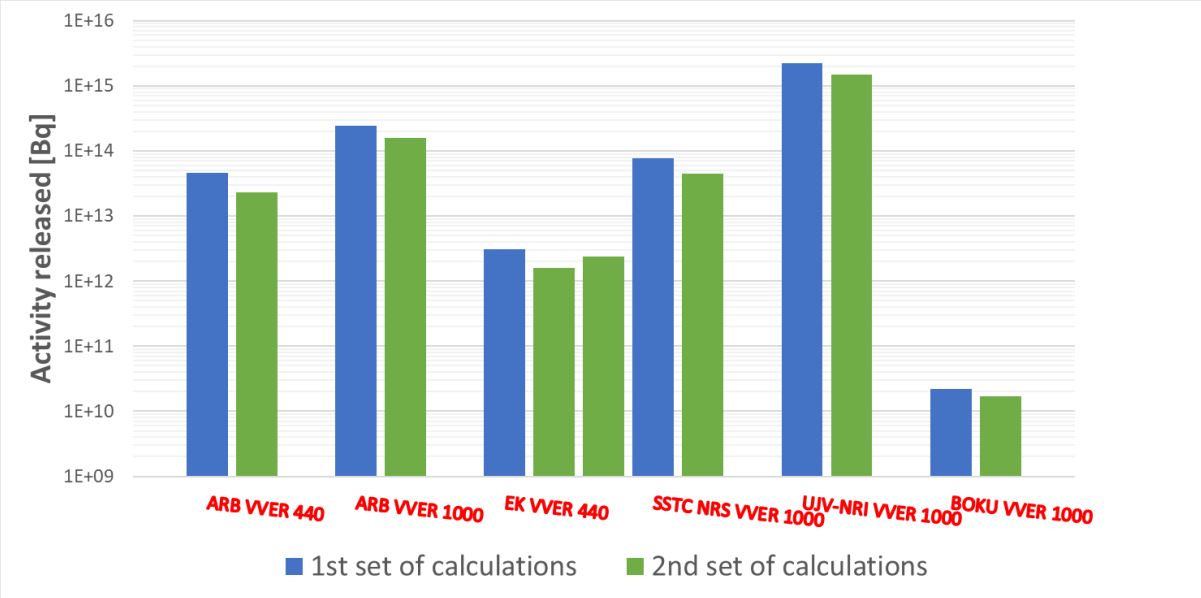

Figure 20. Activity in environment in the case of the SGTR transients for VVER type DBA scenarios from initial and final calculations.

For instance, regarding the large activity releases calculated by UJV-NRI for VVER-1000 (1.5e+15 Bq compared to 1.8e+13 Bq for ARB), for the same scenario (1 SG tube rupture) several explanations can be found:

- The use of conservative initial and boundary conditions with maximum allowable activity concentration in the RCS considered for UJV-NRI (I131: 2.36e+15 Bq vs 2e+13 Bq for ARB).
- Depressurization of the RCS is slow compared to ARB leading to a flow rate at the SGTR break which becomes never zero (cumulative mass from RCS to SG is 250 t compared to 40 t for ARB).
- In the SG, depressurization is also very slow and ends at the end of the calculation (22000 s) provoking constant release of water/steam through the RV: 590 t are released in the environment compared to 90 t for ARB.

On the other hand, for BOKU, low activity releases are calculated (around 1e+10 Bq) for VVER-1000 compared to ARB and SSTC for the same scenario (SG collector lift-up). This may be explained by several reasons:

- Compared to ARB and SSTC NRS, initial RCS contamination and spiking is one order of magnitude lower.
- Only Iodine 131 is considered.
- Compared to 1st set of calculations, implementation of clean up system in the RCS and pool scrubbing in the SG (for scenarios for which the affected SG contains liquid water) in 2nd set may explain the lower releases.
- As the cumulative water/steam release to environment is consistent with what is observed for similar scenarios from other partners (ARB/SSTC), differences may reside only on the reasons explained before.

Meanwhile, for VVER 440 calculations, only ARB and EK provided results. EK computes activity releases which are one order of magnitude lower than the ones calculated by ARB for equivalent scenarios. As a matter of fact, initial radionuclide inventory in the RCS is higher for EK than for ARB (~2e+15 Bq compared to 4.6e+13 Bq for ARB), but releases from SG for EK are first going to containment and then to environment. There is a lot of retention in containment and only 218 kg of water/steam is released from containment for EK compared to 189 tons for SG collector lift up 40 mm and 101 tons for 3 tubes SGTR calculated by ARB.

Eventually, radiological consequences have been evaluated by most of the partners. All population age groups are represented. The same observations as for the activity releases can be noticed, i.e. reduction of radiological

consequences, between 11% and 89% for VVER DBA calculations (both for thyroid and total effective dose). The thyroid dose calculated for the VVER 440 transients is ranging from 0.16 to 7.44 mSv while for VVER 1000 transients, thyroid dose is ranging from 0.79 to 304 mSv (see Figure 21). The total effective dose calculated for the VVER 440 transients is ranging from 0.01 to 0.197 mSv while for VVER 1000 transients, total effective dose is ranging from 0.063 to 15.5 mSv (see Figure 22). The large discrepancies on the dose for the VVER 1000 transients may be explained by what was already stated for the activity releases, but also by the fact that even if the radiological consequences tool is common for all partners, the use of this tool may be different between partners: FPs considered, height, distance considered and if the partner only considered steam releases or both releases in liquid and steam phases.

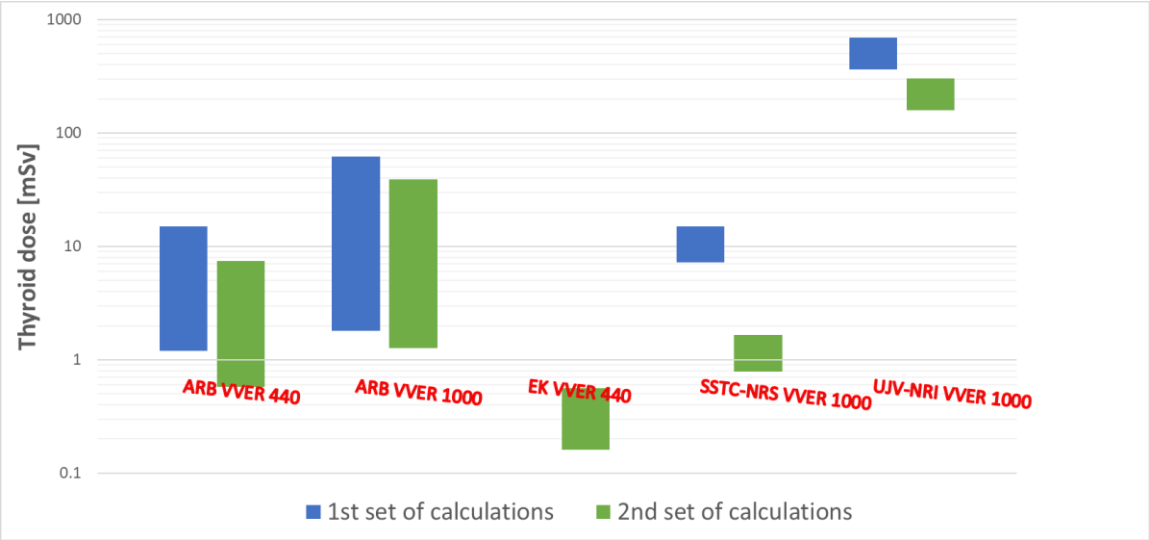

Figure 21. Thyroid equivalent dose for all population age groups in the case of the SGTR transient for VVER type DBA scenarios from initial and final calculations.

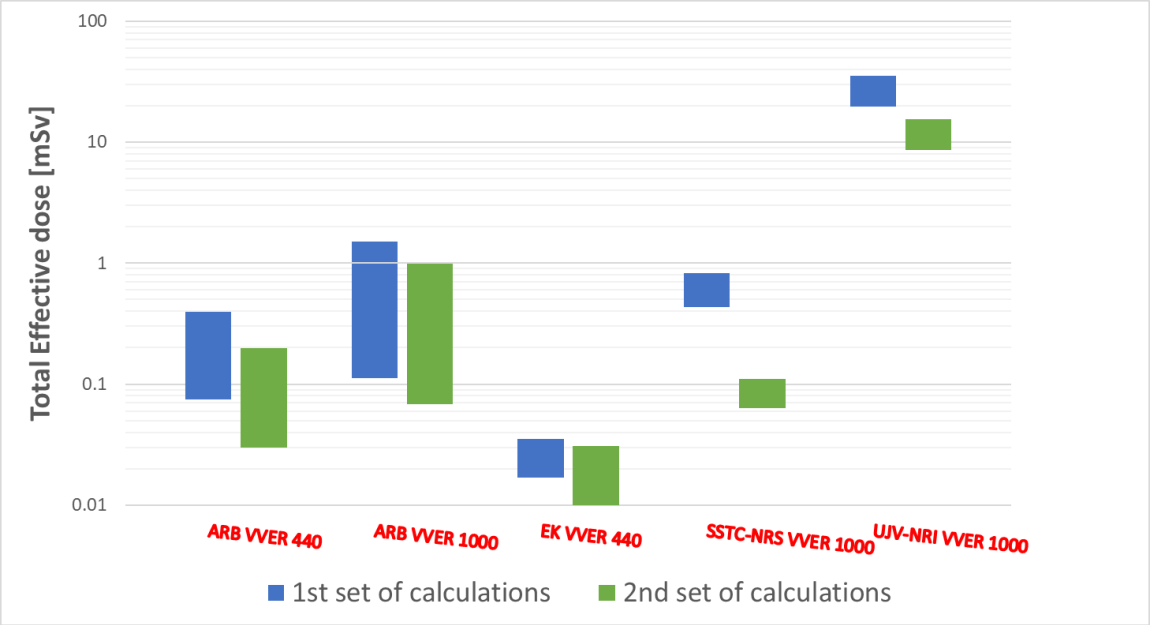

Figure 22. Total effective doses for all population age groups in the case of the SGTR transient for VVER type DBA scenarios from initial and final calculations.

VVER calculations, DEC-A scenario.

For VVER type reactors (440 and 1000), SGTR transients in the case of the DEC-A scenario, 17 calculations from 3 partners were provided. The initiating event was not the same for all partners (break in the SG collector of different sizes, break of SG tube(s), number/diameter of broken tubes,) but some identical initiating events may be found for different partners. The main improvements made by the partners between 1st and 2nd set of calculations are diversified and identical compared to DBA scenario: improvement of the SG relief/safety valves thermohydraulic correlation (ARB), consideration/improvement of the dilution in the RCS (ARB, SSTC NRS, BOKU), improvement of the spiking model (BOKU), improvement of the FP transport (SSTC NRS, BOKU) and improvement of the pool scrubbing model in the SG (BOKU). For the VVER reactor calculations, only ARB improved their TH with the use of a refined model for SG relief/safety valves correlations with DRIFT FLUX. Thanks to this improvement, the affected SG cumulative liquid and steam masses released to the environment was slightly reduced (less than 8%) for the 2nd set of calculations compared to the 1st one (see Figure 23). Overall, the cumulative liquid water and steam released to the environment is between 60 and 430 t for the VVER 440 calculations. For VVER 1000 calculations, the cumulative liquid water and steam released to the environment is between 90 and 820 t. As explained in D2.5 [16], differences observed in the primary to secondary and secondary to environment discharges could be explained mainly by the differences in the scenario, in the SGTR break sizes, the IS duration, automatic procedures and operator actions, in the secondary to environment discharge capacities (SG relief and safety valves discharge capacities, setpoints, failures, operator actions, etc.) and in the considered initial and boundary conditions (additional single/multiple failure(s), best estimate/penalized parameters). These differences may also impact the evolution of the pressure in the RCS and in the affected SG that will further influence the water and steam released.

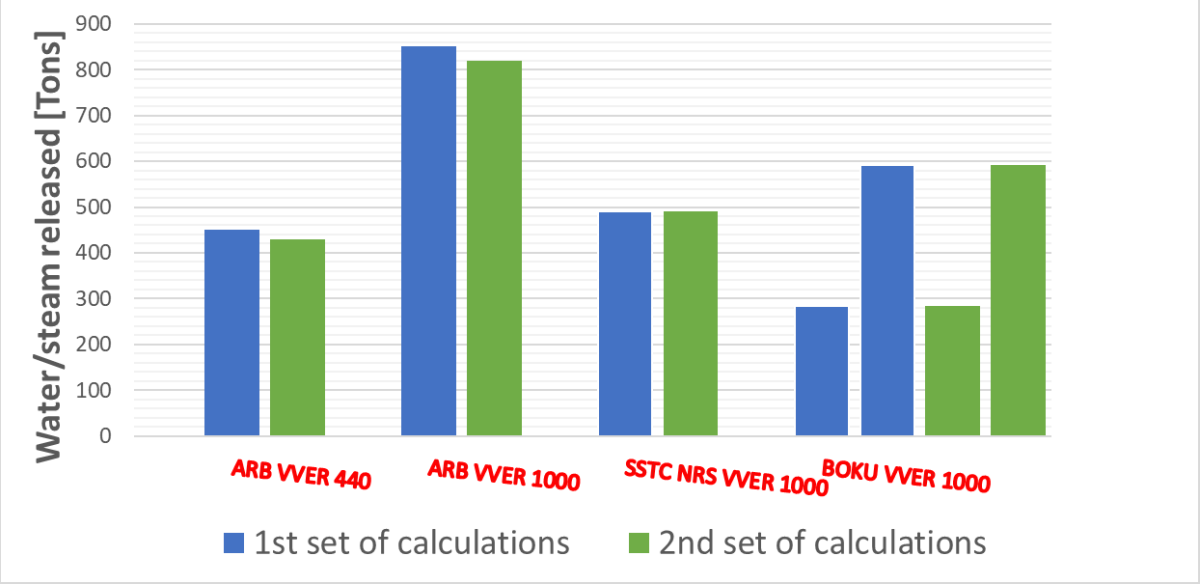

Figure 23. Cumulative liquid water and steam released to environment for VVER type SGTR DEC-A from initial and final calculations.

Thanks to the improvements made by partners, the calculated activity released to the environment is reduced between 18% to 71% for the 2nd set of calculations compared to the first one (see Figure 24). For VVER-440 reactor type, the calculated integral activity released to the environment from the 2nd set of calculations is ranging from 5.8e+12 Bq to 2.5e+13 Bq. For VVER-1000 reactor type, the calculated integral activity released to the environment from the 2nd set of calculations is ranging from 8.0e+9 Bq (BOKU) to 1.7e+14 Bq (ARB). When comparing to DBA results, releases are generally higher for DEC-A thanks to additional failure, except for the BOKU DEC-A scenario SGTR + MSLB because MSLB is inside containment while DBA scenario release directly to environment. The calculation results show that the results may differ up to 4 orders of magnitude. The differences

may be due to several reasons (same ones as for DBA): the ones already listed before for the water/steam released in the environment, differences on the initial FP inventory and spiking, differences on the isotopes considered, differences on the dilution in the RCS, differences on the transport phenomena through the SGTR break and in the SG (atomization, flashing, partitioning, scrubbing), differences in the consideration of activity releases in the steam phase only or in both liquid and steam phases and time period considered for the releases etc.

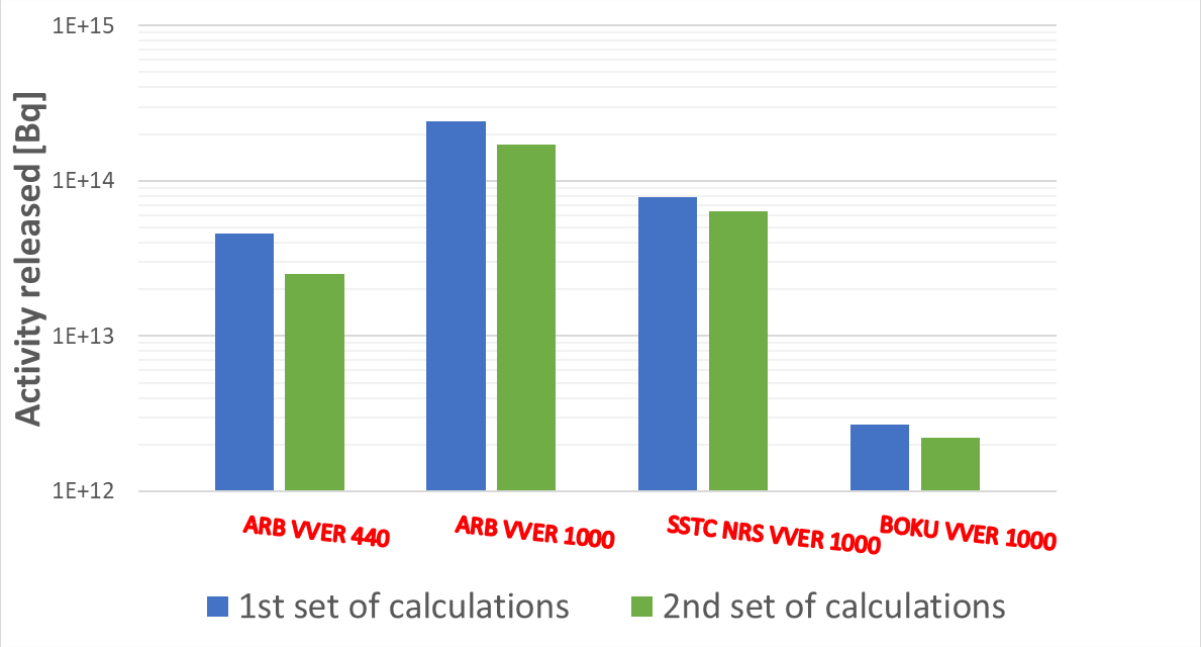

Figure 24. Activity in environment in the case of the SGTR transients for VVER type DEC-A scenarios from initial and final calculations.

For instance, for BOKU, low activity releases are calculated compared to ARB and SSTC NRS. The same reasons given for DBA can explain the differences.
On the other hand, SSTC NRS and ARB provide close results (6.4e+13 vs 1.6e+14 Bq) when comparing DBA scenario of ARB and DEC-A scenario of SSTC (collector cover lift up 100 mm + BRU-A [SG RV] stuck open) even if conservative conditions are considered by ARB and more realistic conditions are considered by SSTC NRS. Indeed, initial radionuclide inventory in the RCS and spiking is the same between both partners. But differences remain due to faster depressurization for SSTC NRS than for ARB: for SSTC NRS one train is unavailable so there is less HPSI and hydro accumulators mass flowrate and operators' actions are faster than ARB. Therefore, cumulative mass flow at the break is lower for SSTC NRS: 550 t compared to 800 t for ARB. In the end, cumulative water/steam released to environment is of 490 t for SSTC NRS and 820 t for ARB. On top of that, ARB considers activity releases in both liquid and steam phases while SSTC NRS only considers activity releases in steam/gas phase.
Eventually, radiological consequences have been evaluated by most of the partners. All population age groups are represented. The same observations as for the activity releases can be noticed, i.e. reduction of radiological consequences, between 27% to 84% for VVER DEC-A calculations (for thyroid and total effective doses). The thyroid dose calculated for the VVER 440 transients is ranging from 0.58 to 8.07 mSv while for VVER 1000 transients, thyroid dose is ranging from 1.12 to 40.6 mSv (see Figure 25). The total effective dose calculated for the VVER 440 transients is ranging from 0.03 to 0.216 mSv while for VVER 1000 transients, total effective dose is ranging from 0.07 to 1.07 mSv (see Figure 26). SSTC NRS and ARB provide relatively close results on the radiological consequences for VVER-1000 with only one order of magnitude of difference between results. However some discrepancies are still observable and they may be explained by what was already stated for the

activity releases, but also by the fact that even if the radiological consequences tool is common for all partners, the use of this tool may be different between partners: FPs considered, height, distance considered and if the partner only considered steam releases or both releases in liquid and steam phases.

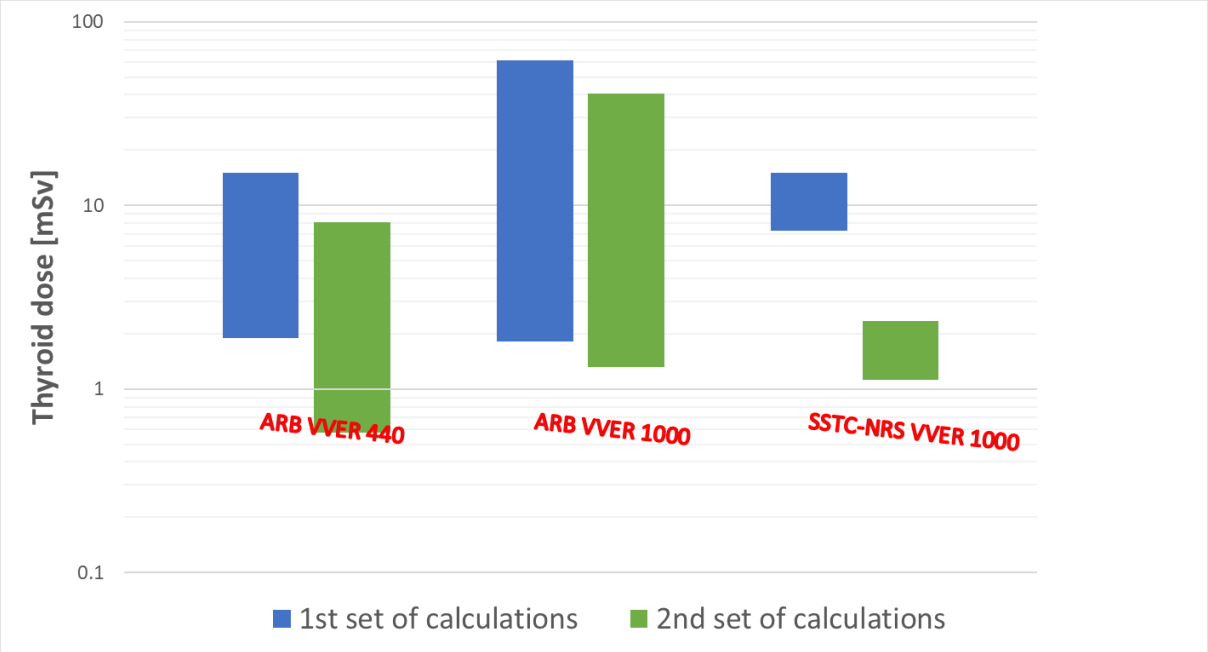

Figure 25. Thyroid equivalent dose for all population age groups in the case of the SGTR transient for VVER type DEC-A scenarios from initial and final calculations.

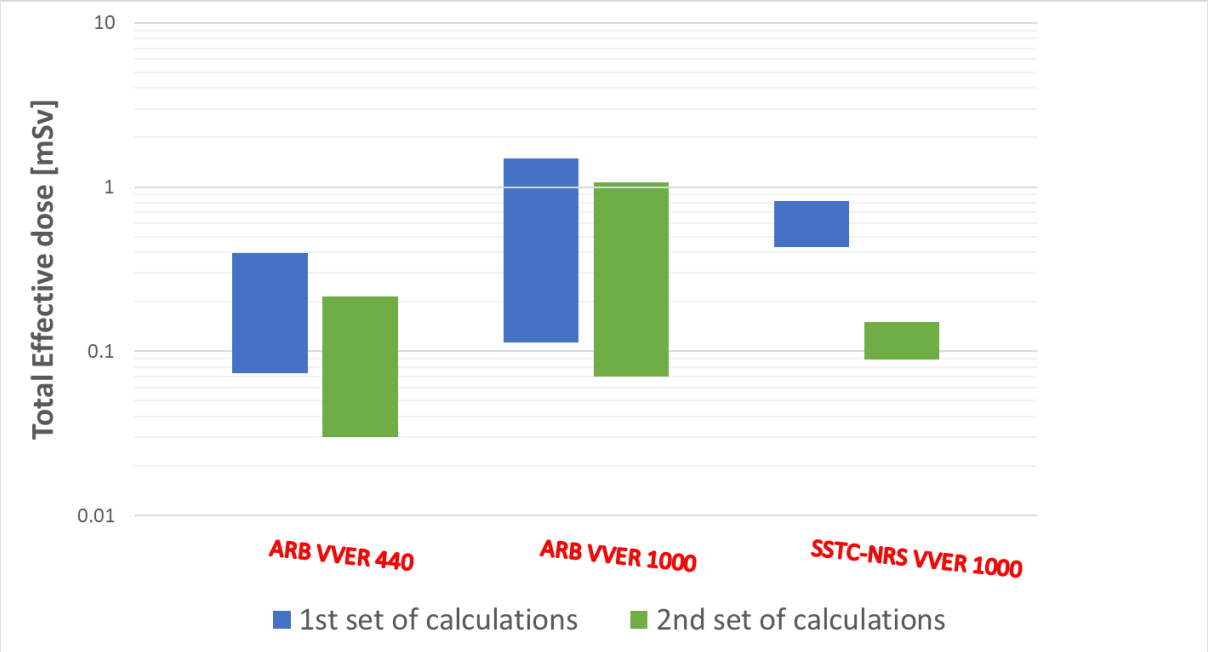

Figure 26. Total effective doses for all population age groups in the case of the SGTR transient for VVER type DEC-A scenarios from initial and final calculations.

PWR calculations, DBA scenario.

For PWR type reactors, SGTR transients in the case of the DBA scenario, 4 calculations from 4 partners were provided. The initiating event was rather close for all partners (SGTR 1 tube) and almost similar for IRSN, Bel V and CIEMAT (SGTR 1 tube + SG RV stuck open). The main improvements made by the partners between 1st and 2nd set of calculations are all related to FP/radionuclides physics/phenomena: improvement of the dilution in the RCS (BOKU, IRSN), improvement of the spiking model (BOKU, IRSN, CIEMAT, Bel V), improvement of the FP transport between primary and secondary and inside SG [atomization, partitioning, scrubbing, flashing] (BOKU, IRSN, Bel V, CIEMAT) and consideration of FP speciation (IRSN). For the PWR SGTR calculations within DBA conditions, no partner improved the thermohydraulic of their calculation, only slight changes were observed for IRSN and Bel V. Overall, the cumulative liquid water and steam released to the environment is between 74.8 and 172 t for the 2nd set of PWR DBA calculations (see Figure 27). As explained in D2.5 [16], differences observed in the primary to secondary and secondary to environment discharges could be explained mainly by the differences in the scenario, in the reactor model, in the SGTR break sizes, the IS duration, automatic procedures and operator actions, in the secondary to environment discharge capacities (SG relief and safety valves discharge capacities, setpoints, failures, operator actions, etc.) and in the considered initial and boundary conditions (additional single/multiple failure(s), best estimate/penalized parameters). These differences may also impact the evolution of the pressure in the RCS and in the affected SG that will further influence the water and steam released.

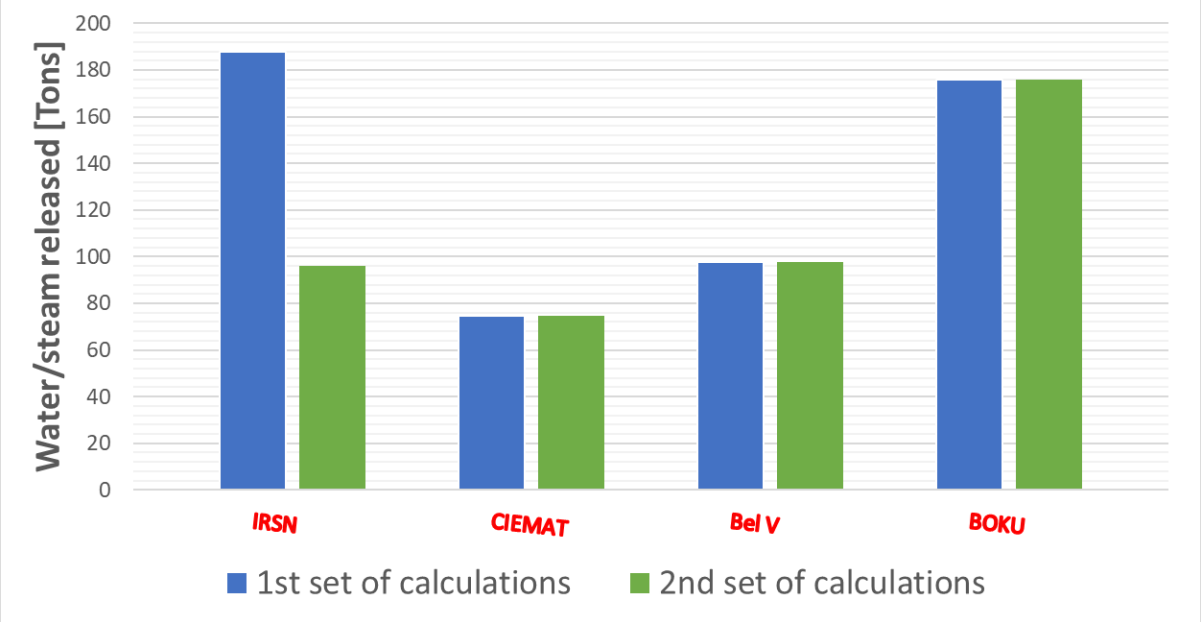

Figure 27. Cumulative liquid water and steam released to environment for PWR SGTR DBA from initial and final calculations.

Thanks to the improvements made by the partners, the calculated activity released to the environment is reduced between 24% to 80% for the 2nd set of calculations compared to the first one for BOKU and CIEMAT (see Figure 28). For Bel V, the improvements do not lead to noticeable changes in the activity releases. However, for IRSN, activity releases in 2nd set of calculations are twice the ones computed in the 1st set of calculations. Given that the cumulative liquid steam releases to environment are consistent with other partners (Bel V and CIEMAT), increase of activity releases in 2nd set of calculations may be explained by of the new calculation chain used in the 2nd set of calculations impacting FP dilution/filtration/transfer in RCS (thus initial RCS contamination and spiking), FP transport/physics between RCS and SG and inside failed SG (i.e. flashing) and FP speciation.

In the end, the calculated integral activity released to the environment is in the range of from 2.8e+8 Bq to 9.5e+13 Bq for PWR DBA in the 2nd set of calculations. The calculation results show that the results may differ up to 5

orders of magnitude. The differences may be due to several reasons: differences on the initial FP inventory and spiking, differences on the isotopes considered, differences on the dilution in the RCS, differences on the transport phenomena through the SGTR break and in the SG (atomization, flashing, partitioning, scrubbing), differences in the consideration of activity releases in the steam phase only or in both liquid and steam phases etc.

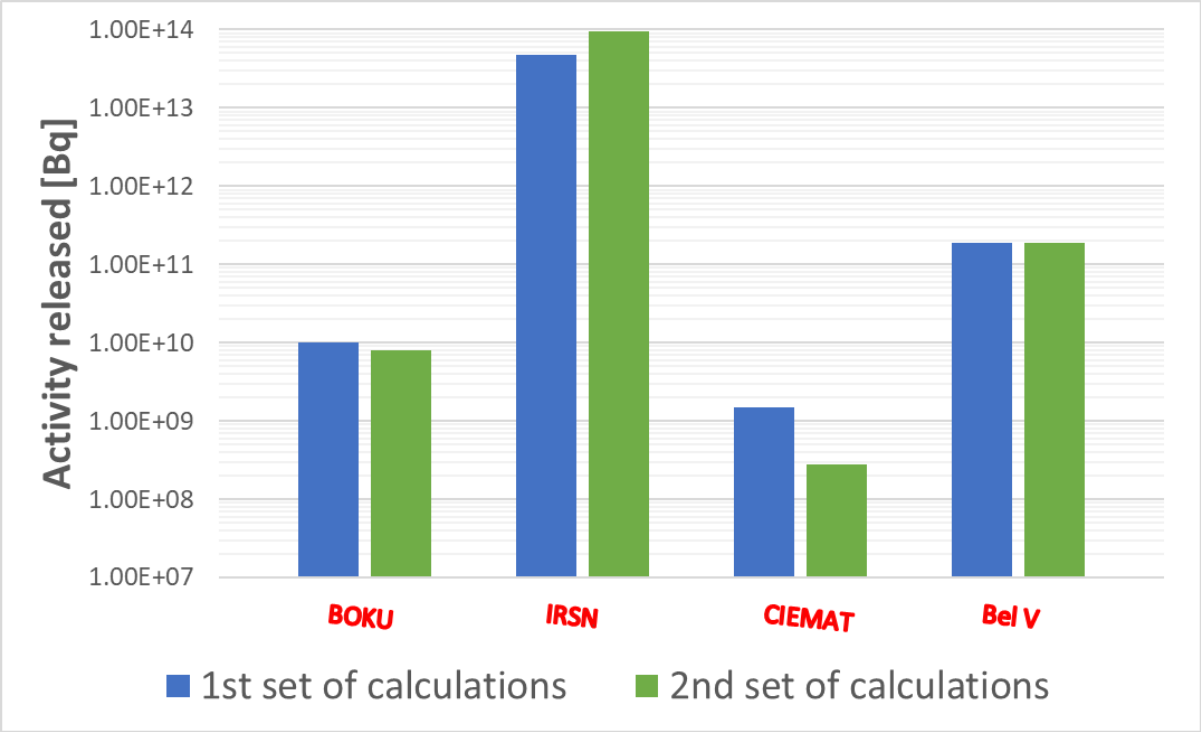

Figure 28. Activity in environment in the case of the SGTR transients for PWR type DBA scenarios from initial and final calculations.

For instance, it is not exactly clear how CIEMAT computes the lowest releases, given that:

- The water/steam released to environment is equivalent with IRSN and Bel V.
- Initial contamination and spiking are only 3 times lower than Bel V while there are 3 orders of magnitude difference on the activity releases.

One plausible explanation may be linked to the FP transport model difference used by the partners.

Additionally, BOKU provides lower activity releases compared to Bel V but higher compared to CIEMAT. Several observations can be noted:

- Initial activity in RCS and spiking is higher than CIEMAT and Bel V (BOKU used a 1300 MWe PWR model while CIEMAT and Bel V used a 1000 MWe model to do their calculations).
- The cumulative water/steam released to environment is higher than other partners with the scenario SGTR 1 tube (IRSN/CIEMAT/Bel V) considering a longer time period for releases, but reactor type considered in the calculation is different (1300 MWe vs 1000 MWe).
- There is no consideration of SG RV stuck open in the BOKU scenario.
- Eventually, compared to 1st set of calculations, implementation of clean up system in the RCS and pool scrubbing in the SG in 2nd set of calculations may explain the differences with Bel V.

Ultimately, radiological consequences have been evaluated by half of the partners. All population age groups are represented. The same observations as for the activity releases can be noticed, i.e. reduction of radiological

consequences of 77% for CIEMAT (for thyroid and total effective dose). For IRSN, there is an increase of the radiological consequences between 1st and 2nd set of calculations of between 79% to 125%. As a remainder, radiological consequences in term of dose were not evaluated by BOKU and Bel V. In the end, the thyroid dose calculated for the PWR DBA transients is ranging from 0.01 to 0.48 mSv (see Figure 29). The total effective dose calculated for the PWR DBA transients is ranging from 0.0005 to 0.045 mSv (see Figure 30). What can be observed is that IRSN and CIEMAT results are closer for the thyroid dose compared to the total effective dose. Indeed, for CIEMAT, activity releases are almost entirely the consequence of iodine releases while for IRSN, it is the opposite and iodine releases are contributing to a very small part of the activity releases. As the equivalent thyroid dose is almost solely linked to iodine toxicity and given the far lower activity releases for CIEMAT compared to IRSN, it is normal to witness closer thyroid dose between both partners in this case than closer total effective dose. However, discrepancy on radiological consequences between CIEMAT and IRSN is reduced to 2 orders of magnitude maximum while the activity releases computed by both partners had more than 4 orders of magnitude difference. It is then clear that even if the radiological consequences tool is common for all partners, the tool has been used differently by CIEMAT and IRSN. For instance, the height of the release point has been chosen as 30 m for CIEMAT while it has been chosen as 60 m for IRSN. Furthermore, the distance considered between the source and the receiver was set to 700 m by CIEMAT and 1 km by IRSN. Finally, the considered FPs in the tool may also have been different between CIEMAT and IRSN.

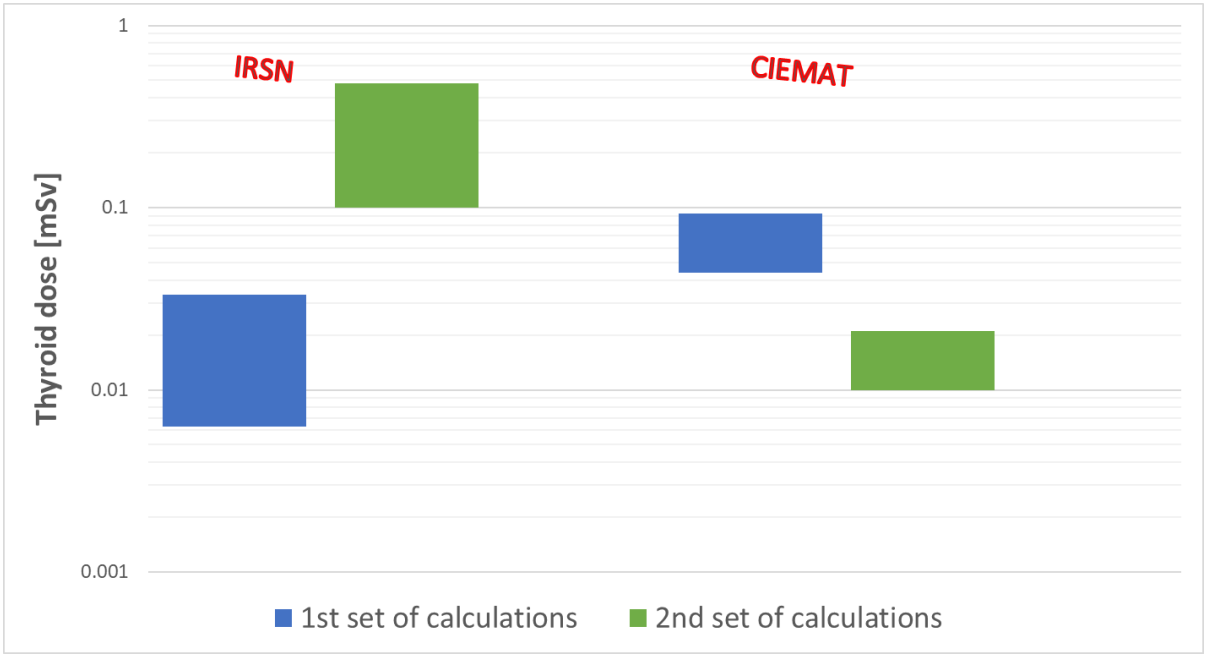

Figure 29. Thyroid equivalent dose for all population age groups in the case of the SGTR transient for PWR type DBA scenarios from initial and final calculations

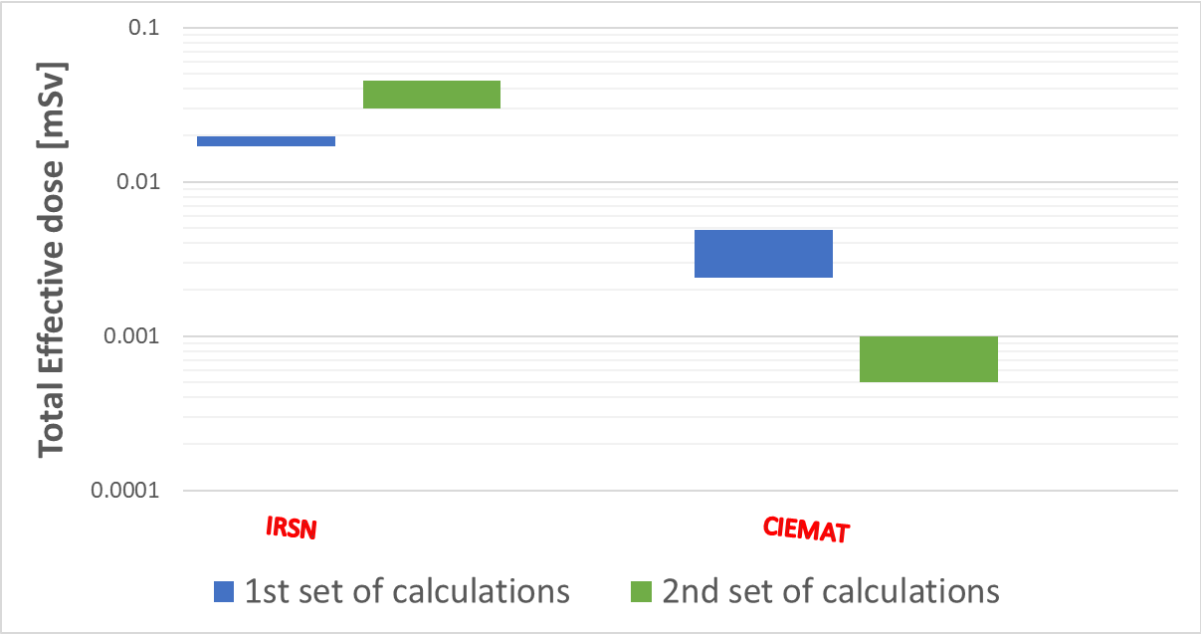

Figure 30. Total effective doses for all population age groups in the case of the SGTR transient for PWR type DBA scenarios from initial and final calculations.

PWR calculations, DEC-A scenario.

For PWR type reactors, SGTR transients in the case of the DEC-A scenario, 4 calculations from 4 partners were provided. The initiating event was identical for Bel V and TRACTEBEL (SGTR 3 tube at the bottom of the SG + simultaneous non-isolable SLB outside containment) and is almost the same for CIEMAT but the SLB is isolable which will lead to far different results. On the other hand, BOKU considered a SGTR 1 tube with SG RV stuck open and LPIS failure. The main improvements made by the partners between 1st and 2nd set of calculations are diversified: improvement of the dilution in the RCS (BOKU), improvement of the spiking model (BOKU, CIEMAT, Bel V), improvement of the FP transport between primary and secondary and inside SG [atomization, partitioning, scrubbing, flashing] (BOKU, TRACTEBEL, Bel V, CIEMAT) and consideration of new EOPs for operators' actions to depressurize RCS as fast as possible (TRACTEBEL). For the PWR type DEC-A calculations, only TRACTEBEL improved their TH with the use of improved EOPs to depressurize the RCS as fast as possible in order to faster reduce the flow rate at the SGTR break and to reach earlier pressure equilibrium between primary and secondary and cancellation of the break-flow. Thanks to this improvement, the affected SG cumulative liquid mass released to the environment is reduced from 130 t in the 1st set of calculations to 40 t for the 2nd set of calculations (see Figure 31). Overall, the cumulative liquid water and steam released to the environment is between 4 and 389 t for the PWR DEC-A calculations (see Figure 31). As explained in D2.5 [16], differences observed in the primary to secondary and secondary to environment discharges could be explained mainly by the differences in the scenario, in the SGTR break sizes, the IS duration, automatic procedures and operator actions, in the secondary to environment discharge capacities (SG relief and safety valves discharge capacities, setpoints, failures, operator actions, etc.) and in the considered initial and boundary conditions (additional single/multiple failure(s), best estimate/penalized parameters). These differences may also impact the evolution of the pressure in the RCS and in the affected SG that will further influence the water and steam released.

More particularly for CIEMAT who computed only 4 t of water (liquid and steam) releases, the SLB is isolated only 12 s after initiating event. Then, releases are only occurring while SG RV is cycling. These facts are explaining entirely why releases for CIEMAT are so low.

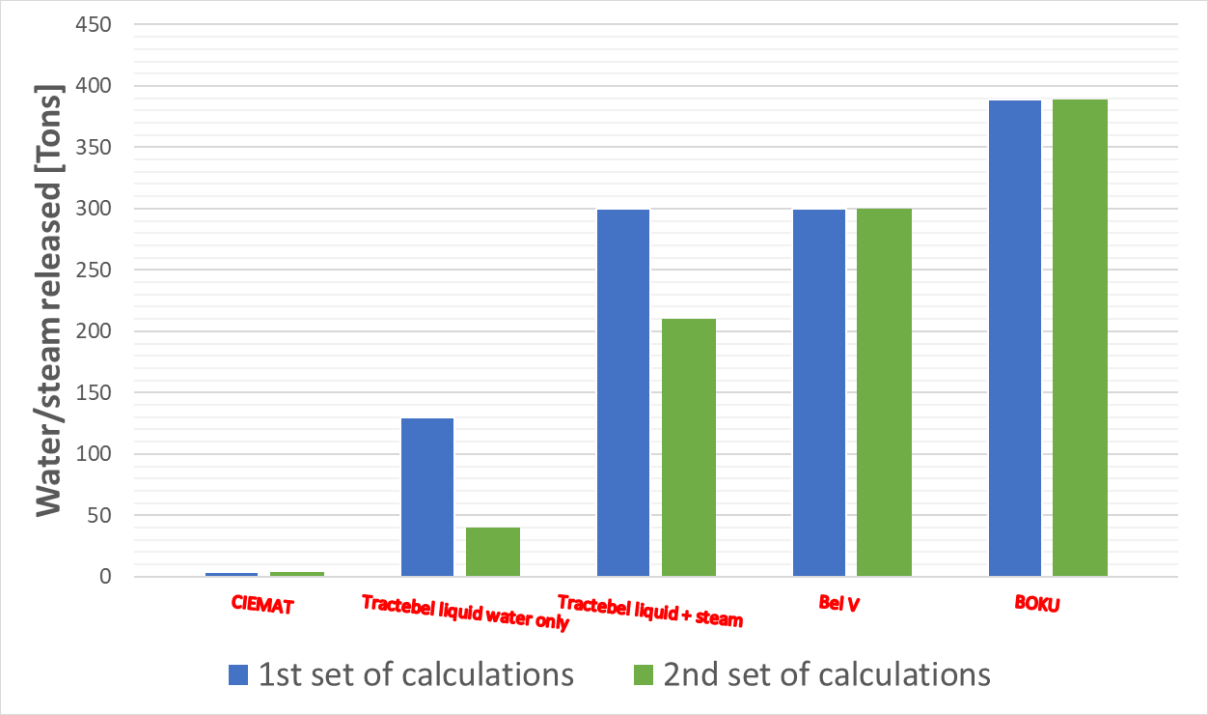

Figure 31. Cumulative liquid water and steam released to environment for PWR type SGTR DEC-A from initial and final calculations.

Thanks to the improvement made by the partners, the calculated activity released to the environment is reduced between 17% to 97% for the 2nd set of calculations compared to the first one for all partners, except Bel V (see Figure 32). For Bel V, while activity releases in liquid phase were not considered in 1st set of calculations, they are now considered in 2nd set of calculations leading to an increase of the activity releases of 800% (releases of 2nd set = releases of 1st set times 9). In the end, the calculated integral activity released to the environment is in the range of from 1.8e+7 Bq to 3.6e+12 Bq for PWR DEC-A calculations. When comparing with DBA results, releases are higher for DEC-A thanks to additional failure (consideration of SLB and 3 tubes break instead of1or failure of all LPIS), except for the CIEMAT DEC-A scenario because SLB is isolated 12 s after transient initiation while for DBA RV is stuck open. The calculation results show that the results may differ up to 5 orders of magnitude. The differences may be due to several reasons: the ones already listed before for the water/steam released in the environment, differences on the initial FP inventory and spiking, differences on the isotopes considered, differences on the dilution in the RCS, differences on the transport phenomena through the SGTR break and in the SG (atomization, flashing, partitioning, scrubbing), differences in the consideration of activity releases in the steam phase only or in both liquid and steam phase, differences in time release period considered etc.

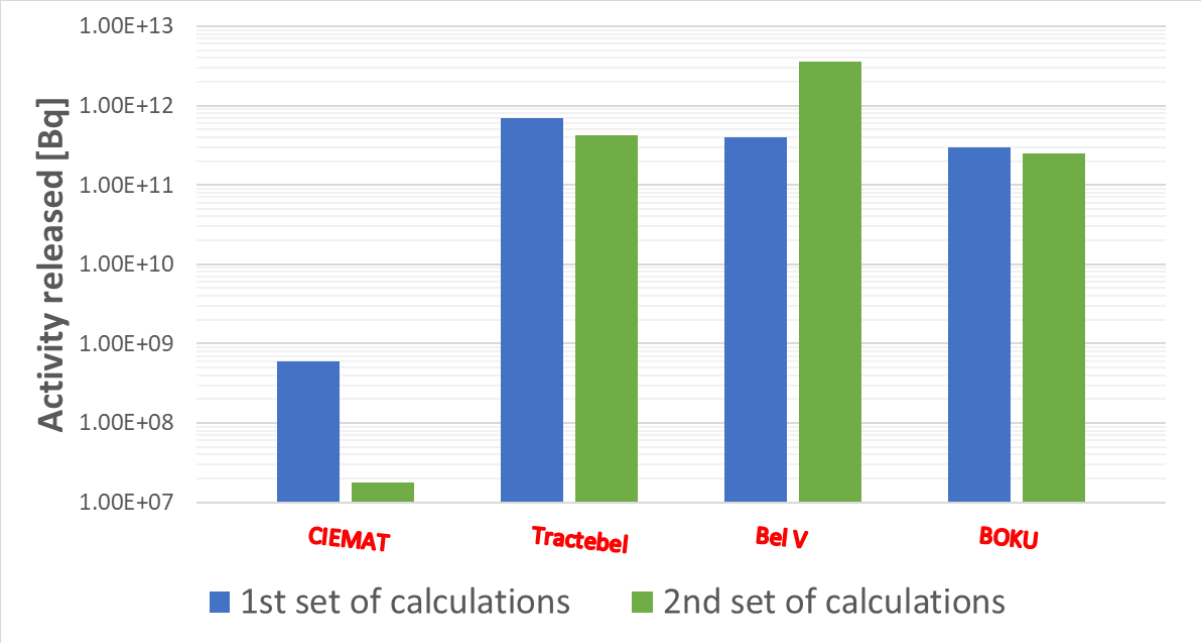

Figure 32. Activity in environment in the case of the SGTR transients for PWR type DEC-A scenarios from initial and final calculations.

For CIEMAT, the isolation of the SLB 12 s after transient initiation partly explain the low releases compared to other partners.

On the other hand, TRACTEBEL and Bel V provide close results (4.2e11 vs 3.6e12 Bq) when comparing both DEC-A calculations. It is even more true when the 1st set of calculation of TRACTEBEL is compared to the Bel V's 2nd set of calculations. Indeed:

- Almost same operators' actions and same timings are used between TRACTEBEL 1st and Bel V 2nd set of calculations (TRACTEBEL modified the operators' actions timing in 2nd set of calculations).
- The cumulative liquid water and steam released in the environment was also the same in 1st set of calculations, meaning that the codes and TH modelling is similar between TRACTEBEL and Bel V.
- Initial RCS contamination and Iodine spiking is around 18 times higher for Bel V.
- When comparing iodine activity released through the liquid phase between the 1st set of calculations of TRACTEBEL and the 2nd set of calculations of Bel V (2.19E11 Bq vs 3.1E12 Bq), the iodine spiking difference (ratio of 18) explains mainly the difference of activity releases in liquid phase.
- However, differences remain on the gas phase iodine releases in 2nd set of calculations as Bel V computes 5 times more releases compared to TRACTEBEL. Differences between Bel V and TRACTEBEL are here due to the FP transport model inside the SG (partitioning, atomization, flashing) which is different between both partners.

Eventually, radiological consequences have been evaluated by half of the partners here. All population age groups are represented. The same observations as for the activity releases can be noticed, i.e. reduction of radiological consequences, between 20% to 97% for PWR DEC-A calculations (for thyroid and total effective dose). As a reminder, radiological consequences in term of dose were not evaluated by BOKU and Bel V. In the end, the thyroid dose calculated for the PWR DEC-A transients is ranging from 0.0013 to 1.61 mSv (see Figure 33). The total effective dose calculated for the PWR DEC-A transients is ranging from 0.00007 to 0.085 mSv (see Figure 34). The large discrepancies found on the radiological consequences between CIEMAT and TRACTEBEL are first mainly explained by the differences on the activity releases. Then, even if the radiological consequences tool is

common for all partners, the use of this tool may be different between partners: FPs considered, height, distance considered and if the partner only considered steam releases or both releases in liquid and steam phases.

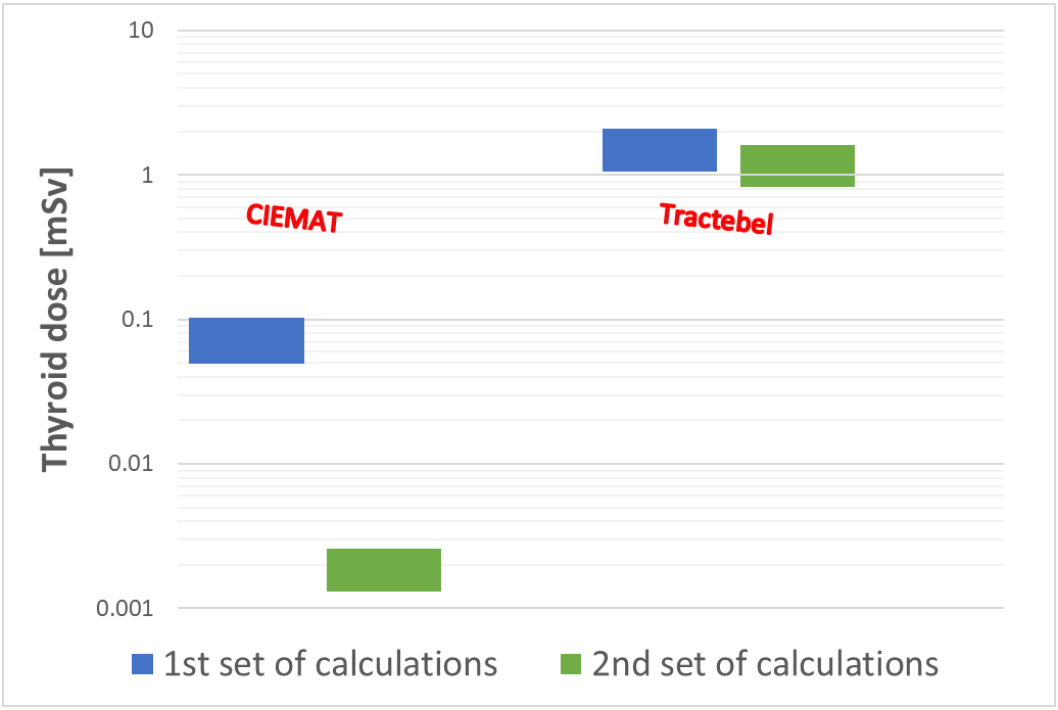

Figure 33. Thyroid equivalent dose for all population age groups in the case of the SGTR transient for PWR type DEC-A scenarios from initial and final calculations.

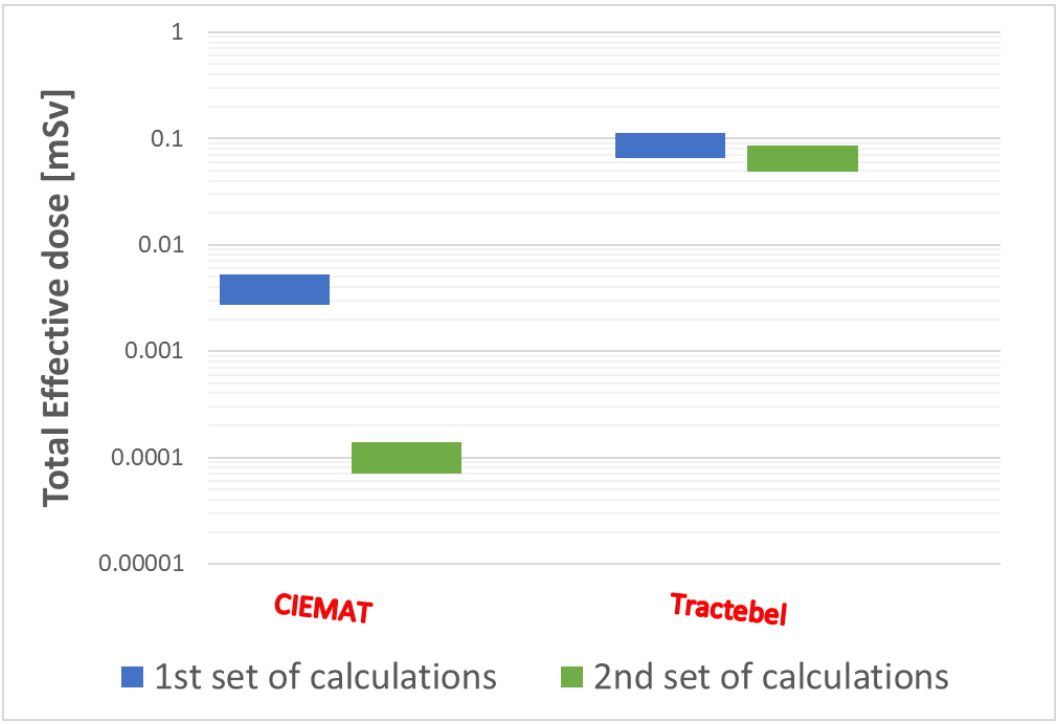

Figure 34. Total effective doses for all population age groups in the case of the SGTR transient for PWR type DEC-A scenarios from initial and final calculations.

4 Uncertainty & sensitivity analyses

The safety assessments of Nuclear Power Plants (NPP) generally consist in performing DBA analyses together with considering more severe situations (the so-called design extension conditions, DEC). These are generally addressed taking into account additional events/failures or combination of initial independent events. The development of specific countermeasures (procedures and hardware) for these conditions is then explicitly included in the design of the NPP. DEC includes two different kinds of conditions: DEC-A conditions, for which the prevention of significant core degradation through Emergency Operating Procedures is achieved by dedicated system intervention and/or operator actions and DEC-B conditions covering core melting occurrence for which severe accident management (SAM) procedures are developed to mitigate the accident consequences.
Previously for RC evaluations of DBAs (also for some of DEC-As) conservative and decoupled approaches were applied because some relevant elements concurring to the results of the safety analyses were poorly known: such as some phenomena taking place during the accident, relevant initial and boundary conditions, evolution of these conditions during the NPP operational phase. In addition, the code capabilities to reproduce the behaviour of the plant were not properly quantified. The progressive overcome of those aspects due to improvements in the knowledge of phenomena and the availability of more powerful and complex computational tools, have led to the gradual replacement of conservative approaches with Best Estimate (BE) approaches.
However, the use of a BE approach requests to evaluate the uncertainties connected with the elements of the analysis to derive the total uncertainty related to the code results in reproducing the behaviour of the plant during the accident. The uncertainty quantification is of course a relevant aspect in the assessment of assumptions, models, and simulation codes to derive realistic safety margins in DBA and DEC-A conditions.
Extensive uncertainty quantification analyses were beyond the scope of the project. However, most of the partners provided parametric analyses determining the sensitivity of the results to main relevant parameters. This analysis is also useful for the calibration, preparation of the reference case calculation when the code users evaluate the influence of the most important initial parameters, assumptions, computational models and its parameters. The summary of the sensitivity (parametric) analyses performed by the different partners are presented in Table 18 while some examples of provided analyses are presented in sections 4.1.1, 4.1.2 and 4.1.3.
In addition, despite the fact, that according to the project work plans it was not required, some specific methods for uncertainty quantification were proposed (i.e. for coupled code calculations) and the CIAU and GRS methodologies were applied for some uncertainty quantification (Table 19). Application of the CIAU method to a SGTR transient simulation is presented in section 4.2. Application of the GRS method to a LOCA transient simulation is presented in section 4.3.

4.1 Sensitivity (parametric) analysis

In this section is presented Table 18 and Table 19 which summarises the activities provided by partners in the field of uncertainty quantification analyses. Table 18 gives summary of the sensitivity (parametric) analyses performed by the different partners. This information was also used to for the calibration, preparation of the reference case calculation. Table 19 gives summary of uncertainty and sensitivity analyses performed by different partners, GRS and CIAU methods were used.

	LOCA	
	Initial/boundary conditions	**Models**
IRSN, PWR-900	1. Fuel rod internal pressure (30 and 50 bars). 2. Axial power profile: flat and peaked. 3. Radial Power factor distribution.	1. Chapman vs Edgar for clad burst criteria. 2. Core modelling: 5 rings vs realistic 1/8th core - 26 FAs. 3. 1D vs 3D in-core T/H modelling. 4. Fuel gas permeability coefficients.
ENEA, PWR-900	1. Accumulator water mass: reference value vs 20% reduction 2. Neutronic power after the scram: reduced with respect to reference case. 3. Decay heat: increase by 5% with respect to reference case	1. CHAPMAN and NUREG-630 models vs EDGAR model for clad burst criteria 2. User dependent maximum hoop strain for clad burst vs reference case. 3. Burst criteria: BE-exponential, Mean, Min, Max, CHAPE, CHAPMAN
HZDR, PWR-Konvoi	1. Fuel rod internal pressure (2.25MPa and 3.6 MPa) 2. Power profiles (best-estimate and peaked)	
VTT, EPR-1600	Cladding burst models	
LEI, BWR-4		1. Cathcart, Urbanic, Prater. 2. Modelling parameters: minimum temperature to start the reaction of oxidation, maximal hoop creep allowed before burst and axial extension of the cracking after the clad burst.
	SGTR	
	Initial/boundary conditions	**Models**
IRSN, PWR-900	Transient activity peak onset.	1. Iodine flashing vs no iodine flashing. 2. Iodine speciation.
SSTC-NRS, VVER		1. Gas transfer coefficient in affected SG
BOKU, VVER	Fuel cycle position for iodine spiking impact	
TRACTEBEL, PWR-1000		1. Iodine pool model. 2. Iodine partitioning model 3. EOP operators' actions timings

Table 18. Summary of sensitivity analyses (parametric analyses) performed by different partners on initial/boundary conditions and model parameters.

LEI, BWR-4	Uncertainty and sensitivity analyses of TRANSURANUS calculation results of a LOCA transient using GRS methodology. Selected uncertain parameters: pellet radius, inner cladding radius, outer cladding radius, gap pressure, outer pressure.
BOKU, VVER	Uncertainty analysis of SGTR transient using CIAU methodology.

Table 19. Summary of uncertainty and sensitivity analyses performed by different partners.

4.1.1 Sensitivity calculations performed by IRSN for LOCA final calculations

Several sensitivity studies were performed by IRSN on several parameters. In this section are described those that have been carried out for updated DRACCAR calculations where the impact of axial power profile, axial gas transport (i.e. fuel permeability) and in-core flow modelling (i.e. 1D vs 3D models) were especially analysed. The obtained results are summarized below for each analysis.

1. Impact of Axial power profile

The impact of axial power profile (peaked vs flat) on thermos-mechanical response of fuel rods was investigated with DRACCAR realistic core model used in the second set of reactor calculations for evaluation the activity release from a PWR 900 in case of LOCA. The maximum power axial factor was set in the 2/3 highest elevation of fuel rod i.e. in a region of the core which is early uncovered during the DBA scenario. For the DBA scenario, for most of the fuel rods, peaked profile led to higher maximum cladding temperatures (especially for hottest fuel rods). Maximum increase of peak cladding temperature is 30 K. Due to higher cladding temperatures, the number of failed fuel rods also increases (23% with the peaked axial profile instead of 10% for the reference case.
However, from the analysis it could not be concluded that considering a peak axial profile leads systematically to decrease the margin to the burst criteria. Indeed, if the general trend shows that the peaked axial profile is associated to an increase of the maximum cladding temperatures and a decrease of the margins to the burst criteria, some of the rods behave unexpectedly by reaching a quasi-equal PCT and having a slightly lower burst margin. Therefore, for the burst risk assessment, it was recommended to consider a wide range of the axial power profile (including different axial profiles for each assembly) and manage it through uncertainty analysis.

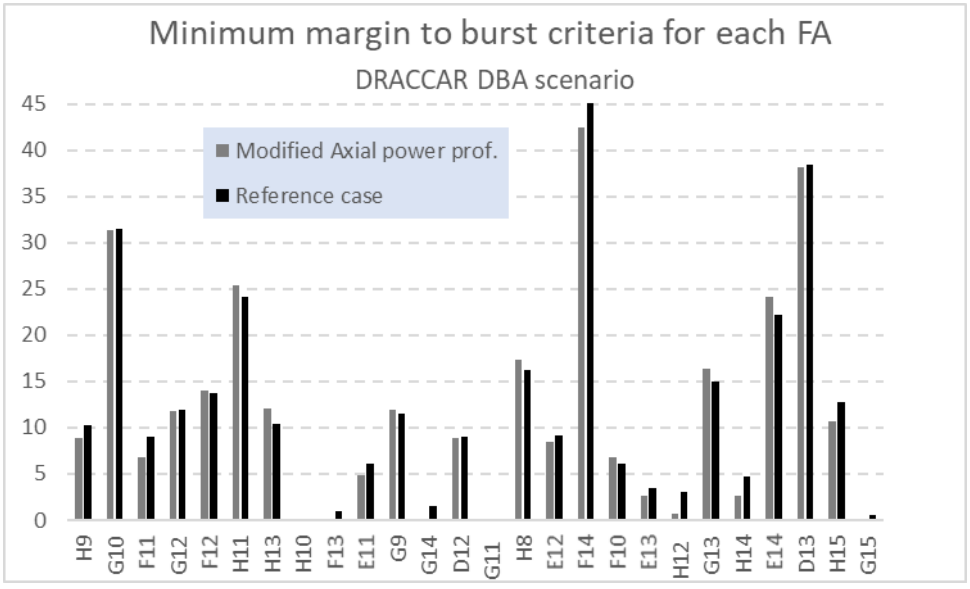

Figure 35. Evolution for LOCA DBA scenario in PWR 900 of the minimum burst margins with different axial power profiles for each rod simulated by DRACCA realistic core model.

2. Impact of axial gas transport in fuel rods

The impact of axial gas transport in rod free volumes on rod internal pressure and mechanical stress on the cladding was investigated. Different calculations were performed using a uniform distribution of the pressure all along the rod length and in plenums or more advanced modelling using a pressure network (i.e. different local pressure at different axial levels) coupled to an axial gas transport model where the axial gas velocity in the fuel is represented by an axial gas equivalent permeability. Sensitivity calculations on this latter parameter which is rather uncertain were performed with eight different permeabilities applied as a first approach for all the fuel rods whatever their burn-up. The pressure of the gas involved in the fuel to clad heat transfer as it influences gas properties (such as the thermal

conductivity) and in the creep (gap thickness) impacts the fuel to gap exchanges and the local stress. In case of DBA scenarios, these impacts were however expected to be limited.
The gas permeability was found to have a largest impact on the maximum cladding temperature evaluation (timing and magnitude) than expected. The most probable explanation corresponds to an undirect link between permeability and PCT evolution by a complex combination to thermal hydraulics sensitivity. It's known that some phasis of LOCA simulation are highly sensitive for example to the time discretization or modelling (i.e. accumulator discharge, fast uncovering and reflooding of the core) and still remain tricky to simulate. These phenomena last during 40 s to 250 s in the scenario. Therefore, small variations associated to gas permeability could act as a trigger of larger deviation on thermal hydraulics response and so on PCT. This behaviour could be attributed to the sensitivity of core reflooding simulation.
For the investigated values of permeabilities, the prediction of the number of burst fuel rods varies from 5% to 15%, being 10% for the reference case. Furthermore, for a given threshold value of 5% on the minimum burst margin, the potential number of failed fuel rods varies from 22% to 30%.

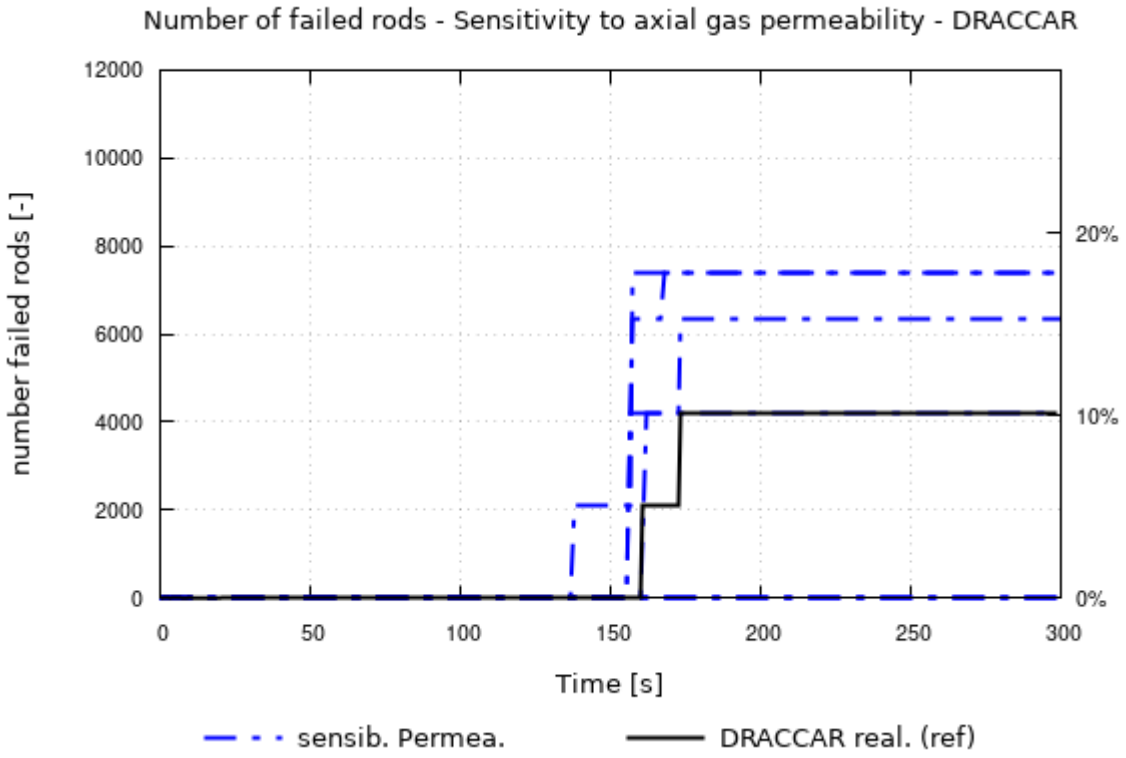

Figure 36: Evolution of the number of failed rods with different gas permeability modelling for LOCA DBA scenario in a PWR 900 simulated with the DRACCAR realistic core model.

This sensitivity analysis shows an unexpected response of simulations when investigating variation of a given parameter. As shown by this example, it's sometimes hard to understand the link between scattering of results and the initial entry input variation. This is often observed when the simulations are subject to cliff edge effect driven by binary test conditions in models (i.e. for this case threshold for the wall to fluid heat transfer model selection…). Regarding such simulation results, it was concluded that LOCA analysis shouldn't rely on a single simulation case but on a larger panel whose results should be processed by statistical analysis.

3. In-core flow modelling

Sensitivity analysis on in-core flow modelling was performed by carrying-out DRACCAR simulations using the 3D "realistic" core model or an axial mutli-1D core model (i.e. disabling the transverse flow through vertical faces of core mesh volumes). In this latter configuration, all the fuel assembly channels are independent and only connected from bottom and top respectively to the lower plenum volume and to the upper plenum volume. The peak cladding temperature evolution was found to be drastically different. In a first phase, from blowdown to the end of hydro-accumulators discharge (~100 s), a higher PCT is observed for the multi-1D case. Then during reflooding of the core, the PCT is widely under-estimated in comparison to 3D case whereas the delay to quench the hottest channels is increased. The axial multi-1D model led to radically different results in comparison to 3D core model. This highlights the necessity to adopt 3D core model to prospect the LOCA accident.

4.1.2 Sensitivity calculations performed by ENEA for LOCA final calculations

Several parameters have been considered by ENEA for sensitivity studies, as reported in Table 18. The effect of burst criteria, proposed by IRSN in the project work package dedicated to experimental database re-assessment and model/code improvements [2], on the computed number of failed rods was studied in the final phase of reactor calculations and the main outcomes are briefly reported hereafter.

The cladding burst is determined in ASTEC code by the fulfilment of selected main burst criterion or by the achievement of the maximum allowed cladding hoop strain, that is a user parameter set to 40% by default.

The following burst models proposed by IRSN were implemented and selected as main burst criterion in the ASTEC input data-deck: "BE-exp", that is the best fit of experimental data of true burst stress vs. temperature; "Mean", that is the mean value of true burst stress vs. temperature; "Min" and "Max", that are the minimum and maximum values of true burst stress vs. temperature and "CHAPE", that is a Chapman-like criterion based on a burst temperature function of the engineering cladding stress. The effect of maximum allowed cladding hoop strain was also investigated in the case of DBA.

The analysis of performed calculations of DBA scenario shows that, as a function of adopted main burst criterion and user options on maximum allowed hoop strain, the number of failed fuel rods can range from **0 to 66.88%** of the total (Figure 37) demonstrating that the modelling of cladding burst is a relevant source of uncertainties for the estimation of failed fuel rods number in the studied scenario.

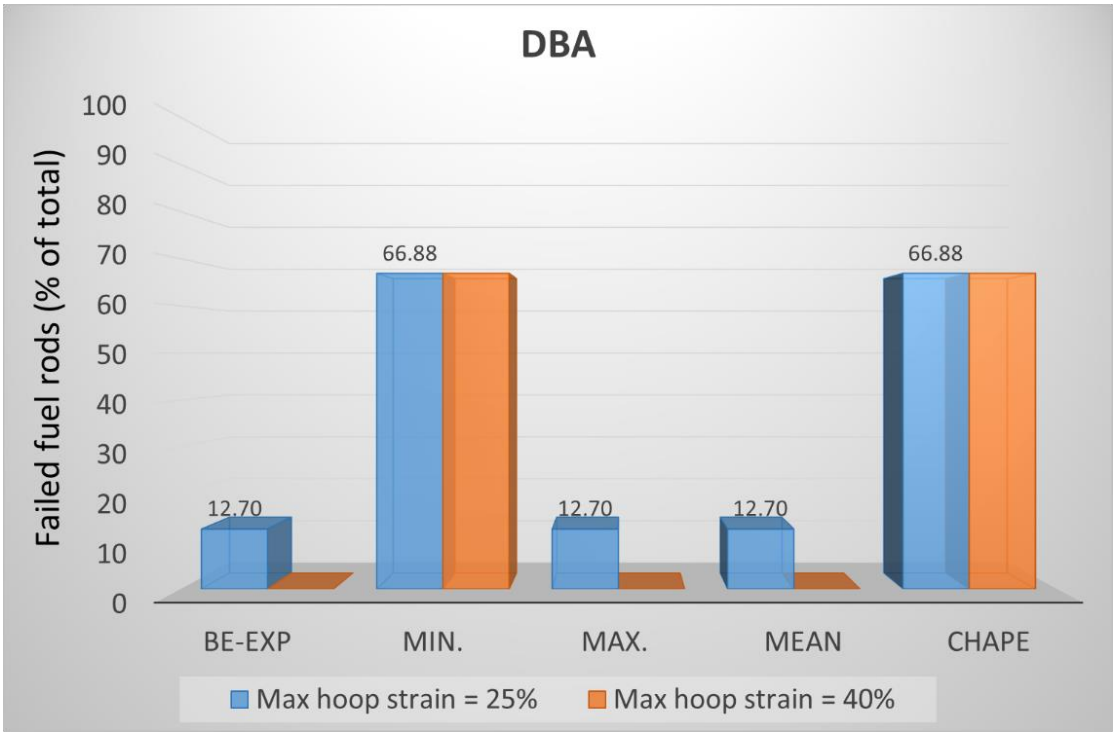

Figure 37. Number of failed fuel rods (% of the total fuel rods) in DBA scenario.

DEC-A calculations were performed with the default value of the maximum allowed cladding hoop strain (40%). The results, presented in Figure 38, show that the adopted main burst criterion has a minor effect on the estimation of failed rods number, ranging from **66.88% to 71.97%** of the total. Nonetheless, the obtained result can be misleading because, even if BE-exp, Mean, Max and CHAPE predict the same number of failed rods (66.88%, corresponding to the fuel rods in the 4 innermost fluid rings) only CHAPE criterion is really fulfilled while, in the other cases, the claddings failure is triggered by the reaching of maximum allowed hoop strain (40%). It is worth noting that the constraint on cladding hoop strain is needed to avoid too large deformations, out of the application domain of ASTEC, since the contact between neighbouring fuel rods is not managed by the code models. The most penalizing Min burst criteria is reached, other than in the fuel rods of the 4 innermost fluid rings, also in a fraction of fuel rods in the 5th and outermost fluid ring leading to the maximum number of failed fuel rods (71.97% of the total).

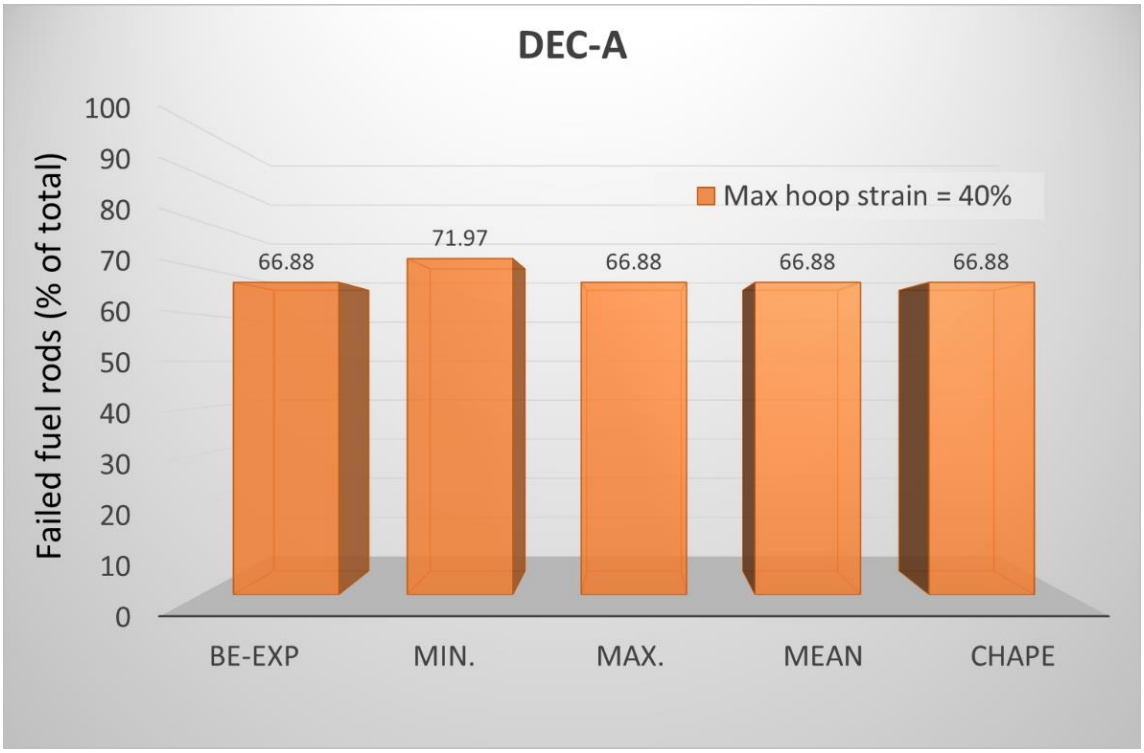

Figure 38. Number of failed fuel rods (% of the total fuel rods) in DEC-A scenario.

4.1.3 Sensitivity calculation performed by TRACTEBEL for SGTR DEC-A final calculations

Several sensitivity studies were performed by TRACTEBEL. In this section is described one of these that has been carried out for a SGTR DEC-A transient with updated MELCOR calculation where the impact of the iodine pool model of MELCOR was analysed.

In this analysis, instead of using the homemade partitioning model used for the first set of reactor calculations (see §2.4.2), TRACTEBEL performed a sensitivity calculation using the MELCOR iodine pool model. Due to this model, chemistry is actuated in SG 1 (affected SG) and molecular iodine is highly impacted. Figure 39 shows the iodine molecular releases with this sensitivity: only $1.65 \cdot 10^{11}$ Bq of molecular iodine are released for this sensitivity compared to $2.19 \cdot 10^{11}$ Bq for the first set of reactor calculations. A part of the iodine is also released as IM "Pool iodine bound in chemical species other than iodine or Cs" with a value of $0.187 \cdot 10^{11}$ Bq. The sum of this pool iodine and the molecular iodine is not equal to the value of the reference calculation $2.19 \cdot 10^{11}$ Bq. That means that another part of the molecular iodine has been transformed into other iodine species in the SG 1 and a larger part of the molecular iodine initially present is retained in the SG 1 compared to the reference calculation without the iodine pool model active.

Anyway, because of the fact that this iodine pool model is only intended to be used for the chemistry in the containment and is not qualified to be used in SG conditions (higher pressures and temperatures), the calculation with the iodine pool model has not been used as a reference by TRACTEBEL.

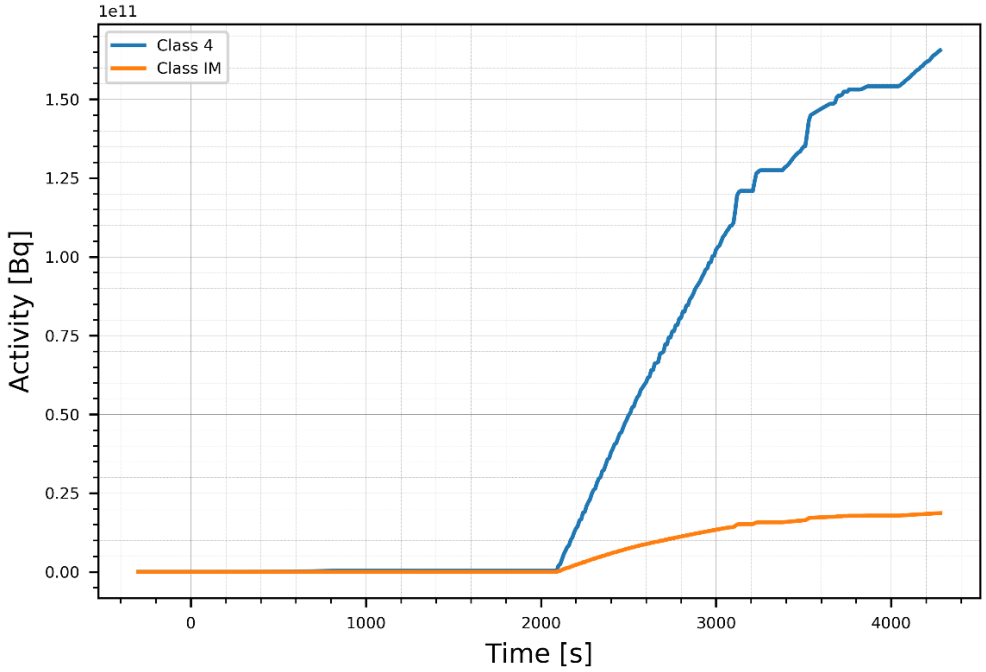

Figure 39. Iodine releases during a SGTR DEC-A transient using MELCOR iodine pool model.

4.1.4 Sensitivity calculations performed by SSTC-NRS for SGTR DBA and DEC-A final calculations

In the frame of the second set of calculations, SSTC-NRS assessed the impact of fission products transport from liquid to gas phase in the affected SG by performing different sensitivities on the gas transfer coefficient K_g. Different values of the gas transfer coefficient K_g from 0 to 1 were used to calculate the final releases. For the DBA simulation, the fraction of RCS activity transferred to SG in case of such break is about 0.64. The total amount of activity coming to environment (gas+liquid) depends on the transfer coefficient from liquid to gas phase and corresponds to the value 0.345 for K_g=0 and to 0.64 for K_g=1 (as for non-condensable gases).
The following figure represents the fraction of RCS initial activity release to SG and environment in both gas and liquid phase for different gas transfer coefficients K_g for the DBA simulation.

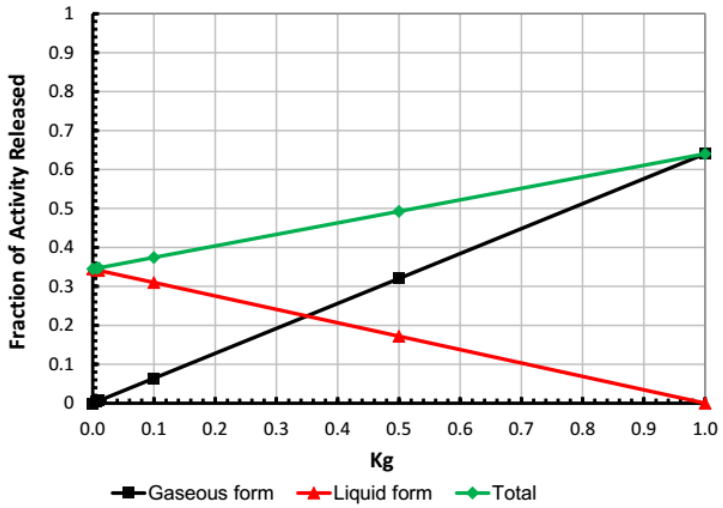

Figure 40. Activity fraction transported to SG and environment for different Kg – SSTC-NRS SGTR DBA.

The final source term calculated with the second set of calculations used different gas transfer coefficient Kg for each isotopes:

- K_g = 1 for noble gases
- K_g ~ 0.01 for iodine species and Sr
- K_g < 0.01 for other less volatiles species

For the DEC-A simulation, the fraction of RCS activity transferred to SG in case of such break is about 0.91. The total amount of activity coming to environment (gas+liquid) depends on the transfer coefficient from liquid to gas phase and corresponds to the value 0.74 for K_g=0 and to 0.91 for K_g=1 (as for non-condensable gases).
The following figure represents the fraction of RCS initial activity release to SG and environment in both gas and liquid phase for different gas transfer coefficients K_g for the DEC-A simulation.

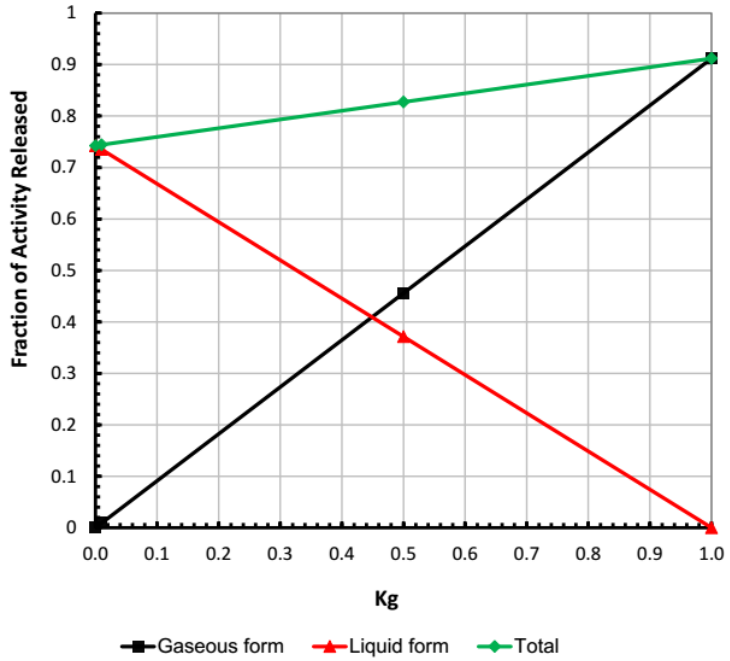

Figure 41. Activity fraction transported to SG and environment for different Kg – SSTC-NRS SGTR DEC-A.

As for DBA, the final source term calculated with the second set of calculations used different gas transfer coefficient Kg for each isotope:

- K_g = 1 for noble gases
- K_g ~ 0.01 for iodine species and Sr
- K_g < 0.01 for other less volatiles species

4.1.5 Sensitivity calculations performed by BOKU for SGTR DBA and DEC-A final calculations

In the frame of the second set of calculations, BOKU assessed the impact of fuel cycle position on iodine spiking. Indeed, the current position in the fuel cycle is an important indicator as an iodine spiking only can take place if there are small breaks at the fuel rods. Those defects develop over time. Therefore, it can be assumed that if the reactor is further in the fuel cycle it is more likely to have defects at the fuel rods. For this reason, the iodine spiking model of BOKU has been used at 3 different time positions in the fuel cycle, namely after, 6, 12 and 18 months. The same sensitivities have been performed for all studied BOKU cases (VVER-1000 and PWR-1300, DBA and DEC-A). In order to not overload this paragraph and because the sensitivity results on the same trend for all studied BOKU cases, only the VVER-1000 BDA simulation and the PWR-1300 DEC-A simulation will be specifically presented here.
For the VVER-1000 DBA simulation, the maximum I131 concentration reached in the primary system is between 2.2e+13 Bq to 3.2e+13 Bq at about 400s for time position in the fuel cycle between 6 and 18 months (Figure 42). The released I131 activity to the environment has been evaluated to be between 1.2e10 to 1.7e10 Bq for the 3 sensitivities studied in second set calculations (Figure 43). As expected, if the reactor is further in the fuel cycle, it is more likely to have defects at the fuel rods. Therefore, activity in the primary is more important and releases also.

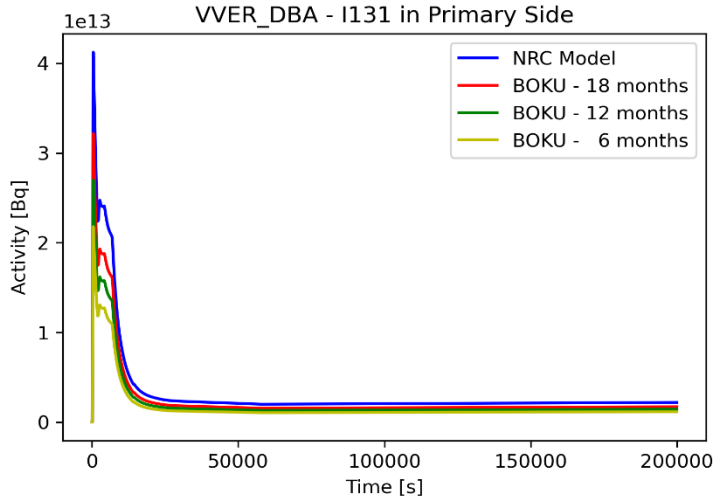

Figure 42. I131 activity in the primary side – BOKU SGTR VVER-1000 DBA.

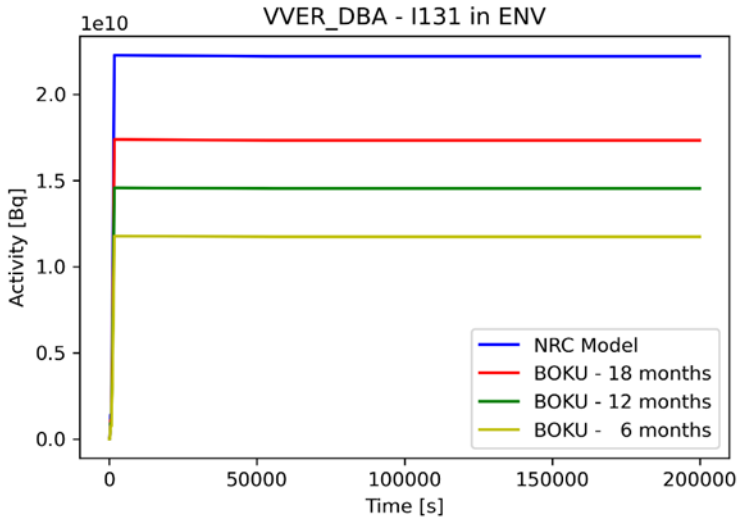

Figure 43. I131 activity in the environment – BOKU SGTR VVER-1000 DBA.

For the PWR-1300 DEC-A simulation, the maximum I131 concentration reached in the primary system is between 1.5e+14 Bq to 2.2e+14 Bq for time position in the fuel cycle between 6 and 18 months (Figure 44). The released I131 activity to the environment has been evaluated to be between 1.6e+11 to 2.5e+11 Bq for the 3 sensitivities studied in second set calculations (Figure 45). As for VVER-1000 DBA, if the reactor is further in the fuel cycle, it is more likely to have defects at the fuel rods. Therefore, activity in the primary is more important and releases also.

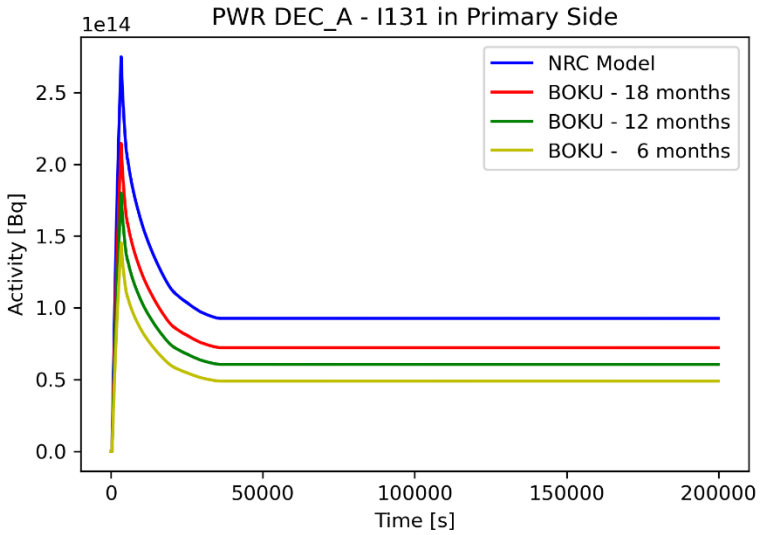

Figure 44. I131 activity in the primary side – BOKU SGTR PWR-1300 DEC-A.

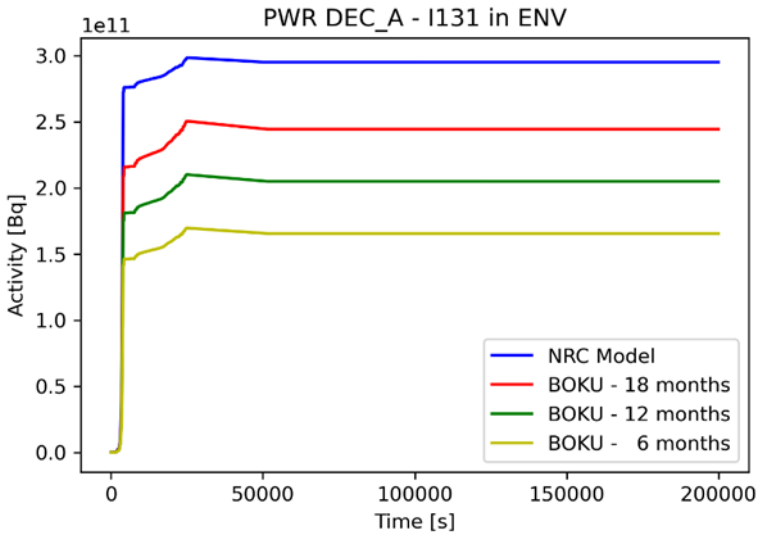

Figure 45. I131 activity in the environment – BOKU SGTR PWR-1300 DEC-A.

4.2 Implementation of the CIAU method to evaluate the uncertainty of a SGTR transient simulation

Thermohydraulic simulations of transients are always subject to uncertainties. For licensing purposes in principle an uncertainty analysis must be conducted, whenever the best estimate method is applied. Therefore, several methods have been developed to determine this uncertainty, including the GRS method, the UMAE and the CIAU (Code with capability of Internal Assessment of Uncertainty) of the University of Pisa [17]. Since the CIAU method is currently maintained by NINE, BOKU decided to perform this analysis together with NINE to determine the uncertainty of the transient calculations.

Description of the CIAU Method:
Compared to the GRS method, the CIAU approach requires only one (best estimate) simulation and afterwards the results are compared with the weighted average of a set of experimental data. The main ideas of the methodology are:

1. Any transient scenario assumed in the reference systems can be characterized by the time and by a limited number of variables. The boundaries of variation for those variables and the time are identified.
2. The ranges of variation for those variables and the transient time are subdivided into intervals. Hypercubes result from the combination of variables intervals (Figure 46).
3. The NPP status is formed by the combination of one hypercube and one time interval.
4. It is assumed that uncertainty can be associated to any NPP status.

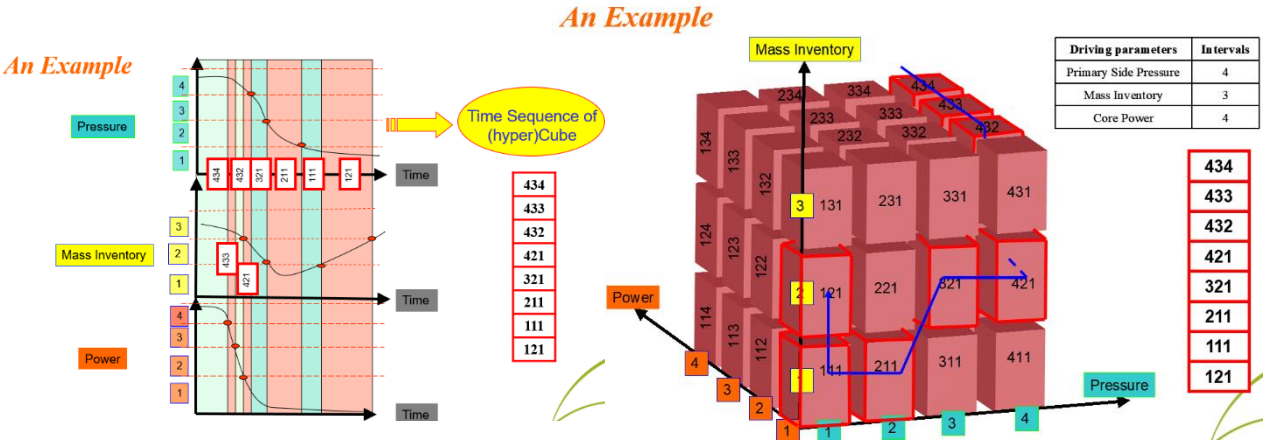

Figure 46. Allocation of simulation results to hypercubes.

In Figure 46 a hyper cube is included. Furthermore, it is shown, how the alternating values of each parameter lead to the sequence of the (hyper) cube.

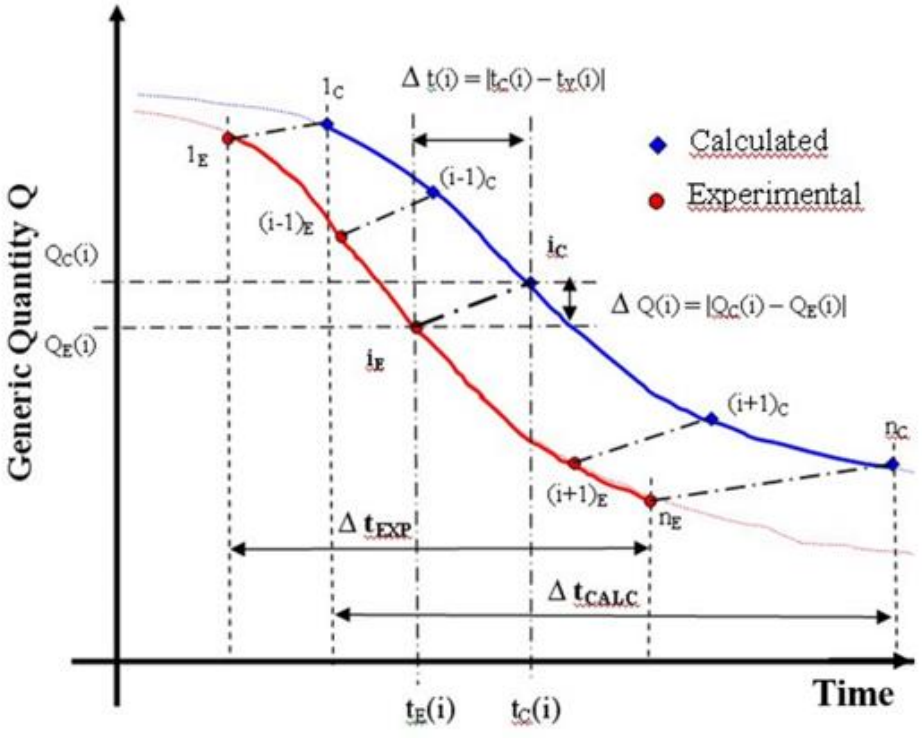

Figure 47. Schema of CIAU Results.

The CIAU method is capable to assess quantitative and time errors to create uncertainty bands (see Figure 47 and Figure 48Figure 48).

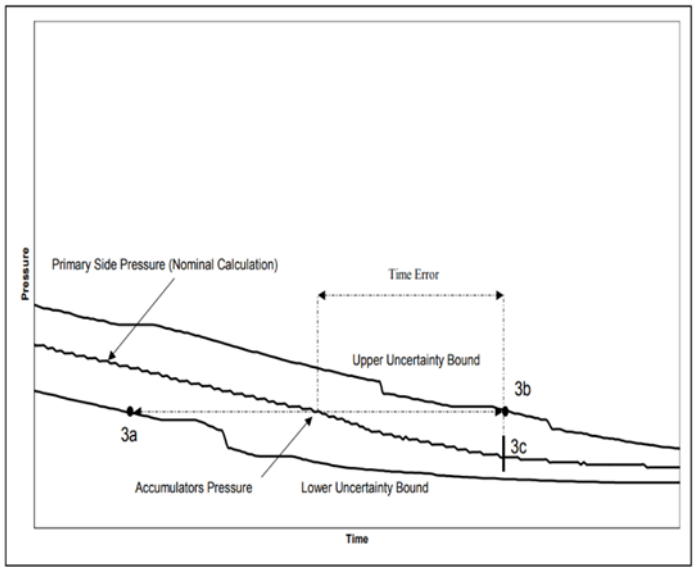

Figure 48. Example result of the CIAU method (D'Auria, 2002).

Uncertainty of IS simulation:

The standard CIAU procedure assesses the uncertainty of the following 3 parameters:

- Upper plenum pressure
- Primary side mass
- Cladding Temperature at 60% core height

In principle any parameter could be included in the analysis if there is sufficient experimental data in the developed databank. However, for iodine transport this is not the case as up to now not enough studies have been published, that address this parameter. Therefore, it was considered how the uncertainty of the iodine concentration could be derived from the basic parameters of the CIAU method. Since in our scenarios the iodine transport to the environment occurs always via a containment bypass over the secondary side, the pressure difference between the steam generator and the environment is mainly responsible for the contamination of the environment. Therefore, it would be reasonable to consider the uncertainty of the secondary side pressure as the main driver for the uncertainty of the iodine transfer into the environment.

Results:

The results of the CIAU analysis are included in Table 20 and are shown graphically as well (see Figure 49 to Figure 51). It is visible that the uncertainty of the calculation of the mass inventory larger than the other parameters. Regarding the figures it can be detected that the uncertainty band changes over time, as each timestep can be in a different hypercube which has a different uncertainty due to the experimental data it contains.

	Lower Band (mean) [%]	Nominal Value	Upper Band (mean) [%]
Primary side pressure	0.85	1.00	1.14
Mass inventory	0.77	1.00	1.24
Cladding temperature	0.90	1.00	1.11

Table 20. Average deviation of uncertainty bands from CIAU method application on SGTR transient.

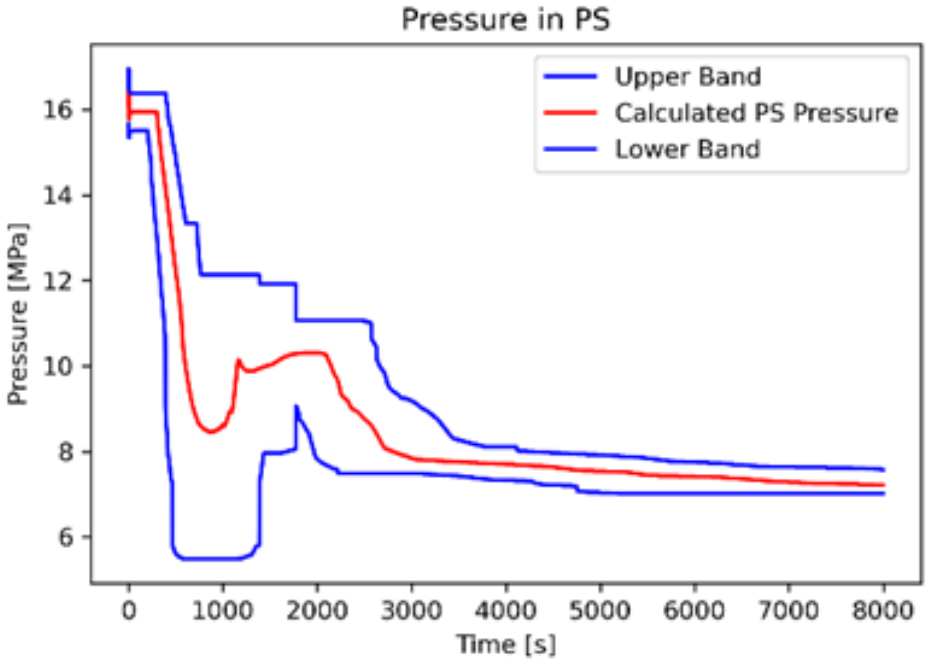

Figure 49. Uncertainty of PS Pressure evolution during a SGTR transient calculated by the CIAU method.

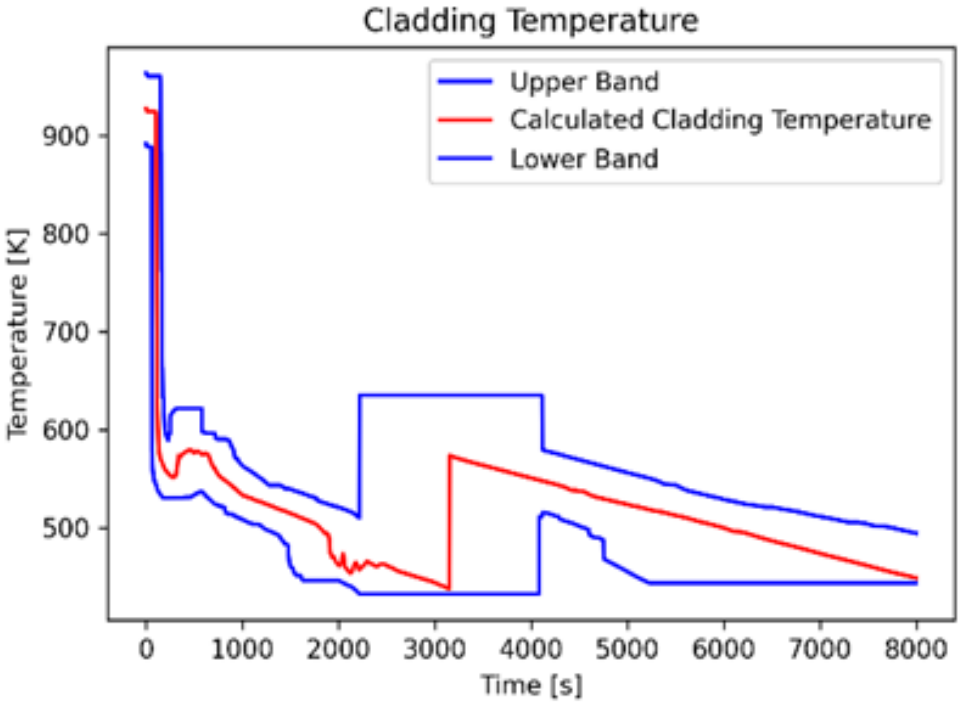

Figure 50. Uncertainty of Cladding Temperature evolution during a SGTR transient calculated by the CIAU method.

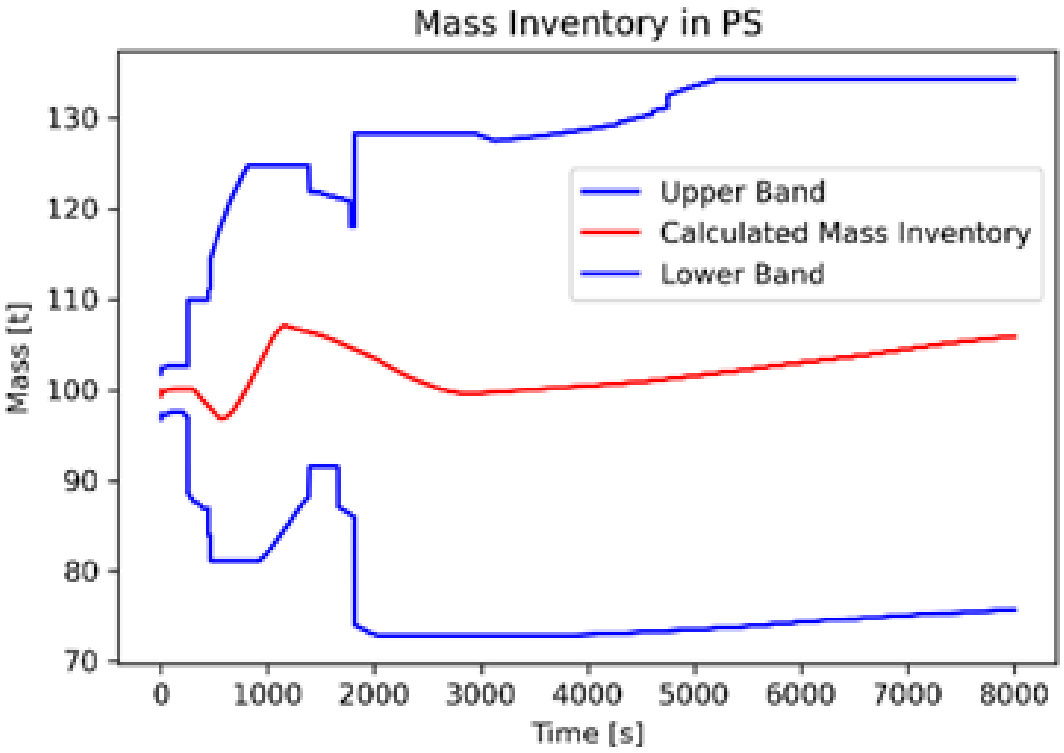

Figure 51. Uncertainty of Mass Inventory evolution in PS during a SGTR transient calculated by the CIAU method.

The analysis with the CIAU method shows the limitations of the simulation by calculating the uncertainty bands of significant parameters. Further steps, beyond the project, will focus on the development of a way to derive the uncertainty of the iodine simulation based on the results of the CIAU.

4.3 Implementation of the GRS method to evaluate uncertainty of a LOCA transient

For this analysis, LEI considered a generic Boiling Water Reactor (BWR) of class 4 with Mark I containment. The thermal power of the reactor is 2381 MW. The calculation results of the basic ASTEC BWR model for a LOCA DEC-A transient predicted the clad rupture of all fuel rods in two of the five concentric rings used for the core nodalisation, corresponding to 55% of all the fuel rods in the core. To verify the ASTEC calculation results; more detailed calculations were also carried out using the TRANSURANUS fuel performance code.

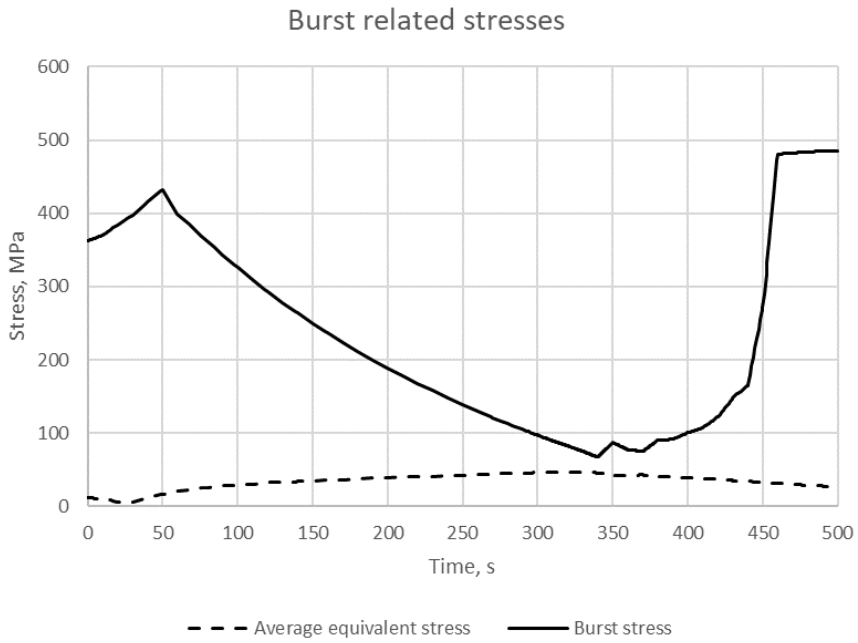

Figure 52. TRANSURANUS calculated average equivalent stress and burst stress during a LOCA DEC-A transient in BWR-4.

The TRANSURANUS code was used for a more detailed analysis of the processes occurring in the fuel during a LOCA DEC-A transient considering ASTEC code calculated fuel cladding temperatures for FA results with the concentric ring at relative power of 0.98. The calculation results did not indicate cladding rupture, corroborating the findings from the ASTEC calculations. Figure 52 presents the average equivalent stress, representing the forces acting on the cladding, and burst stress, corresponding to the cladding's capacity to withstand bursting. The obtained margin between the average equivalent stress and the burst limit was only ~10 MPa and might fall within the range of uncertainties. Thus, it was decided to conduct uncertainty quantification of TRANSURANUS calculation results.

Conservative rupture parameters are being considered as presented in other cases. Five parameters were considered for uncertainty quantification. Uncertain parameters and selected uncertainty ranges for the uncertainty quantification are presented in Table 21. Uncertainty ranges and probability distribution function (PDF) were selected according to the previously provided work and engineering judgment, after the separate sensitivity analysis.

Uncertain parameter	Default value	Uncertainty range	PDF
Pellet radius, mm	4.335	±1%	Normal Distribution
Inner cladding radius, mm	4.420	±1%	
Outer cladding radius, mm	5.025	±1%	
Gap pressure, MPa	3.000	±2%	
Outer pressure, MPa	According to ASTEC calculations	±1%	

Table 21. Uncertain parameters and selected uncertainty ranges for the uncertainty quantification.

TRANSURANUS code has its in-build Uncertainty and Sensitivity tool which was used for this analysis. For the uncertainty analysis, 100 calculations were performed. Results of the uncertainty analysis are presented in Figure 53 to Figure 56. All presented figures show the results obtained at the 14th axial segment of TRANSURANUS fuel rod model.
As it is presented in Figure 53, the average equivalent stress varies in the range of up to ~60 MPa (Percentile 95%), still below the burst stress. The calculated burst stress did not show any significant uncertainty since it is entirely dependent on the cladding temperature which has fixed values according to the ASTEC calculations.

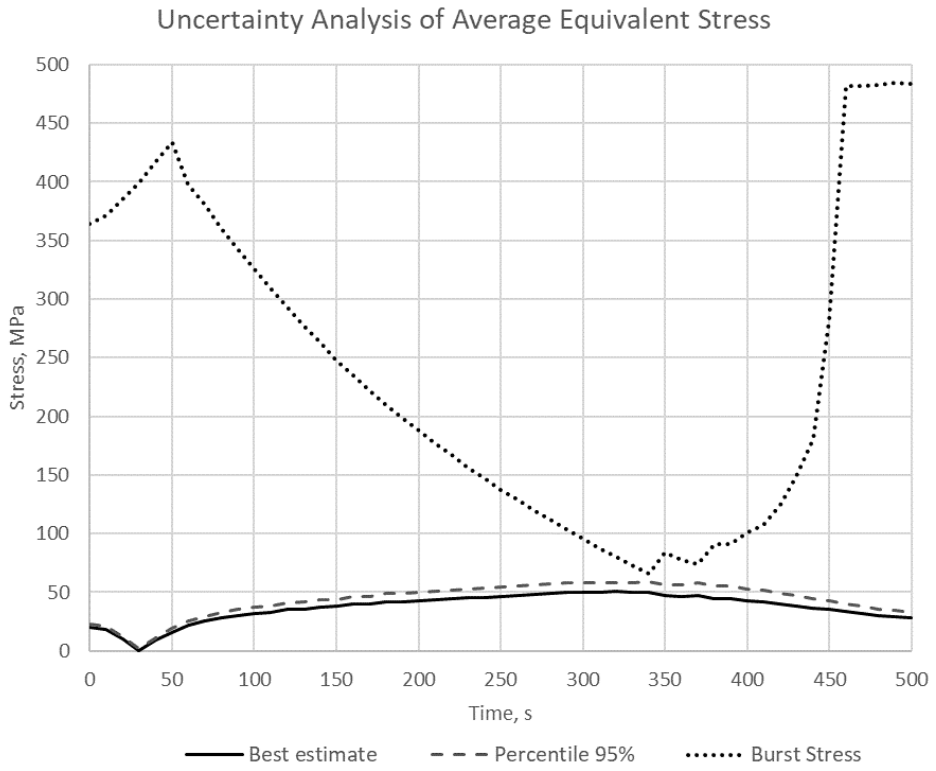

Figure 53. TRANSURANUS calculated best-estimate and 95% percentile average equivalent stresses with burst stress in cladding for a LOCA DEC-A transient in BWR-4.

Figure 54 and Figure 55 present the pressure evolution in the gap between fuel pellet and cladding and the gap width changes at the 14th segment. Especially high variations are observed in the gap width at 300 s after the transient initiation. The minimum gap width was ~200 µm, while the maximum value reaches ~1600 µm. The outer oxide layer at the 14th segment is presented inFigure 56. Discrepancies in the calculation results are uniform during the whole presented calculation period.

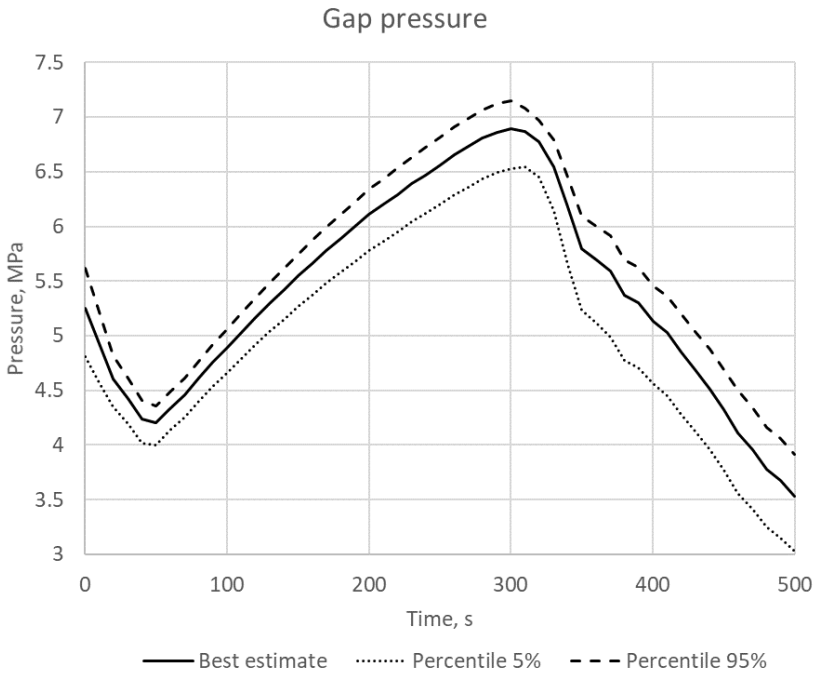

Figure 54. TRANSURANUS calculated gap pressure evolution during a LOCA DEC-A transient in BWR-4.

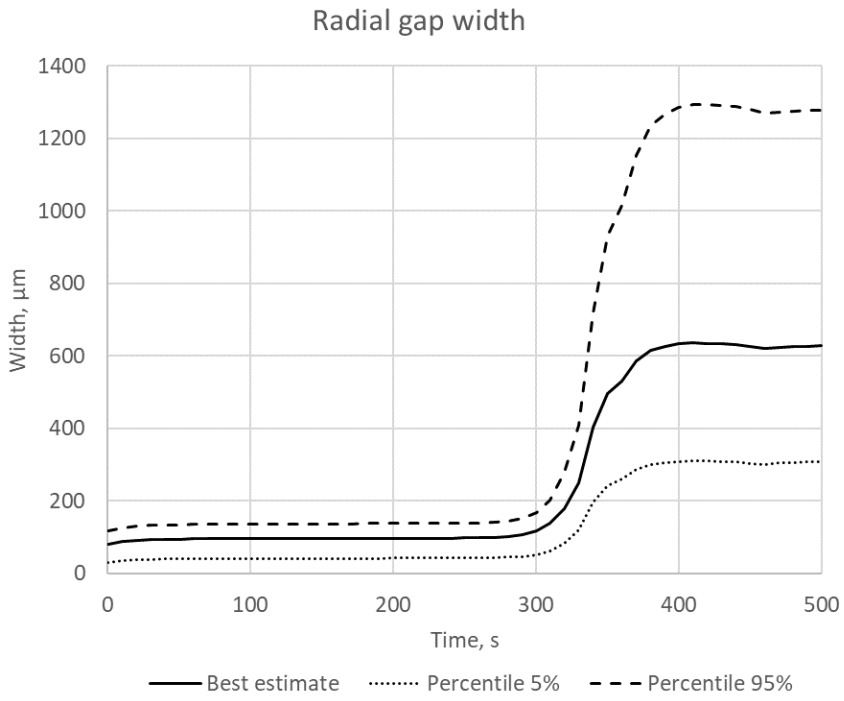

Figure 55. TRANSURANUS calculated gap width evolution during a LOCA DEC-A transient in BWR-4.

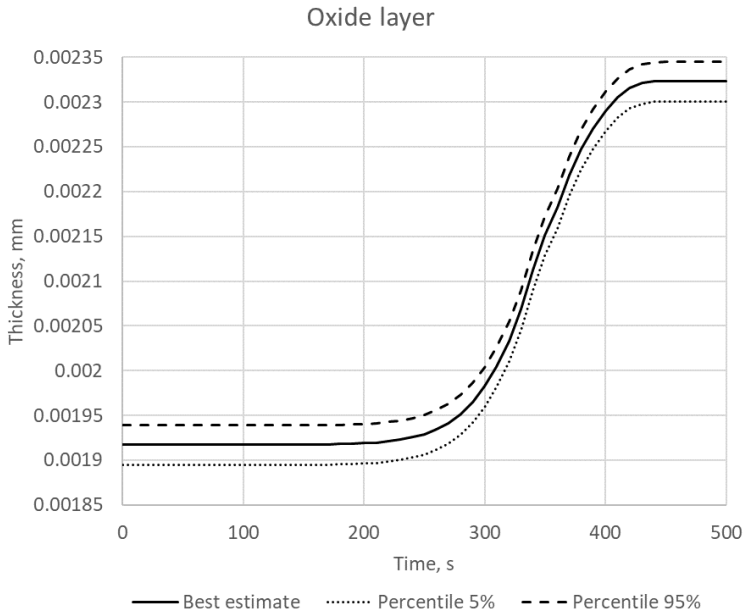

Figure 56. TRANSURANUS calculated outer oxide layer thickness evolution during a LOCA DEC-A transient in BWR-4.

For the Sensitivity analysis the Spearman correlation was used. Figure 57 to Figure 59 present the sensitivity analysis results (Spearman's ranks and scattering plots at the beginning of the LOCA transient and 340 s after the LOCA transient onset) for the gap pressure calculation results. The results of the sensitivity analysis to the gap pressure calculation shows that in the first ~300 s of the start of the accident the cladding inner radius and fuel outer radius have the highest effect. Later the influence is changing – the most important parameter become cladding outer and inner radius. Scatter plots provided in the moment at the beginning of the LOCA transient and 340 s after the LOCA transient confirms this this. However, it is needed to note that the results scattering amplitude is high.

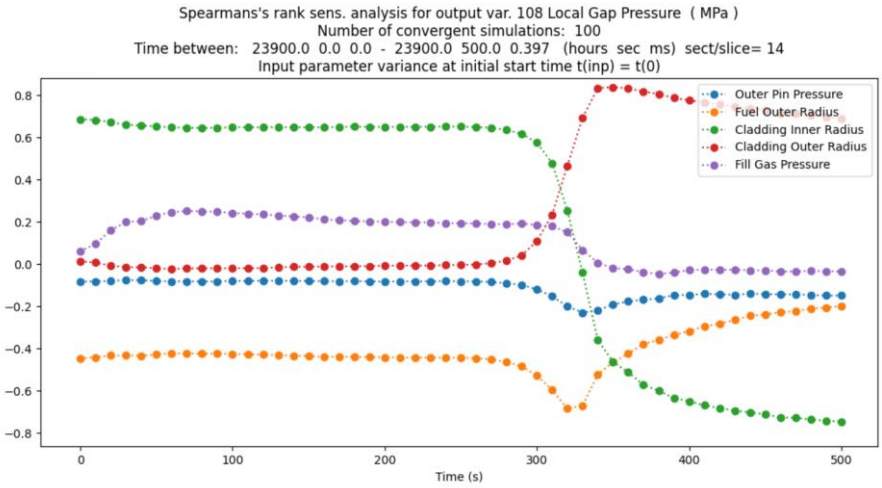

Figure 57. Spearman's ranks for gap pressure in a LOCA DEC-A transient in BWR-4.

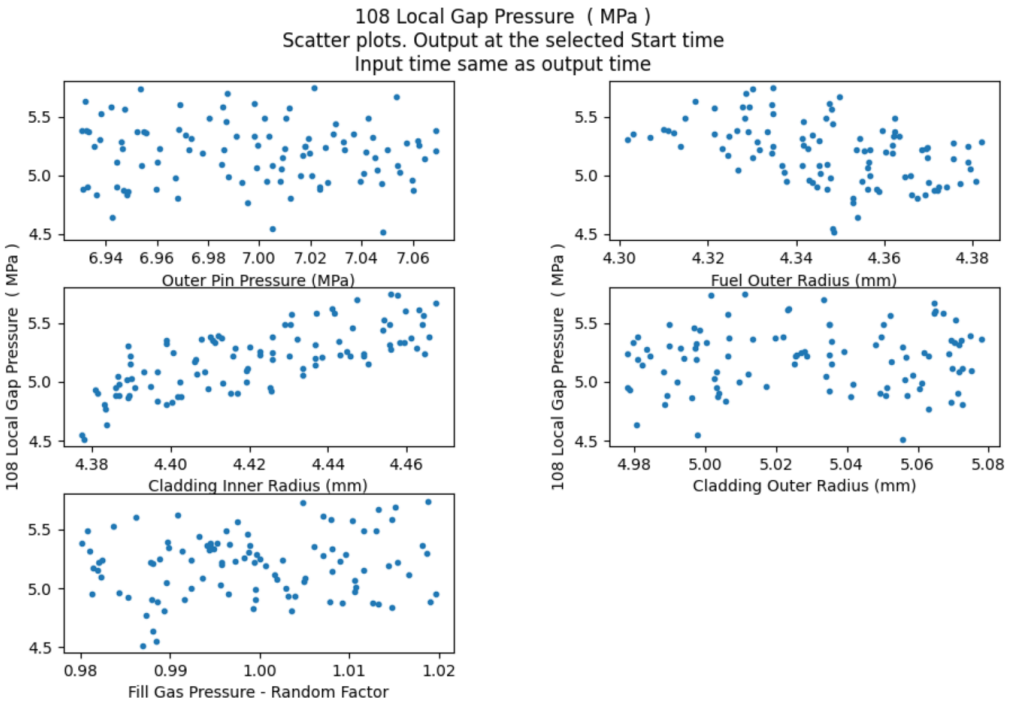

Figure 58. Scatter data plots for gap pressure, at the beginning of the LOCA DEC-A transient in BWR-4.

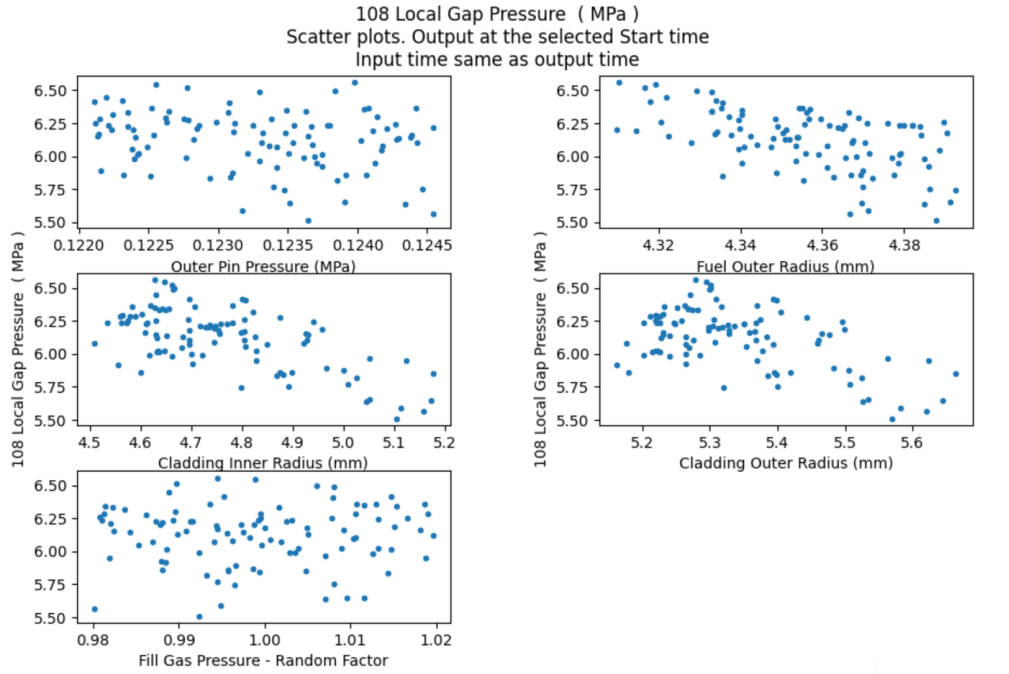

Figure 59. Scatter data plots for gap pressure, 340 s after the LOCA DEC-A transient onset in BWR-4.

Figure 60 to Figure 62 present the sensitivity analysis results (Spearman's ranks and scattering plots for time moment at the beginning of the LOCA transient and 340 s after the LOCA transient) to the average equivalent stress calculation results. The results of the sensitivity analysis to the equivalent stress shows that the cladding inner and outer radius have highest effect during all calculated transient period. This in principle indicate the

thickness of the cladding. Scatter plots provided in the moment at the beginning of the LOCA transient and 340 s after the LOCA transient confirms this this.

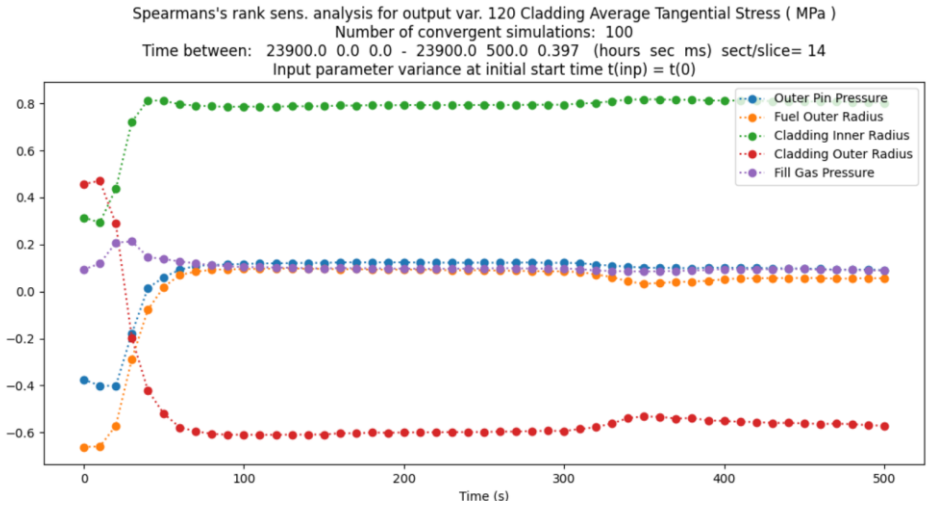

Figure 60. Spearman's ranks for average equivalent stress for a LOCA DEC-A transient in BWR-4.

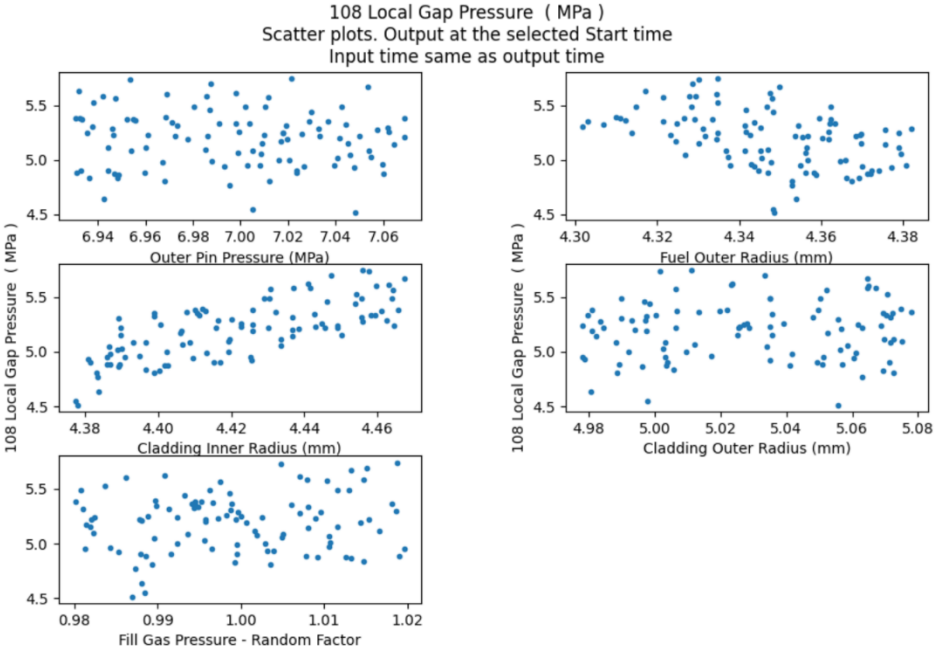

Figure 61. Scatter data plots for average equivalent stress, at the beginning of the LOCA DEC-A transient in BWR-4.

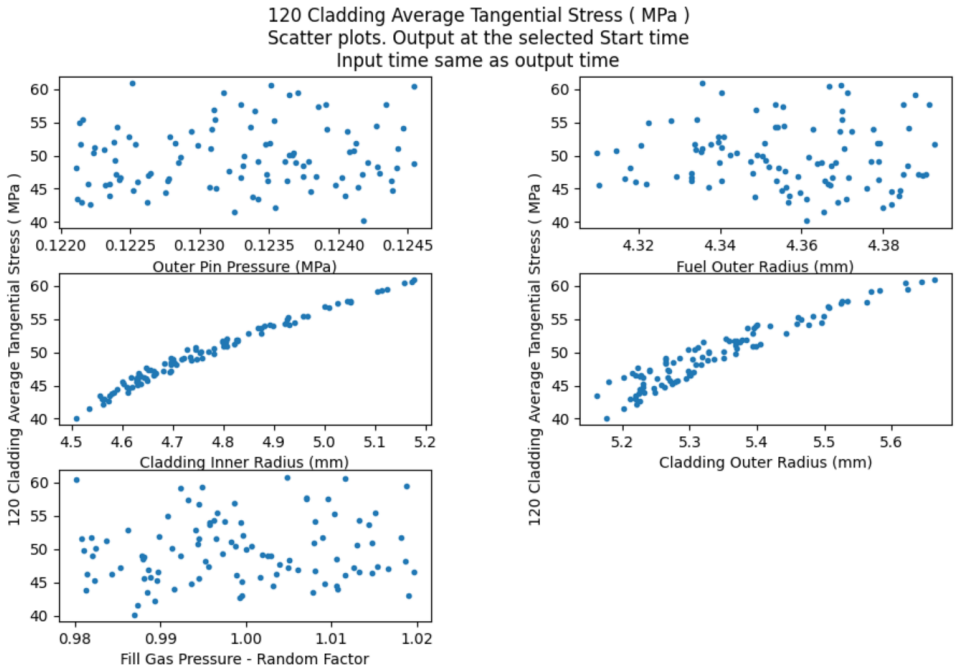

Figure 62. *Scatter data plots for average equivalent stress, 340s after LOCA DEC-A transient onset in BWR-4.*

Provided uncertainty analyses confirmed that even with considering uncertainty bounds fuel claddings with 0.98 relative power will remain intact. However, a high discrepancy in average equivalent stress was calculated and for the maximal case the limit between Burst stress and average stress was found to be very narrow. Sensitivity analysis indicated that the most influencing parameter is Cladding inner and outer diameter.

5 Main final remarks

The first set of reactor calculations was used to identify the needs in terms of code/model improvements and upgrade of calculation chains by including for example more detailed (mechanistic) computer codes to be made to reduce as much as possible some of the conservatisms used in modelling assumptions/models and avoid decoupling factors.
In the first set of the calculations received results, experience and remarks served as a reference point for the second set of simulations, analysing the same LOCA and SGTR transients and taking advantages of some of the improvements made during the project in models, simulations tools and calculation chains. In the end, comparison of both calculation sets helped to quantify the gains in terms of radiological consequences (RC) provided by the updated calculation methodologies.
This represents a first step towards best estimate evaluations. These latter needed to be associated to systematic Sensitivity Analyses an Uncertainty Quantifications were indeed beyond the scope of the project. However, from the updated evaluations, the parameters having the most impactful effect on results were identified and recommendations formulated.
Key points in calculation improvements done within the project, used methodologies, identification of the most influent parameters as well as remaining limitations and further needs are summarized below respectively for LOCA and SGTR.

Regarding LOCA calculations, the main improvements made by the partners for the 2nd set of calculations are linked to clad deformation and creep models and clad burst criteria (in temperature, stress and/or strain) more

appropriate for DBA and DEC-A conditions, refined core modelling (incl. 3D T/H core modelling), refined fuel gap inventory (incl. 3D burn-up distribution), and to a less extent to FP transport/behaviour in containment.
These improvements have led generally to a decrease in burst fuel rod ratio and in environmental activity releases. This was especially the case for VVER for which a very conservative assumption of 100% burst fuel rods had been used in initial calculations. However, it was still observed discrepancy between the results - up to 4 orders of magnitude difference between minimum and maximum activity releases calculated. The remaining discrepancies can be explained by differences in initial and boundary conditions, in modelling (model assumptions, modelling tools, calculation methodologies etc.) and in NPP operation (design containment leakages, CSS operation and efficiency etc.). For example, regarding fission product modelling during LOCA transient such differences concerned initial gap inventory, list of isotopes considered, consideration/modelling of iodine speciation and chemistry (if iodine chemistry considered or not). The conservatism and decoupled approaches have been reduced in the updated calculations. Except of very few of calculations due to low calculated PCT and no clad failure were predicted.
Some parameters/models have significant influence on the radiological consequence evaluation:

- Clad burst criteria: failed fuel rod ratio in a core is of first importance and is directly linked to the activity releases. The use of updated clad burst criteria more appropriate to DBA/DEC-A conditions (i.e. lower PCT and clad deformation…) should be used as more realistic and accurate thermomechanical calculations should be preferred. To do so, modelling of the axial gas transfer in fuel rods during the transient also must be refined.
- Fuel rod initial conditions: the difference in fuel rod initial conditions in a core (i.e., burn-up, internal rod pressure, specific power, etc…) greatly impact their thermomechanical behaviour and should be properly taken into account.
- Core nodalisation: the use of a detailed 3D core modelling allowed for better differentiation of FA characteristics (power distribution) and better reproduce the asymmetric character of a LOCA transient. However, as these calculations are very challenging in terms of computational effort, the level of details in the model must be balanced with computational capabilities or specific methodologies will have to be used to cope with it.
- Gap inventory: considering different gap inventories function of the FA irradiation history/burn-up/location in the core bases on the results of detailed neutronic calculations (i.e., provide multi-inventory, 3D burn-up distribution…) is recommended.
- FP behaviour in containment: the set of a dedicated calculation tool/module for modelling the complex and time dependent iodine behaviour/chemistry is necessary.

Also, several methodologies were developed/updated using various simulation tools that also influence the results:

- Calculation chain approach sequentially coupling a thermohydraulic system code to a thermomechanical code.
- Integral approach with a coupling between thermohydraulic and thermomechanical models within the same simulation tool.

Many other modelling improvements were made (generally more mechanistic) which will be of benefit in future reactor calculations (i.e. FP releases from fuel during transients, high burn up structure evolution and associated FP releases, fuel oxidation, etc...). Regarding code improvements, enhanced couplings of fuel performance code with FP codes were also performed as well as enhanced built-in capabilities to support the statistical analysis methodology.

Regarding SGTR calculations, main improvements made by the partners for the 2nd set of calculations are linked to the initial FP inventory and spiking, and the FP transport phenomena in the RCS, between the RCS and the SG, and in the SG. These improvements have led generally to a decrease in the activity releases. Even if for some partners, activity releases have not decreased with the improvements, the provided results are more realistic. However, it was still observed that there was a large discrepancy between the results (up to 5 orders of magnitude difference between minimum and maximum activity releases calculated).

For SGTR transients, some parameters, models, phenomena have been observed to have significant influence on the calculation results:

- Initial RCS contamination and spiking is of first importance and will directly be linked to the activity releases (the use of real NPPs data can for instance be preferred to be more realistic).
- List of isotopes considered is also very important as consequences can highly be impacted (e.g only consideration of I-131 or iodine + noble gases + Cs etc.).
- Dilution in the RCS and CVCS clean up impact have to be considered (e.g. when Severe Accidents integral codes are used).
- Related to TH: Choice of scenario, single failure, additional failure assumptions (LOOP, 1 train lost etc.), initial and boundary conditions, use of integral TH code, operators' actions, modelling of the SGTR/SLB, RV/SV correlation etc. are important and one should move towards more realistic assumptions.
- All transport phenomena through the SGTR break and in the SG (atomization, flashing, partitioning, scrubbing) should be considered and simulated based on feedback from the TH part and based on latest international references, codes or experiments in test facilities.
- For the transfer to the environment, as consequences of activity releases in liquid water or in steam phases are not the same, each phase must be considered separately.

Several methodologies using different modelling computer codes or process assessment methods were applied by the partners that are also influencing the calculation results:

- Partners used thermohydraulic codes which tend to be more faithful to simulate TH transient compared to integral SA codes. To simulate FP transport and behaviour in RCS and SG:
    - Some partners used in-house conservative and simplified methodologies leading generally to conservative results in the 1st set of calculations. In the 2nd set of calculations, they tried to reduce the conservatisms considering different phenomena or by using modules embedded in their TH simulation code to simulate FP transport and behaviour.
    - Other partners used specific and dedicated codes for radionuclides transport.
    - While other partners directly used modules and capabilities of their TH simulation code to simulate FP transport and behaviour.
- Partners used integral Severe Accidents codes to simulate at the same time TH and FP transport and behaviour.
    - Some partners in this case had to developed dedicated in-house methodologies in order to simulate specific FP transport phenomena (atomization, partitioning, flashing for instance) as the SA code was not able to reproduce those phenomena because the code is not designed for that.
    - Other partners directly used the capabilities of their integral SA codes to simulate radionuclides transport and behaviour.

Further needs of improvements observed in the project.

Many improvements were made within the project. However, there is still room for additional improvements as some remaining limitations were identified during the project.

From LOCA calculations:

- Whatever the methodology used during the project to calculate the fuel burst ratio in a core none of them properly addressed the fuel assembly behaviour at a sub-channel code (i.e. able to deal with rod-to-rod interaction, considering guide tubes….);
- The burst strain should be revised for DBA/DEC-A conditions;
- The computational cost associated to 3D approach is not compatible with the need to manage uncertainties in rod burst ratio evaluation methodology;
- In addition to the fuel gap inventory releases some additional FP releases from fuel might occurs during the transient due to the variations of mechanical stress in fuel pellets, the evolution of the high burn-up structure and/or the oxidation of fuel.

From SGTR calculations:

- Retention and deposition of FP/radionuclides in the RCS/SG (in the swirl-vane or chevron separators for instance) should further be looked at. It can be simulated by detailed transport cods or by driven-correlation models taking advantage of available experimental data (i.e. form ARTIST program)
- The radiological consequences of activity releases with liquid water phase should be better described so that they can be fully and independently considered.
- The development of mechanistic codes which can simulate the FP spiking phenomenon based on gap inventory, fuel burnup/history and feedback from TH code to simulate the FP escape rate from the defective fuel rod may be an improvement. However, the ratios between improvement of the spiking modelling, computing resources and added value of a more accurate spiking model compared to more simplistic model should be considered.

6 References

[1] Adam Kecek (UJV), R2CA deliverable D3.2

[2] Tatiana Taurines, Sébastien Belon (IRSN): Rod cladding failure during LOCA – Final report on experimental database re-assessment and model/code improvements (IRSN), R2CA deliverable D3.4, February 2023

[3] Arndt Schubert: Fuel rod behaviour during LOCA transient – Final report (JRC), R2CA deliverable D3.6, December 2022

[4] Luis E. Herranz, Rafael Iglesias, (CIEMAT), Raphael Zimmerl (BOKU), Jeremy Bittan (EDF), Francois Kremer (IRSN), Adam Kecek (UJV), Gumenyuk Dmytro (SSTC). D4.1 Final Report on experimental database reassessment and on model/code improvements for fission product releases during a SGTR transient, July 2023.

[5] Cédric Leclere (IRSN), R2CA deliverable D4.5

[6] Berta Bürger (EK), Zoltán Hózer (EK): Improvement of the iodine and cesium spiking models in the RING code, EK-2021-437-1-4-M0, T4.2. Fission product release from defective fuel rod during SGTR transient (2021)

[7] Berta Bürger (EK), Zoltán Hózer (EK): Simulation of coolant activity concentrations during SGTR with the RING code, Technical report EK-2021-437-1-1-M0, EU R2CA T4.2. Fission product release from defective fuel rod during SGTR transient (2022)

[8] L.E. Herranz, Rafael Iglesias (CIEMAT), Raphael Zimmerl (BOKU), Jeremy Bittan (EDF), Francois Kremer (IRSN), Adam Kecek (UJV), Gumenyuk Dmytro (SSTC), R2CA, D4.1, Progress Report on experimental database reassessment and on model/code improvements for fission product releases during a SGTR transient., 23/11/2021

[9] D. Pizzocri, L. Luzzi, G. Zullo, F. Kremer, R. Dubourg, N. Arnold, N. Muellner, R. Zimmerl, J. Klouzal, D. Gumenyuk, L.E. Herranz, R. Iglesias, M. Cherubini, L. Giaccardi, A. Schubert, P. Van Uffelen, B. Bürger, Z, Hózer, R2CA, D4.3, Progress report on source term for defective fuel rods during SGTR, 29/11/2021

[10] T. Taurines, S. Belon, A. Arkoma, T. Kaliatka, K. Kulacsy, M. Jobst, I. Ovdiienko, P. V. Uffelen, J. Klouzal, R. Calabrese, Rod cladding failure during LOCA- Final report on experimental database reassessment and model/code improvements, 28/02/2023

[11] G. Zullo, D. Pizzocri, L. Luzzi (POLIMI), F. Kremer (IRSN), N. Arnold, N. Muellner, R. Zimmerl (BOKU), J. Klouzal (UJV), D. Gumenyuk (SSTC), L.E. Herranz, R. Iglesias (CIEMAT), M. Cherubini, L. Giaccardi (NINE), A. Schubert, P. Van Uffelen (JRC), B. Bürger, Z, Hózer. D 4.4 Final report on rod cladding failure during SGTR, R2CA Project, 2022.

[12] L.E. Herranz, Rafael Iglesias (CIEMAT), Raphael Zimmerl (BOKU), Jeremy Bittan (EDF), Francois Kremer (IRSN), Adam Kecek (UJV), Gumenyuk Dmytro (SSTC), D4.2 – T4.1, Final Report on experimental database reassessment and on model/code improvements for fission product releases during a SGTR transient, R2CA Project, 2023.

[13] Walter Giannotti, D2.6 - T2.4. Addressing uncertainty evaluation, R2CA Project, 2023

[14] R. Zimmerl, W. Giannotti, Y. Janal, B. Hrdy, N. Muellner, Extended CIAU Uncertainty Method-Evaluation of iodine release, to be submitted in ANE special issue on R2CA project

[15] L. Cantrel and P. March, Mass Transfer Modeling with and Without Evaporation for Iodine Chemistry in the Case of a Severe Accident, Nuclear Technology, 154:2, 170-185, DOI: 10.13182/NT06-A3726, 2006

[16] Tadas Kaliatka (LEI) et al., D2.5 – T2.3 Reactor test case simulations, R2CA project, 2021

[17] F. D 'Auria, CIAU method for uncertainnty evaluation, 2002